UNIVERSITÀ DEGLI STUDI DI TRIESTE

XXXVIII CICLO DEL DOTTORATO DI RICERCA IN BIOMEDICINA MOLECOLARE

This work was sponsored and funded by GlaxoSmithKline Biologicals SA.
GSK Vaccines Institute for Global Health srl is an affiliate of GlaxoSmithKline Biologicals SA.

Characterization of multivalent vaccines against antimicrobial resistant pathogens

Settore scientifico-disciplinare: BIOS-07/A

DOTTORANDA
Roberta Di Benedetto

COORDINATORE
Prof. Alessandro Tossi

SUPERVISORE DI TESI
Prof. Paola Cescutti

CO-SUPERVISORE DI TESI
Dr. Carlo Giannelli
GSK Vaccines Institute for Global Health

Dr. Francesca Micoli
GSK Vaccines Institute for Global Health

ANNO ACCADEMICO 2024/2025

UNIVERSITÀ
DEGLI STUDI
DI TRIESTE

UNIVERSITÀ DEGLI STUDI DI TRIESTE

XXXVIII CICLO DEL DOTTORATO DI RICERCA IN BIOMEDICINA MOLECOLARE

This work was sponsored and funded by GlaxoSmithKline Biologicals SA.
GSK Vaccines Institute for Global Health srl is an affiliate of GlaxoSmithKline Biologicals SA.

Characterization of multivalent vaccines against antimicrobial resistant pathogens

Settore scientifico-disciplinare: BIOS-07/A

DOTTORANDA
Roberta Di Benedetto

COORDINATORE
Prof. Alessandro Tossi

SUPERVISORE DI TESI
Prof. Paola Cescutti

CO-SUPERVISORE DI TESI
Dr. Carlo Giannelli
GSK Vaccines Institute for Global Health

Dr. Francesca Micoli
GSK Vaccines Institute for Global Health

ANNO ACCADEMICO 2024/2025

TABLE OF CONTENTS

ABSTRACT

In recent years, the threat of antibiotic-resistant bacteria has become increasingly concerning. Vaccines are crucial tools in the fight against antimicrobial resistance (AMR), and multivalent polysaccharide-based vaccines are promising candidates for addressing this issue. However, developing these vaccines requires additional efforts, e.g. in terms of immunological evaluation including eventual immuno-interference, development of analytical methods for determining the characteristics of single antigens and the stability of the final multivalent combination.

Generalized Modules for Membrane Antigens (GMMA) and glycoconjugation were compared for the development of an O-antigen-based tetravalent vaccine against Shigella, leading bacterial cause of diarrheal disease in low- and middle-income countries (LMICs). GMMA offers good immunogenicity, functionality, and simplified manufacturing, making it a viable strategy for vaccine development.

Originally targeting *Shigella* strains *S. sonnei* and *S. flexneri* 1b, 2a, and 3a, the vaccine's multivalency was expanded to hexavalency by adding glycoconjugates against *Salmonella* Typhi and Paratyphi A. This combination could address a significant unmet need and substantially contribute to AMR reduction. The technical feasibility of combining these six antigens was demonstrated, with no negative impact on the humoral immune response elicited by each of them in different animal models.

The *S. flexneri* O-antigens have identical sugar compositions, posing challenges for individual quantification. To address this, a liquid chromatography-mass spectrometry method was developed to differentiate monomers based on their linkages in the O-antigen chain.

Assessing vaccine stability is critical for safe and effective patient administration. Accelerated stability studies on the tetravalent *Shigella* GMMA vaccine have been conducted, and predictive models established to foresee vaccine behavior during storage and expedite vaccine development.

Overall, this work advances multivalent saccharide-based vaccine development, contributing to AMR reduction and public health efforts.

.

LIST OF ABBREVIATIONS

5 PL	**Five parameter logistic**
A	**Pre-exponential factor**
Abe	**Abequose**
ABS	**Absorbance**
Abs	**Antibodies**
ACN	**Acetonitrile**
Ag	**Antigen**
altSonflex1-2-3	**tetravalent *Shigella* GMMA vaccine**
AMR	**Antimicrobial resistance**
AMR MPTF	**AMR Multi-partner Trust Fund**
ANOVA	**Analysis of Variance**
APCs	**Antigen-presenting cells**
BSA	**Bovine serum albumin**
CDAP	**1-cyano-4-dimethylaminopyridine tetrafluoroborate**
cELISA	**Competitive Enzyme-linked immunosorbent assay**
CHIM	**Controlled Human Infection Model**
CIES	**Carrier-induced epitopic suppression**
CPS	**Capsular polysaccharides**
CQA/CQAs	**critical quality attributes**
CRM_{197}	**Cross Reacting Material 197**
DALYs	**Disability-adjusted life-years**
DCM	**Dichloromethane**
DLS	**Dynamic Light Scattering**
DMSO	**Dimethylsulfoxide**
dNTS	**diarrheagenic non-typhoidal *Salmonella***
dRI	**Differential Refractive Index**
Ea	**Activation energy**
ELISA	**Enzyme-linked immunosorbent assay**
ESI	**Electrospray ionization**
FacE	**Formulated Alhydrogel competitive ELISA**
Fuc	**Fucose**
Gal	**Galactose**
GAP	**WHO Global Action Plan**
GBD	**Global Burden of Disease**
GCs	**Germinal centers**
GLASS	**WHO Global Antimicrobial Resistance and Use Surveillance System**
Glc	**Glucose**
GlcNAc	***N*-acetylglucosammine**
GMMA	**Generalized Modules for Membrane Antigens**
GMP	**Good Manufacturing Practice**
GVGH	**GSK Vaccines Institute for Global Health**
HCD	**Higher-energy collisional dissociation**
HIC	**Hydrophobic interaction chromatography**
HICs	**High-income countries**

HPAEC-PAD	**High-performance anion-exchange chromatography with pulsed amperometric detection**
HPLC-SEC	**Size Exclusion High Performance Liquid Chromatography**
ICH	**International Conference on Harmonization**
Ig	**Immunoglobulins**
IL-6	**Interleukin 6**
IMPDs	**Investigational Medicinal Product Dossier**
INDs	**Investigational New Drug application**
iNTS	**Invasive non-typhoidal *Salmonella***
KDO	**3-deoxy-D-manno-oct-2-ulosonic acid**
LC	**Liquid chromatography**
LMICs	**Low- and medium-income countries**
LPS	**Lipopolysaccharide**
LTA	**Lipoteichoic acids**
Man	**Mannose**
MAPS	**Multiple Antigen Presenting System**
MAT	**Human monocyte activation tests**
MDR	**Multidrug resistance**
MeI	**Iodomethane**
micro BCA	**micro Bicinchoninic Acid protein assay**
MS	**Mass spectrometry**
MW	**MW molecular weight**
n	**Order of reaction**
NIH	**U.S. National Institutes of Health**
NTS	**Non-typhoidal *Salmonella***
O:2	***S.* Paratyphi A OAg**
O:2-CRM$_{197}$	***S.* Paratyphi A glycoconjugate**
OAg	**O-antigen**
OMVs	**Outer Membrane Vesicles**
ON	**Over night**
PAMPs	**Pathogen-Associated Molecular Patterns**
Par	**Paratose**
PBS	**Phosphate Buffer Saline**
PCVs	**Pneumococcal conjugate vaccines**
PI	**Prediction intervals**
PMP	**1-phenyl-3-methyl-5-pyrazolone**
PS	**Polysaccharide**
QA/QAs	**Quality attributes**
Rha	**Rhamnose**
RMSE	**Root mean square error**
RNA	**Ribonucleic acid**
RT	**Room temperature**
rt	**Retention time**
RU	**Repeating units**
***S.* Enteritidis**	***Salmonella* Enteritidis**
S. flexneri	***Shigella flexneri***
***S.* Paratyphi A**	***Salmonella* Paratyphi A**
S. sonnei	***Shigella sonnei***

***S.* Typhimurium**	***Salmonella* Typhimurium**
SBA	**Serum bactericidal activity**
spp	**Species**
SSE	**Sum of squares error**
t_0 / t_∞	**Values of starting (t_0) and final (t_∞) QA**
TA	**Teichoic acids**
TFA	**Trifluoroacetic acid**
TLR	**Toll-like Receptor**
Tyv	**Tyvelose**
UPLC-PRM MS	**Ultra Performance Liquid Chromatography coupled with Mass Spectrometry in Parallel Reaction Monitoring mode**
UPLC-RP	**Reversed Phase-UPLC**
Vi-CRM_{197}, TCV	**Typhoid conjugate vaccine**
WHO	**World Health Organization**
WTA	**Wall teichoic acids**

1. INTRODUCTION

1.1. Antimicrobial resistance (AMR): a global threat to public health

The introduction of antibiotics in the 20th century marked one of the greatest medical breakthroughs, initiating a "golden age" of antibiotic discovery that peaked in the 1950s. However, decades of overuse and misuse of antibiotics in humans and animals have driven the emergence of multidrug-resistant pathogens, making infections harder to treat and complicating procedures such as surgeries, chemotherapy, and organ transplants, giving rise to the current antimicrobial resistance (AMR) crisis [1, 2]. Indeed, AMR has emerged as one of the leading public health threats of the 21st century [3, 4], becoming an endemic and widespread problem. Although it affects high-income countries (HICs), the burden is disproportionately higher in low- and middle-income countries (LMICs) [5, 6].

AMR develops when microorganisms—bacteria, viruses, fungi, and parasites—mutate over time, causing antimicrobial drugs to become less effective or even ineffective in treating infections [7]. This not only complicates infection treatment but also increases the risk of disease spread, leading to higher rates of severe illness and mortality.

Several factors facilitate the rapid spread of AMR in LMICs, including uncertain access to safe water and proper hygiene conditions, and quality healthcare systems restricted to a minor part of the population. Moreover, suboptimal management and control of drug-resistant infections in both hospital and agricultural settings, together with the high spread of resistant pathogens during food production and processing, have significantly contributed to the issue. Additional factors include inadequate access to affordable drugs, vaccines, and diagnostics, as well as a general lack of awareness and understanding of AMR [6, 8].

In 2019, a global estimate of the burden of bacterial AMR revealed that 1.27 million deaths were attributable to AMR—directly caused by ineffective treatment of drug-resistant infections—while 4.95 million deaths were associated with AMR, indicating that resistance was present even if not the sole cause of death. The highest burdens were observed in Sub-Saharan Africa and South Asia, with six leading pathogens driving these deaths: *Escherichia coli*, *Staphylococcus aureus*, *Klebsiella pneumoniae*, *Streptococcus pneumoniae*, *Acinetobacter baumannii* and *Pseudomonas aeruginosa* (**Figure 1.1**) [9]. Several of these are part of the ESKAPE group, a set of multidrug-resistant bacteria for which effective therapies are urgently needed [10].

A subsequent study [11] presented the first comprehensive assessment of the global burden of AMR from 1990 to 2021, with forecasts extending to 2050. Between 1990 and 2021, deaths caused by AMR

decreased by over 50% among children under 5 years, while they increased by more than 80% in adults aged 70 and older (**Figure 1.2**). Projections for 2050 suggest that AMR could be responsible for approximately 1.91 million deaths directly attributable to resistance and 8.22 million deaths associated with it on a global scale.

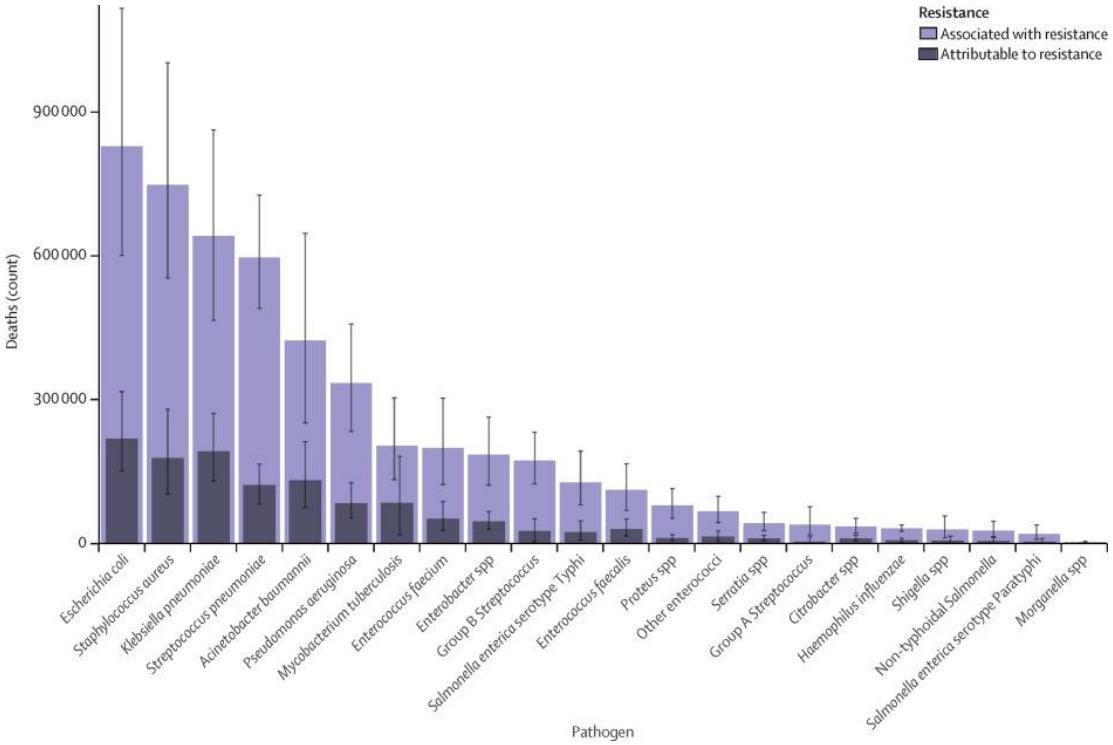

Figure 1.1. Global deaths (counts) attributable to and associated with bacterial antimicrobial resistance by pathogen, 2019. *Reproduced from* [9].

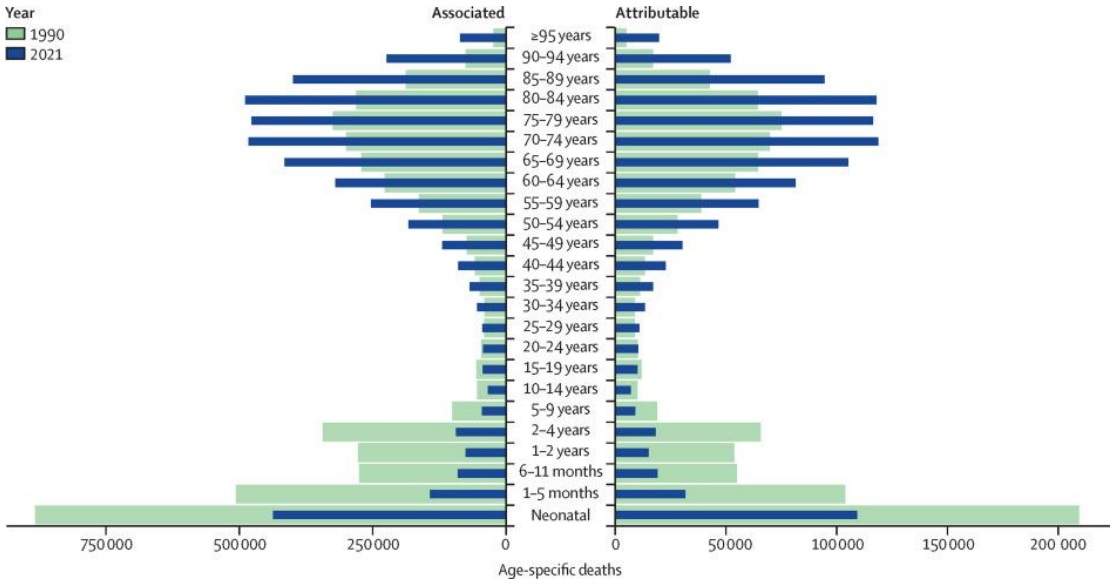

Figure 1.2. Deaths attributable and associated with antimicrobial resistance, by detailed age group, for 1990 and 2021. *Reproduced from* [11].

Over the last few years, the World Health Organization (WHO) and numerous other authorities have called for coordinated action to tackle AMR. In 2015, the WHO launched the Global Action Plan (GAP), emphasizing the need for a "One Health approach", which involves joint efforts across human health, food production, animal, and environmental sectors to achieve improved public health outcomes [12]. That same year, the WHO introduced the Global Antimicrobial Resistance and Use Surveillance System (GLASS), a standardized system for collecting, analyzing, and sharing AMR data from all countries [13].

In 2017, the WHO published the Bacterial Priority Pathogens List [14], which was later updated in 2024 [15]. This document identifies bacterial pathogens of public health significance to guide research, development, and strategies for preventing and controlling AMR. In this report, bacteria were classified as critical, high, or medium priority, according to the urgency of need for new preventive strategies [15] (**Figure 1.3**). Furthermore, the report emphasizes that addressing AMR within the human health sector requires global efforts focused on several key areas: robust infection prevention and control measures, equitable access to diagnostics and treatment, vigilant surveillance to detect emerging trends in AMR, and substantial investment in research and development for the creation of new medicines, diagnostics, and prevention tools [15].

A major step forward in the fight against AMR occurred in 2019 with the launch of the AMR Multi-partner Trust Fund (AMR MPTF), designed to enhance support for LMICs in facing the AMR threat [16].

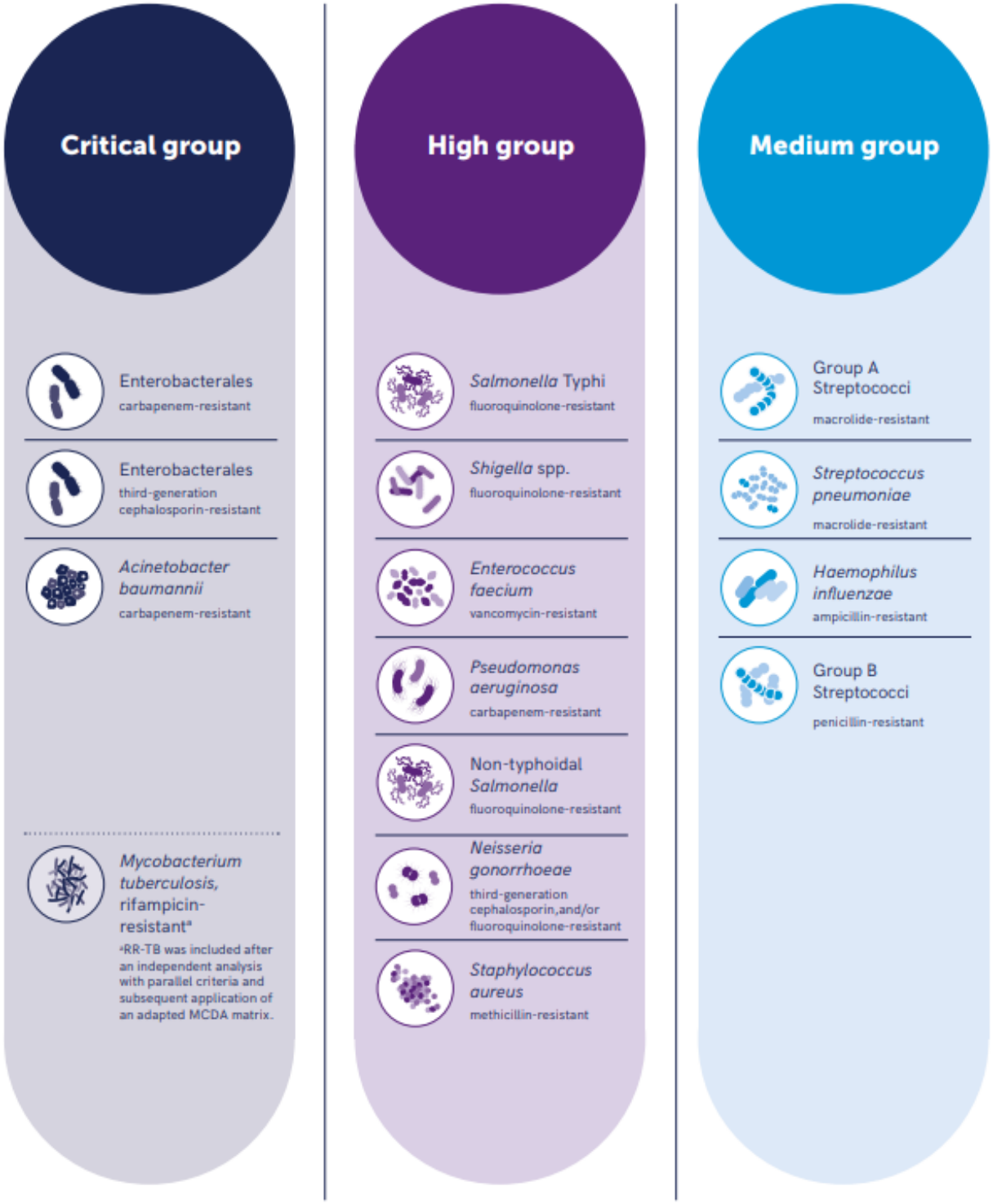

Figure 1.3. WHO Bacterial Priority Pathogens List, 2024. *Reproduced from* [15].

1.1.1. Resistance mechanisms to antibiotics

Antibiotic resistance is driven by several mechanisms [17] and occurs naturally, but the emergence and spread of new resistance mechanisms may have been greatly accelerated by the overuse and misuse of antimicrobials [18]. Indeed, global antibiotic consumption has increased by 65% from 2000 to 2015, mainly in LMICs, and is projected to triple by 2030 without appropriate interventions [19].

Antibiotics may either destroy bacteria (bactericidal) or inhibit their growth (bacteriostatic) and are grouped based on the cellular target or metabolic process they disrupt: (1) inhibitors of cell wall synthesis (e.g., β-lactams and glycopeptides); (2) inhibitors of protein synthesis (e.g., aminoglycosides, tetracyclines, oxazolidinones); (3) inhibitors of nucleic acid synthesis (e.g., quinolones, fluoroquinolones, rifamycins); (4) inhibitors of folic acid metabolism (e.g., sulfonamides and trimethoprim); and (5) cell membrane disruptors (e.g., polymyxins) [17, 20].

Bacteria may naturally exhibit resistance to antibiotics, but they can also acquire resistance through chromosomal mutations or acquisition of genetic material via horizontal gene transfer [21, 22]. A bacterial strain is considered intrinsically resistant when it resists the effects of a specific antibiotic because the antibiotic's target is either absent or structurally/chemically different. In addition to intrinsic resistance, bacteria can develop or acquire antibiotic resistance through three main mechanisms (**Figure 1.4**) [21, 22].

(1) Restriction of antibiotic access to the target. Bacteria can reduce the permeability of their outer membranes—either by downregulating porins or expressing more selective ones—or they can actively expel antibiotics through efflux pumps. Overexpression of these efflux pumps, often resulting from mutations in transcriptional regulators or as an adaptive response during host colonization, can lead to high levels of resistance. When these pumps have broad substrate specificity, they contribute to multidrug resistance (MDR) and are referred to as MDR efflux pumps.

(2) Modification of the antibiotic target. To exploit their function, antibiotics typically bind to specific bacterial targets, thereby disrupting essential physiological processes. Bacteria can impair this binding either by producing mutant variants of the target through point mutations or genetic recombination, or altering the target post-translationally via the addition of chemical groups by specific enzymes.

(3) Antibiotic inactivation. Bacteria can neutralize antibiotics by expressing enzymes that either degrade the antibiotic molecules or chemically modify them, which prevents effective binding to their targets.

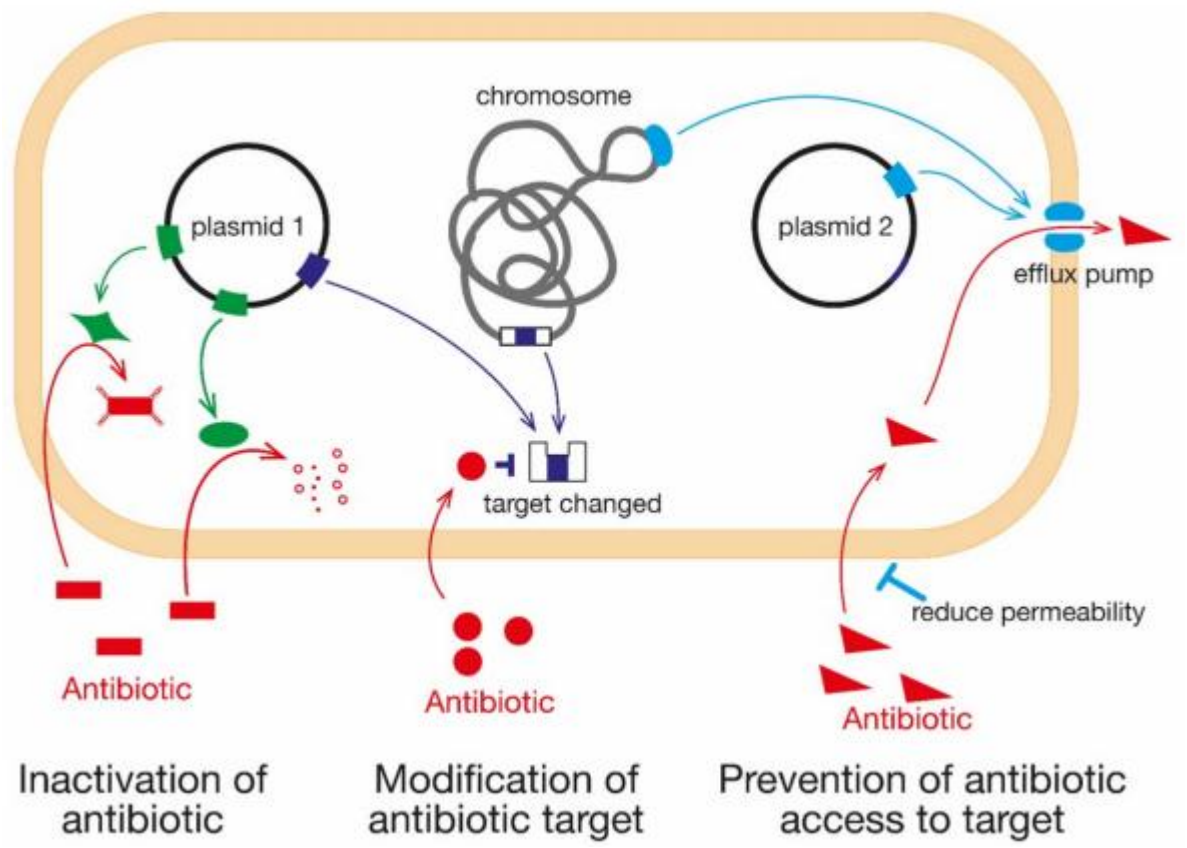

Figure 1.4. Main mechanisms mediating antibiotic resistance. *Reproduced from* [21].

Since resistance evolves rapidly against each new class of antibiotic—often emerging shortly after their introduction [23]—and new effective drugs are increasingly hard to develop, it is clear that relying solely on antibiotics is insufficient [5, 24]. Therefore, to combat AMR, scientific research is now focusing extensively on innovative, alternative strategies. An integrated approach that combines novel antibiotics with the use of vaccines, diagnostic tools, monoclonal antibodies, microbiota interventions, and bacteriophages is considered a more effective solution [21, 25, 26].

1.2. The role of vaccines in addressing antimicrobial resistance

Preventing disease is crucial in the fight against AMR, and vaccines are central to this strategy [2, 21, 27, 28]. Since the introduction of Jenner's vaccine against smallpox in 1798, vaccines are considered one of the most successful public health interventions preventing millions of deaths, improving the quality and prolonging life expectancy [29]. Vaccines work through multiple mechanisms to reduce AMR [30]. They not only directly prevent or reduce life-threatening diseases—thereby decreasing healthcare costs and post-infection sequelae—but also indirectly limit the use of antibiotics, reducing the symptoms that usually trigger their use [21]. This effect has been demonstrated by studies that report reductions in antibiotic prescriptions ranging from 13% to 64%, not only limiting drug use but also decreasing the spread of resistance [31, 32].

Alongside hygiene measures [33], vaccines and antibiotics are essential in controlling infections. Antibiotics are the only life-saving tool during acute bacterial infections, whereas vaccines prevent the initiation of infections, thereby limiting bacterial proliferation and reducing opportunities for mutation [34]. In contrast, antibiotics must treat ongoing infections where bacteria multiply and mutate, often selecting for resistant variants. Moreover, while antibiotics typically target a limited number of metabolic pathways, vaccines stimulate a protective immune response against multiple antigens and epitopes, further reducing the chances for vaccine escape mutants [21, 35].

Vaccines offer lasting protection with a much lower likelihood of resistance emerging compared to antibiotics, as they act prophylactically rather than therapeutically (**Figure 1.5**) [35, 36]. However, there are few cases of vaccine resistance. This outcome may occur for various reasons. For example, while some vaccines effectively prevent disease, they might not entirely block pathogen colonization or transmission, as observed with the acellular pertussis vaccine. Additionally, serotype replacement can occur when vaccines do not target all the serotypes, as is the case with pneumococcal vaccines. Consequently, developing improved protective antigens remains crucial, especially for infections associated with antibiotic resistance [35, 36]. Nevertheless, even in the rare instances where vaccine resistance has been observed, a measurable reduction in disease burden has still been achieved, primarily due to the preventive nature of vaccination, the establishment of indirect protection (herd immunity), and the durability of protective effects [31, 37, 38]. This contrasts sharply with antibiotics, where even minimal resistance can completely nullify therapeutic benefits.

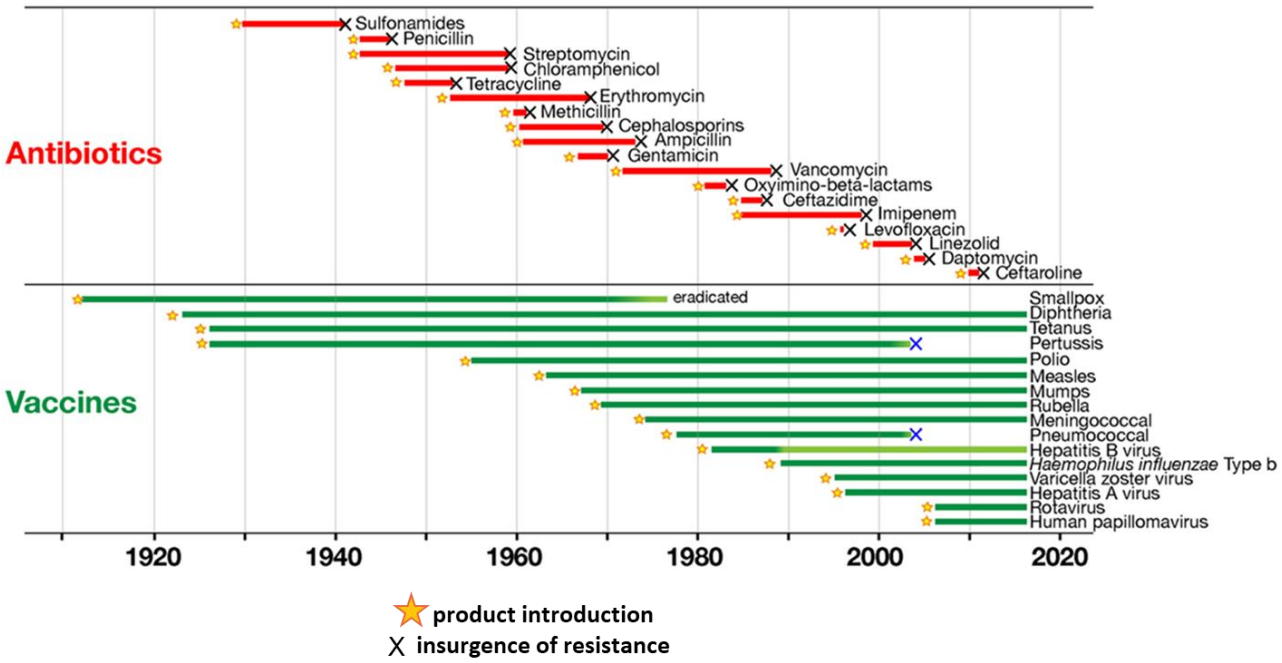

Figure 1.5. Time to detection of resistance of human pathogens to antimicrobials (in red) and to vaccines (in green). *Adapted from* [35].

The WHO has emphasized the importance of maximizing the use of existing vaccines and accelerating the development of new ones against AMR pathogens [39]. Predictions suggest that vaccines could have a substantial impact in controlling infections caused by antimicrobial-resistant pathogens [40], even though, except for *S. pneumoniae* and *Mycobacterium tuberculosis,* vaccines against the top 10 causes of global deaths due to antimicrobial-resistant pathogens (**Figure 1.1**) are still missing.

Traditional vaccines initially employed live attenuated or inactivated organisms to elicit an immune response with minimal illness while promoting memory cell activation [41]. However, these approaches are often associated with high reactogenicity, posing challenges in balancing safety and efficacy [42]. Recent advancements in various scientific disciplines have paved the way for new vaccine technologies, including glycoconjugation, bioconjugation, Multiple Antigen Presenting System (MAPS) technology, reverse vaccinology, structural vaccinology, Generalized Modules for Membrane Antigens (GMMA), nanoparticle vaccines, ribonucleic acid (RNA)-based vaccines, and novel adjuvants [26].

In the next paragraphs, traditional glycoconjugates and GMMA will be described more in depth.

1.2.1. Mode of action of vaccines

Vaccines work by priming the adaptive immune response—both the humoral immunity mediated by B cells and the cell-mediated immunity driven by T cells—to protect against future infections [43]. By exposing the immune system to live attenuated or inactivated forms of a pathogen (or parts thereof), vaccines mimic natural infection without causing disease, thereby teaching the body to rapidly recognize and efficiently combat the real pathogen upon future exposure. This process involves the generation of immunological memory, ensuring that the immune system can mount a quick and robust response when needed. Although it takes 2–3 weeks for vaccines to elicit these immune responses, they confer long-lasting protection [26].

For most vaccines, the induction of antibodies (Abs) is critical to confer protection [43]. B cells produce antibodies (immunoglobulins, Ig) that bind specifically to antigens (Ag), such as exotoxins or bacterial surface molecules (proteins and polysaccharides), effectively neutralizing the pathogen. These antibodies interfere with infection in the following ways (**Figure 1.6**):

(1) Blocking the pathogenic process by neutralizing toxins produced by bacteria.

(2) Enhancing opsonophagocytosis, thus promoting the elimination of internalized bacteria by enhancing the opsonophagocytic activity of macrophages.

(3) Initiating the complement cascade, ultimately leading to the generation of the membrane attack complexes, causing perforation of bacterial cell membranes and subsequent bacterial lysis.

(4) Disrupting adhesion and biofilm formation, by binding adhesins on bacterial surfaces to interfere with adhesion/invasion of epithelial barriers and prevent biofilm formation.

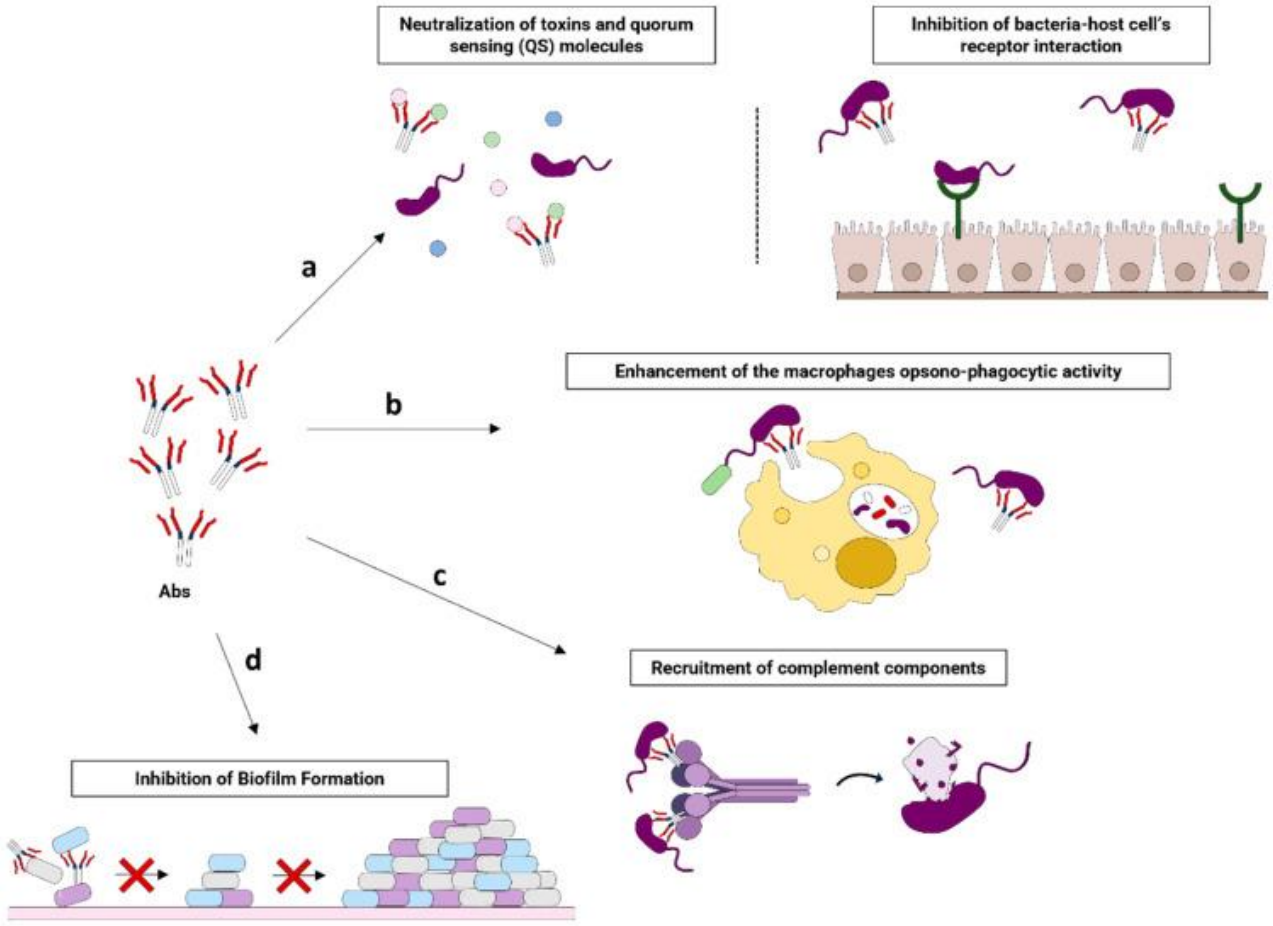

Figure 1.6. Mechanisms of action of antibodies. *Reproduced from* [26].

In addition to antibody-mediated defense, the cellular adaptive immunity plays an essential role [43]. T cells can contribute to effective and long-lasting immune responses in two main ways: through CD4+ T-helper cells, which recognize peptides presented by major histocompatibility complex (MHC) class II molecules, and secrete cytokines that stimulate B cells to produce antibodies; through CD8+ cytotoxic T cells, which recognize peptides in the context of MHC class I molecules, and are crucial for eliminating intracellular pathogens and for tumor surveillance [44-46].

1.3. Bacterial carbohydrates in vaccine development: from plain polysaccharides to glycoconjugate vaccines

Most bacteria possess a surface polysaccharide (PS) network known as the *glycocalyx*. This complex layer comprises: (1) Lipid-linked structures such as lipopolysaccharides (LPS) in Gram-negative bacteria (which include lipid A, a core oligosaccharide, and an O-antigen (OAg) that determines serotype specificity), and teichoic acids (TA) in Gram-positive bacteria (including lipoteichoic acids (LTA) and the more exposed wall teichoic acids (WTA)); (2) Surface peptidoglycans present in Gram-positive species; and (3) Capsular polysaccharides (CPS) found in both Gram-positive and Gram-negative encapsulated bacteria (**Figure 1.7(A)**).

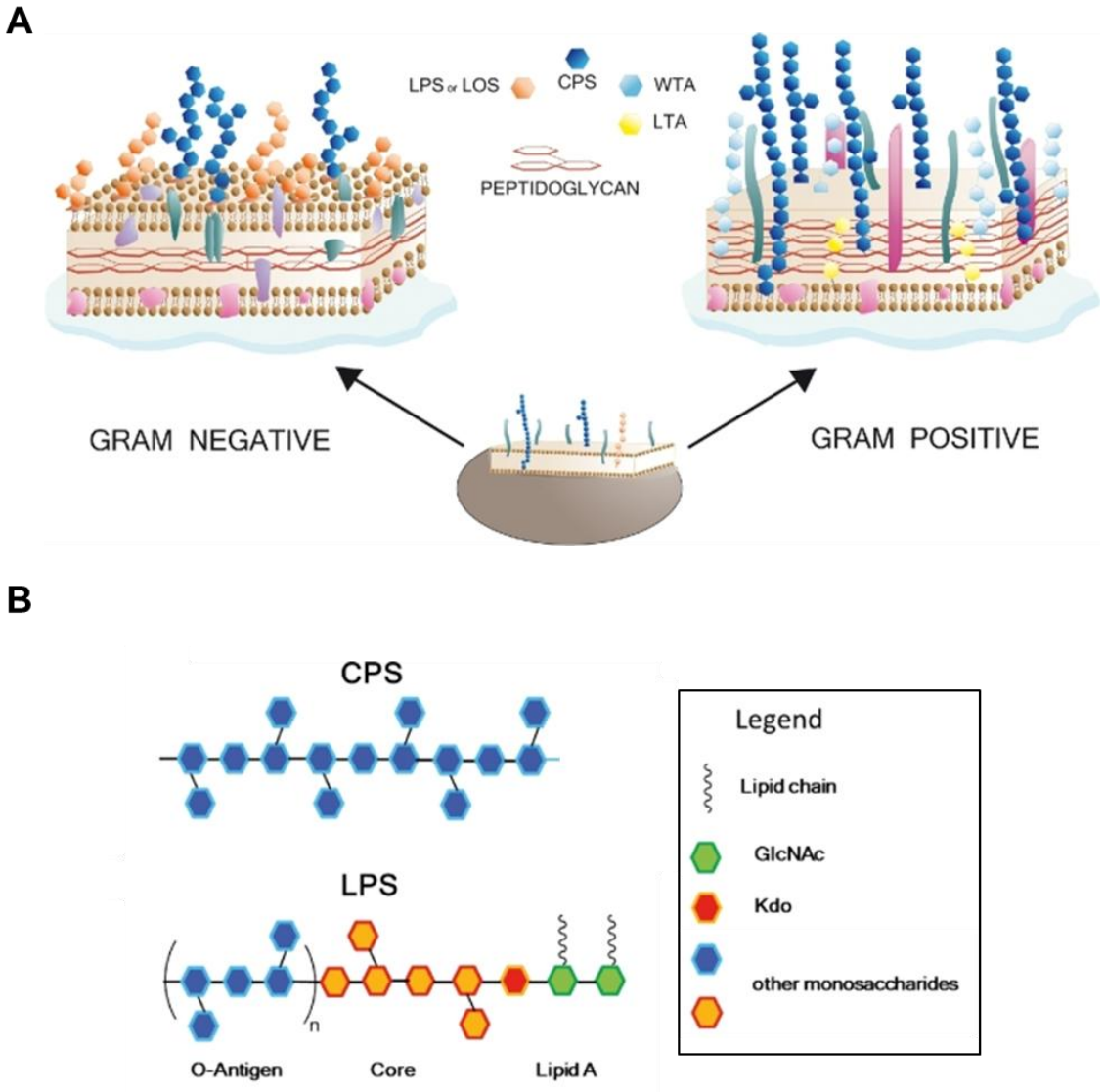

Figure 1.7. (A) Schematic representation of the cell envelope of Gram-negative and Gram-positive bacteria. (B) General structures of bacterial CPS and LPS. *Adapted from* [47].

Surface polysaccharides are critical for multiple reasons. They facilitate bacterial adhesion and host cell infection, protect bacteria by interfering with the host's innate immune mechanisms (for example, by preventing the activation of the alternative complement pathway or by mimicking host self-antigens), and confer a hydrophilic character that helps to prevent desiccation [48-50].

Bacterial carbohydrates have proven to be optimal targets for vaccine development against encapsulated microorganisms [51, 52]. The protective role of antibodies induced by pneumococcal polysaccharides was first examined in the 1930s, and by 1945 the first vaccine composed of purified pneumococcal polysaccharides from selected serotypes was tested in humans [53]. The introduction of antibiotics to treat bacterial infections temporarily slowed vaccine research; however, the rise of drug-resistant strains renewed the interest in vaccines, leading to extensive clinical studies. Consequently, polysaccharide-based vaccines against pneumococcus, meningococcus, and *Haemophilus influenzae* type b were licensed between the 1970s and early 1980s [54, 55].

Due to their T-cell independent nature, these early vaccines effectively protect adults but fall short in eliciting immunological memory or long-lived antibody responses and provide insufficient protection in infants and children under two years of age [56-59].

This limitation is overcome by conjugating—through covalent linkage—the polysaccharide to a carrier protein, which induces a T-cell-dependent immune response to the carbohydrate moiety [52, 60], thereby ensuring effective immunization in both children and the elderly. In the late 1980s, the first glycoconjugate vaccines were licensed [51, 52]. To this day, glycoconjugate vaccines remain among the safest and most successful vaccines ever developed. They represent a breakthrough in vaccinology; for approximately 35 years, they have effectively protected infants, adolescents, and adults from numerous bacterial diseases, as evidenced by dramatic reductions in infections caused by *S. pneumoniae*, *H. influenzae* type b (Hib), and *N. meningitidis* [61-63]. The glycoconjugate vaccines have also achieved significant market success; for example, Pfizer's 13-valent pneumococcal vaccine PCV13 (Prevnar 13) generated USD 6 billion in sales in 2019, making it the company's best-selling individual product [64].

In terms of mechanism of action (**Figure 1.8**), in these vaccines the saccharide moiety supplies the B cell epitopes for recognition, while the protein component offers the T cell epitopes crucial for recruiting effective T-cell help [59]. After immunization, dendritic cells at the injection site capture the conjugate vaccine and transport it to lymph nodes and the spleen within a few days, where the formation of germinal centers (GCs) is initiated. The conjugate is internalized by B cells, through polysaccharide recognition from B cell receptors, and internally processed. The peptide fragments derived from protein processing are presented through MHCII on the B-cell to CD4+ T cells. In

addition to this crucial antigen presentation, co-stimulatory signals are required to fully activate T-cell help for B cells [65, 66]. With T-cell help, B cells undergo proliferation, class switching and differentiation in plasma cells and memory cells, that can rapidly respond to future antigen encounters by producing high levels of antibodies [65, 67-70]. Furthermore, affinity maturation within germinal centers enhances antibody avidity [71].

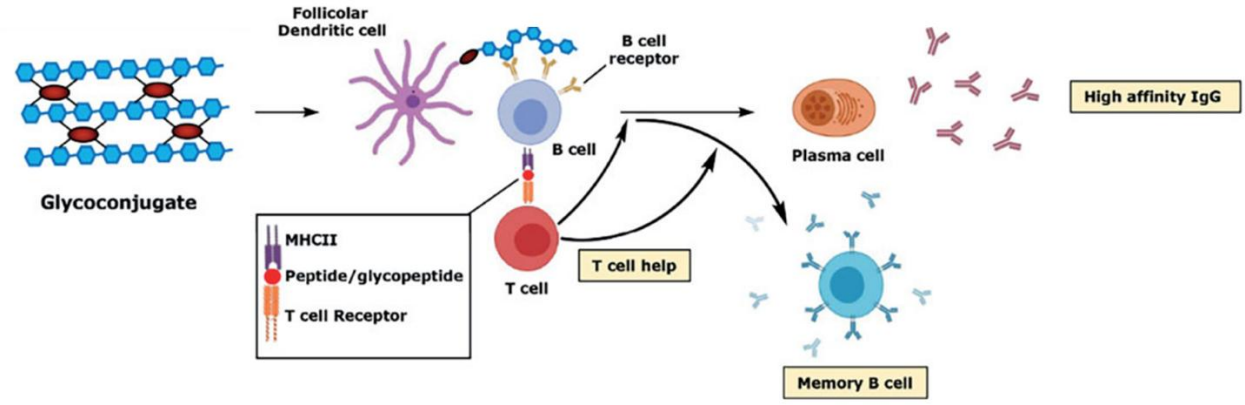

Figure 1.8. Schematic representation of immunological mechanism of action traditionally proposed for glycoconjugate vaccines. *Adapted from* [48].

The glycoconjugate vaccines licensed so far have predominantly been derived from CPS or their fragments (**Figure 1.7(B)**). However, many pathogenic bacteria also express other carbohydrates that may serve as vaccine targets, especially when a pathogen either lacks a capsule (e.g., most *Shigella* species or *Vibrio cholerae*) or produces a capsule that mimics self-antigens (e.g., the α-(2→8) polysialic acid capsule of *Neisseria meningitidis* serogroup B and the polyhyaluronic acid capsule of Group A *Streptococcus*) [47]. In these cases, other glycan structures, such as the OAg of LPS molecules in Gram-negative bacteria (**Figure 1.7(B)**) may be sufficiently exposed to the immune system to be considered as vaccine candidates. Notable examples include targets in *V. cholerae* [72], *Shigella* species [73], *Escherichia coli* [74], and *Salmonella* (Paratyphi A and non-typhoidal) infections [75].

1.4. Alternative carbohydrate-based vaccine technologies: the GMMA platform

Glycoconjugate vaccines were introduced to address the limited protection offered by plain polysaccharide vaccines. Although these vaccines are successful, many diseases still lack effective control. Given the diverse array of glycan antigens found on the surfaces of pathogens for which no vaccines currently exist, carbohydrate-based vaccines are expected to be multivalent formulations, to include multiple antigens from one or more pathogens [75-78]. This is often necessary to achieve broad protection. Moreover, the increasingly widespread use of glycoconjugate vaccines, which commonly rely on a limited repertoire of carrier proteins [79] and involve complex immunization schedules, has sometimes led to suboptimal immunogenic responses to the polysaccharide component. This reduction in efficacy is attributed to pre-existing immunity against the carrier protein, a phenomenon known as carrier-induced epitopic suppression (CIES) [80]. Consequently, there is a need for next-generation vaccines that utilize alternative carriers and technologies, offer simplified formulations and require a lower number of vaccinations to provide protection [60].

In recent years, novel polysaccharide-based platforms have emerged. Conjugates can be directly expressed in *E. coli*, through a process called bioconjugation, or alternative protein delivery systems have been proposed such as Generalized Modules for Membrane Antigens (GMMA), a technology platform based on Outer Membrane Vesicles (OMVs) from Gram-negative bacteria [60, 81].

OMVs are naturally shed by Gram-negative bacteria as membrane blebs, typically ranging in size from 20 to 200 nm [82-84]. These vesicles can have several different roles in the physiology of bacteria releasing them, all aimed at increasing the bacterial fitness in their growing environment. They may aid in biofilm formation and act as decoys, allowing bacteria to evade host immune responses, antibiotics, antimicrobial agents, and bacteriophages. Additionally, OMVs can function as long-distance carriers for toxins, virulence factors, and proteins essential for bacterial growth and survival. In some cases, their release is simply the result of an imbalance between bacterial growth and outer membrane production [82-84].

OMVs have long been considered attractive for vaccine design [82-86], as they are natural subunits of bacterial pathogens that display multiple surface-exposed antigens in their native conformation and orientation [86]. Moreover, OMVs contain pathogen-associated molecular patterns (PAMPs) such as LPS, peptidoglycans, lipoproteins, and flagella. These not only serve as antigens but also stimulate the innate immune system, thereby inducing robust immune responses [82-84, 87-90].

OMV size also facilitates efficient uptake by antigen-presenting cells (APCs), which in turn triggers the T-cell responses necessary for effective immunity [82-84, 91-94].

OMVs have been extensively studied as vaccine components in both preclinical and clinical research. They have been used in human vaccines against *Neisseria meningitidis* serogroup B (MenB) [82-84, 94-97]. Although MenB strains naturally shed OMVs, vaccine production has typically relied on detergent extraction to increase the yield. This process significantly removes LPS and lipoproteins, enhancing vaccine tolerability but also potentially eliminating important antigens such as the lipoprotein factor H binding protein (fHbp) [95-98].

Alternatively, detergent-free methods—such as sonication, vortexing, or chemical treatments—can improve OMV yields while preserving PAMPs, though these techniques require careful purification to avoid contamination with cytoplasmic components [82-86].

To streamline purification and further enhance OMV yields, the GMMA technology platform has been developed [86, 99, 100].

GMMA are OMVs naturally released by Gram-negative bacteria that have been genetically engineered to enhance blebbing [81, 100, 101]. This engineering is typically achieved by disrupting the connection between the outer membrane and the peptidoglycan layer in the periplasm, allowing GMMA to be collected from the bacterial culture supernatant using simple and cost-effective purification methods [99, 102]. Because GMMA retain their native surface lipoproteins, LPS, and other PAMPs—contrary to OMVs obtained via detergent or mechanical extraction—this can pose challenges for vaccine design due to the inherent reactogenicity of the native LPS. To mitigate this, additional genetic modifications are introduced to reduce LPS activity (e.g. by modifying the Lipid A structure) without losing its immunostimulatory properties, a process known as GMMA detoxification [103, 104]. These modifications are crucial because LPS is a potent agonist of Toll-like Receptor 4 (TLR4), which is expressed on various immune cells including APCs [87-89]. Traditionally, to potentially further enhance tolerability, GMMA are also adsorbed onto Alum adjuvant [105-107].

Regarding their mode of action in animal studies, it has been demonstrated that the immunogenicity of GMMA is independent of the TLR2 agonists present in the vesicles (such as lipoproteins and peptidoglycans), but is partially dependent on TLR4 engagement (and thus on LPS). More importantly, GMMA primarily induce immune responses through antigen presentation by follicular dendritic cells to cognate B cells, a critical process for generating germinal centers that drive the differentiation of B cells into antibody-secreting plasma cells or memory B cells [108].

Bacteria engineered to produce detoxified GMMA can further be modified to create tailored vaccines [60, 81, 109]. For instance, bacterial strains can be altered to:

(1) Overexpress selected homologous vaccine antigens or multiple variants of a protective antigen.

(2) Retain and display secreted vaccine antigens on the surface.

(3) Delete unwanted antigens that might negatively affect the induction of an effective immune response.

(4) Display heterologous antigens, like proteins or polysaccharides, from diverse (even phylogenetically distant) pathogens such as viruses, bacteria, or parasites.

By applying these modifications, it is possible to produce a "fit-for-purpose" GMMA tailored to the target vaccine (**Figure 1.9**).

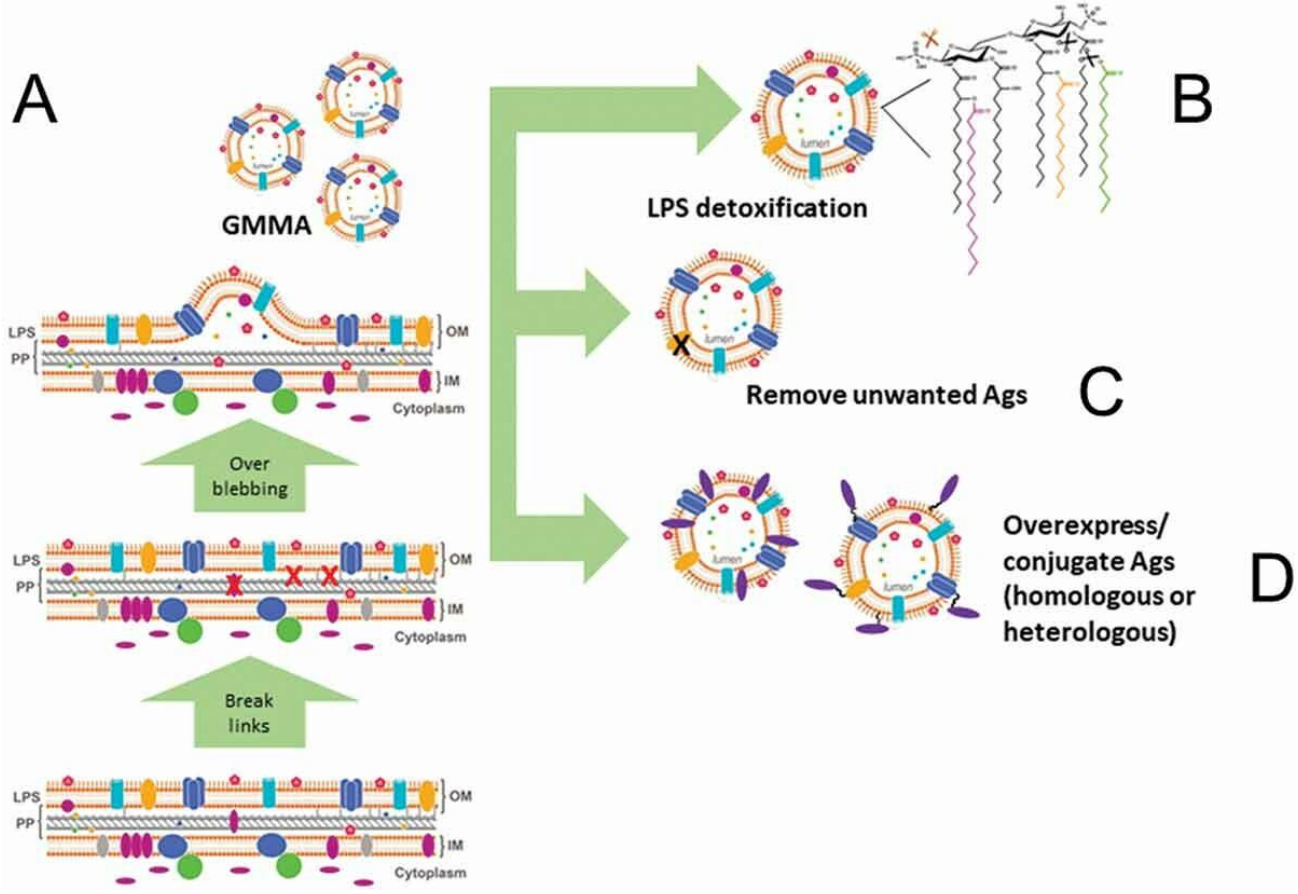

Figure 1.9. Features of GMMA technology. *Reproduced from* [81].

Due to its straightforward manufacturing process, the GMMA platform is particularly attractive for developing affordable vaccines for impoverished countries [81, 110, 111]. Indeed, GMMA-based vaccines have been applied for pathogens causing substantial disease burdens in LMICs, such as

invasive non-typhoidal *Salmonella* (iNTS) [112], *Neisseria meningitidis* [113], and *Shigella* [78, 101].

The first GMMA-based vaccine to enter clinical development was the monovalent *Shigella sonnei* GMMA vaccine (1790GAHB), which was evaluated in phase 1/2 clinical trials in adults in both non-endemic (Europe) and endemic (Kenya) regions, demonstrating good tolerability and immunogenicity [114-118]. Following these promising results, a tetravalent *Shigella* GMMA vaccine, altSonflex1-2-3, which targets *S. sonnei* and *S. flexneri* serotypes 1b, 2a, and 3a, is currently being tested in phase 2 trials among 9-month-old infants in Kenya, where shigellosis is endemic (clinical trials NCT05073003 and NCT06663436) [119]. Additionally, an iNTS-GMMA vaccine has recently completed a first-in-human randomized, dose-escalation trial, demonstrating immunogenicity and a favorable safety profile, which supports its progression to further clinical evaluations [120].

1.5. Antimicrobial resistant pathogens

According to the WHO, *Shigella* spp., *Salmonella* Typhi, and non-typhoidal *Salmonella* are among the high priority pathogens for which the development of new interventions is urgently needed to combat AMR [15].

1.5.1. *Shigella*

Shigella represents the principal bacterial pathogen causing diarrheal illness worldwide. Estimates indicate that this infection results in roughly 270 million cases and about 212,438 deaths annually, with nearly 30% of these fatalities occurring in children under age 5—especially in LMICs where access to clean water, proper nutrition, essential sanitation, and healthcare services is severely limited [121, 122]. Beyond the immediate morbidity and mortality associated with diarrhea, *Shigella* infections may also lead to long-term sequelae such as stunting and cognitive impairments in young children [123, 124]. In LMICs, the limited availability and high cost of diagnostic tests and antibiotics, coupled with WHO guidelines that recommend antibiotic treatment only in cases of dysentery, result in many children with shigellosis not receiving timely treatment. Moreover, the rising incidence of antimicrobial-resistant *Shigella* strains further complicates therapy [125-128]. These challenges underscore the urgent global health priority of developing a vaccine against *Shigella*.

The genus *Shigella* is currently classified into four species based on serological typing: *S. dysenteriae*, *S. boydii*, *S. flexneri*, and *S. sonnei* [129]. Each species is further subdivided into serotypes and subserotypes, defined by the unique saccharide repeating units (RU) present in the OAg portion of their LPS. Specifically, *S. dysenteriae* contains 14 serotypes, *S. boydii* has 19, *S. flexneri* includes 15 serotypes and subserotypes, and *S. sonnei* is represented by a single serotype [130].

The global epidemiological burden of shigellosis is predominantly linked to two species: *S. flexneri* and *S. sonnei*. Traditionally, *S. flexneri* has been associated with developing regions, while *S. sonnei* has been more common in developed areas [131-133]. Yet, emerging evidence reveals that *S. sonnei* is increasingly emerging in countries undergoing economic transition, effectively replacing *S. flexneri* as the primary cause of shigellosis [134].

Transmission of *Shigella* occurs predominantly via the fecal–oral route, either through direct person-to-person contact or through the consumption of food and water contaminated with the pathogen [135].

Several factors complicate efforts to control *Shigella* infections. The bacterium's ability to cause illness with a very low infectious dose, combined with the coexistence of multiple *Shigella* species and serotypes within the same communities, facilitates frequent reinfections. Additionally, treatment is further complicated by the need for antibiotic administration (beyond standard oral rehydration), a factor that contributes to the development of multidrug-resistant strains and threatens the availability of effective and affordable treatments. This situation underscores the critical importance of preventive strategies [136, 137].

To date, there are no widely available vaccines against *Shigella*, although various vaccine candidates aiming for broad protection are under clinical evaluation [138]. Because immunity to *Shigella* appears to be serotype-specific, the OAg has emerged as the main target for vaccine development [139].

In terms of structural diversity, all *S. flexneri* serotypes, excluding serotype 6, share a linear tetrasaccharide OAg repeating unit described as [2)-α-L-Rha*p*^{III}-(1→2)-α-L-Rha*p*^{II}-(1→3)-α-L-Rha*p*^{I}-(1→3)-β-D-Glc*p*NAc-(1→]$_n$, which can be variably modified by O-acetylation and/or glucosylation. In contrast, *S. flexneri* serotype 6 has a different linear polysaccharide backbone, [2)-α-L-Rha*p*^{III}-(1→2)-α-L-Rha*p*^{II}-(1→4)-β-D-Gal*p*A-(1→3)-β-D-Gal*p*NAc-(1→]$_n$ with the first rhamnose^{III} residue variably O-acetylated at either position 3 or 4 [140-142]. The OAg of *S. sonnei* differs considerably, consisting of the following repeating unit [4)-α-L-AltNAcA-(1→3)-β-FucNAc4N-(1→]$_n$ [143].

Given the considerable structural heterogeneity of the OAg across various *Shigella* species and serotypes, a multivalent vaccine approach is crucial to maximize coverage [139, 144-146], further complicating the overall design of a broadly effective vaccine [147].

Based on global epidemiological data, the most advanced *Shigella* vaccine candidates utilize a 4-valent formulation. This formulation typically comprises *S. flexneri* serotypes 2a, 3a, and either 6 or 1b, in conjunction with *S. sonnei* [148, 149]. Such a 4-valent vaccine is estimated to cover approximately 70% of *Shigella* cases, with the potential to extend coverage beyond 85% through cross-reactivity among common epitopes of the *S. flexneri* OAg [73, 149]. Although structural similarities among *S. flexneri* serotypes can elicit cross-reactive immune responses, the specific structural features that mediate this cross-reactivity remain to be fully elucidated [148, 150].

In this regard, the GSK Vaccines Institute for Global Health (GVGH) has proposed the use of GMMA for delivering OAg. The approach involves a four-valent formulation (named altSonflex1-2-3) that combines GMMA derived from *S. sonnei* with those from *S. flexneri* serotypes 1b, 2a, and 3a [78, 148]. After having demonstrated its safety and ability to elicit a functional OAg specific IgG response

in European adults [119], this candidate is currently being evaluated in phase 2 clinical trials in 9-month-old infants in Kenya, a region where shigellosis is endemic (clinical trials NCT05073003 and NCT06663436).

1.5.2. *Salmonella*

Salmonella is a facultative anaerobic Gram-negative bacterium of the *Enterobacteriaceae* family. The organisms that cause human disease are classified into typhoidal and non-typhoidal forms. In high-income countries, non-typhoidal *Salmonella* (NTS)—predominantly the serovars *S.* Typhimurium and *S.* Enteritidis—typically causes self-limiting gastroenteritis [151]. When these bacteria overcome the gastric acid barrier and enter the intestinal epithelium, they trigger inflammation that results in diarrhea, mucosal ulceration, and cell destruction [152]. However, in sub-Saharan Africa, NTS infections in children under five frequently lead to bloodstream infections, known as invasive NTS (iNTS) disease, with case fatality rates as high as 15% [153]. The same serovars are also implicated in a significant global burden of diarrheagenic NTS (dNTS) disease [154].

Typhoid fever, caused by *S.* Typhi, is the most prevalent form of bacterial bloodstream infection in South and Southeast Asia [155, 156]. Transmitted via the fecal–oral route, its clinical presentation varies, but fever is the most consistent symptom. Other reported features include constipation or diarrhea, headache, dry cough, abdominal pain, malaise, anorexia, and vomiting [157]. In the same region, *S.* Paratyphi A causes paratyphoid A fever, a condition clinically indistinguishable from typhoid fever, that accounts for over 25% of enteric fever cases [154].

According to the Global Burden of Disease (GBD) 2019 estimates, typhoid fever is responsible for 40% of all *Salmonella*-related deaths, but only 17% of these occur in children under five. In contrast, iNTS disease accounts for 29% of total *Salmonella* deaths and 45% of deaths in children under five, while dNTS and paratyphoid fever are responsible for 22% (36% in children under five) and 9% (2% in children under five) of deaths, respectively [154].

All four major *Salmonella* serovars are also associated with high levels of AMR [158-160], rendering treatment with current antibiotics increasingly unsuccessful and reinforcing the need for a vaccine-based strategy [15].

Salmonella enterica serovars Typhi, Typhimurium, Enteritidis, and Paratyphi A are differentiated by their OAg, flagellin H-antigen, and the presence or absence of a Vi capsular polysaccharide. Vi is a linear polymer made up of (α1-4)-2-deoxy-2-*N*-acetyl galacturonic acid units, with variable O-acetylation at the C-3 position [161].

Only *S.* Typhi display Vi polysaccharide; thus, Vi-based vaccines do not protect against the other three predominant serovars [75]. While licensed vaccines are available for *S.* Typhi [162, 163], there are currently no approved vaccines for NTS or *S.* Paratyphi A [75]. Except for *S.* Typhi, since immunity against *Salmonella* appears to be serotype-specific, the OAg is recognized as a key antigenic target [164-166], which supports the development of several candidate vaccines targeting this component [75].

The *Salmonella* OAg share a common trisaccharide backbone of α-D-Man(1→4)-α-L-Rha-(1→3)-α-D-Gal-(1→2)), but differ by the attached 3,6-dideoxy monosaccharide to mannose: abequose in *S.* Typhimurium, tyvelose in *S.* Enteritidis, and paratose in *S.* Paratyphi A. Glucose can be found as branched to galactose [167, 168]. The dideoxyhexoses confer *Salmonella* serogroup specificity [169-171]. Moreover, *Salmonella* OAg could show high levels of heterogeneity in terms of chain length and variation in O-acetylation and glucosylation of the repeating units [167, 168, 172-175].

There is a strong rationale for developing *Salmonella* multivalent vaccines to address the antigenic diversity among the several serovars responsible for invasive disease and to overcome the limitations of monovalent formulations in areas where multiple serovars co-circulate, thereby enhancing broad-spectrum protective efficacy [75]. A vaccine comprising these four serovars of *S. enterica* could potentially avoid approximately 274,000 overall deaths (including 111,000 in children under five) and reduce the burden by roughly 20 million disability-adjusted life-years (DALYs), including 9.7 million in children under five [75].

Among the multivalent candidates, a bivalent formulation utilizing GMMA as the delivery system for the OAg of *S.* Typhimurium and *S.* Enteritidis—known as iNTS-GMMA—has been proposed by GVGH. This candidate recently completed a first-in-human, randomized, dose-escalation trial that demonstrated both robust immunogenicity and a favorable safety profile [120, 176, 177]. In addition, GVGH is advancing a trivalent formulation (iNTS-TCV) by combining iNTS-GMMA with the WHO-prequalified typhoid glycoconjugate vaccine TYPHIBEV (by Biological E Ltd., Hyderabad, India) to provide protection against both typhoid fever and iNTS. The iNTS-TCV candidate is currently undergoing Phase 1/2 studies in both non-endemic and endemic populations [177]. Moreover, in collaboration with Biological E, a bivalent glycoconjugate vaccine combining TYPHIBEV with a *S.* Paratyphi A glycoconjugate vaccine [178] is set to progress into phase 2 trials [179].

1.6. Multivalent vaccines: tackling single or multiple pathogens for broad protection

Multivalent vaccines contain antigens from two or more different strains or variants of the same pathogen, or even from multiple pathogens, to provide broader protection than a monovalent vaccine. Also known as combination or multicomponent vaccines, they are designed to mimic the natural exposure of the immune system to multiple antigens, achieving a comprehensive immune response with a single formulation [180-182].

There are clear advantages of using multivalent vaccines versus administering monovalent vaccines separately (**Table 1.1**). Combining several antigens into a single formulation can simplify vaccination schedules, reduce the number of injections, and ultimately increase patient compliance. This is particularly valuable in resource-limited settings, where reducing logistical challenges and the frequency of immunization visits can alleviate strain on healthcare facilities and enhance overall vaccination coverage [183, 184]. Fewer injections also mean less pain and discomfort, a significant benefit for individuals with needle phobia. Furthermore, combination vaccines may transform interventions with low standalone uptake into more impactful measures, especially when targeting related pathogens contributing to similar clinical syndromes (e.g., multiple enteric pathogens that together drive linear growth faltering and stunting) [180].

Despite these advantages, multivalent vaccines also present important challenges. Ensuring that the co-administration of multiple antigens does not compromise the immune response to each single component is a key concern. Immunological interference—where the response to one antigen affects another—must be addressed through rigorous preclinical and clinical studies to demonstrate non-inferiority and acceptable reactogenicity compared with monovalent formulations [185]. Beyond immunological concerns, the production process itself is more complex as individual antigens must be produced according to their specific quality control standards before being combined [186]. This means that any production issue with one antigen can delay, or even interrupt, the entire manufacturing process. Additionally, regulatory pathways originally designed for single-antigen vaccines require adaptation for combination products, further complicating licensure [180, 181].

Examples of successful licensed multivalent vaccines include pneumococcal conjugate vaccines [187, 188] and multivalent meningococcal vaccines [189-193].

.

Table 1.1. Potential value of a combination vaccine versus coadministration of separate antigens. *Adapted from* [180].

	Potential advantages	Potential challenges
Vaccine delivery	• Improved timing of vaccination and increased acceptability among end users and health-care providers. • Higher and more equitable vaccination coverage.	• Need to ensure compatibility of vaccination schedules and routes of administration of each component.
Health impact	• Greater, more equitable impact. • Facilitates targeting less prevalent but still important pathogens. • Creates the opportunity for a syndromic combination—i.e., a single vaccine targeting pathogens responsible for the same clinical syndrome.	• Need to articulate and show incremental health and economic value of overall combination compared with stand-alone components. • Increased difficulty in attributing a safety signal to a specific component.
Vaccine administration efficiency and cost	• Fewer syringes. • Fewer packaging disposal needs. • Less cold chain storage and transportation space required. • Shorter administration time and errors. • Fewer needlestick injuries and therefore improved safety for vaccinators.	• The overall procurement cost could be higher compared to the total cost of buying the component vaccines separately, even if delivery expenses are lower. • The available combination might include more antigens than some countries prefer to introduce.

Vaccine design, development, and supply	• Potentially greater demand for combination than individual components, leading to economies of scale and reduced cost of goods.	• Currently little guidance or recommendations from the public health community regarding combination composition or use preference. • Greater risk of failure due to immunological interference or unacceptable reactogenicity. • More complex, lengthy, and expensive clinical development pathway due to current regulatory guidelines. • Need to develop and validate additional assays to accurately characterize components within complex mixtures. • Need access to multiple components, which could pose substantial commercial and intellectual property complexities.

2. AIM OF MY PROJECT

My PhD project aimed to facilitate the development of complex multivalent polysaccharide-based vaccines, to fight bacterial infections and contribute to AMR reduction. *Shigella* and *Salmonella* PS were used as model antigens. In particular, several aspects like immunogenicity, identification and quantification of single OAg in complex mixture and vaccine stability, all crucial for the success of a vaccine, were deeply investigated.

In detail, the objectives of my PhD project were:

1. Immunological evaluation of multivalent PS-based vaccines, comparing different technologies, with focus on eventual immuno-interference among the different PS components;
2. Development of novel analytical methods to identify and quantify each PS antigen in multivalent formulations;
3. Application of advanced kinetic modelling to predict vaccine stability based on accelerated studies.

3. Comparison of GMMA and glycoconjugation technologies for a vaccine against *Shigella*

This chapter has been already published in [194].

3.1. INTRODUCTION

Shigellosis is the leading bacterial cause of diarrheal disease in LMICs, particularly affecting young children under five years of age [130, 195]. As antibiotic resistance to *Shigella* continues to rise [133, 138, 196], this pathogen has been identified as a priority for vaccine development [15]. Currently, no vaccines are licensed for *Shigella*, but various candidates are under development [73, 139], many of which are based on the O-antigen (OAg) portion of the lipopolysaccharide (LPS) [197-199], recognized as key target for protective immunity [145, 200].

GSK Vaccines Institute for Global Health (GVGH) is developing a four-component *Shigella* vaccine utilizing Generalized Modules for Membrane Antigens (GMMA) as alternative delivery system for the OAg [78, 201, 202].

GMMA are Outer Membrane Vesicles (OMVs) from Gram-negative bacteria, genetically engineered to increase yields and produced through a straightforward and robust detergent-free manufacturing process [99-101]. GMMA are nanoparticle that combine multivalent display of saccharides and proteins in their native outer membrane environment, with the presence of immunostimulatory molecules, such as LPS, lipoproteins and peptidoglycans [81, 86]. Additional mutations can be introduced to modify the lipid A component and reduce endotoxicity, to minimize GMMA's potential to promote reactogenicity [104, 201].

A mono-component *S. sonnei* GMMA vaccine candidate was initially evaluated in phase 1/2 clinical trials in healthy adults from both *Shigella* non-endemic (EU) and endemic (Kenya) regions, demonstrating immunogenicity and good tolerance [114-118]. However, the vaccine did not confer protection against shigellosis in a Controlled Human Infection Model (CHIM) study [203]. Therefore, an improved version of *S. sonnei* GMMA with increased OAg density has been designed and formulated together with GMMA from three *S. flexneri* serotypes (1b, 2a and 3a) into a four-component formulation called altSonflex1-2-3, aiming at providing broad protection against the most prevalent *Shigella* serotypes [148, 149]. The altSonflex1-2-3 vaccine is currently being tested in phase 2 clinical trials in 9-months infants in Kenya, where shigellosis is endemic (clinical trials NCT05073003 and NCT06663436) [119].

As part of my PhD project, the GMMA approach has been compared in animal models, to the more classical glycoconjugation approach for an OAg-based vaccine against *Shigella*. Indeed, conjugation of OAg to appropriate carrier proteins is a well-established approach for improving immunogenicity, providing T-cell stimulation to the OAg which contains only B-cell epitopes [204]. This leads to enhanced memory response, IgG class-switching and improved immunogenicity in both infants and adults [52, 59, 60]. A *S. sonnei* OAg glycoconjugate, developed at the U.S. National Institutes of Health (NIH) [205-207], showed 74% protection in adults after a single dose [208] but failed to protect younger individuals [205]. A well-defined *S. flexneri* 2a synthetic glycoconjugate vaccine, developed at Institut Pasteur (Paris, France) has been shown to be safe and immunogenic in a phase 1 study in adults after a single dose [209], and is now being tested in phase 2 and CHIM trials [199]. Additionally, LimmaTech Biologics produced a bioconjugate against *S. flexneri* 2a, Flexyn2a, which proved to be immunogenic in phase 1 [210] and protective against severe shigellosis in a CHIM study [198]. These findings supported the development of a four-component formulation, composed of bioconjugates of *S. sonnei* and *S. flexneri* 2a, 3a and 6, that is currently tested in an age-descending dose-finding phase 2 trial in Kenya to evaluate vaccine safety and immunogenicity [198].

Alhydrogel is a commonly used vaccine adjuvant due to its safety, low cost, and the adjuvanticity it provides to various antigens [105-107, 211]. Although formulation with this adjuvant is often used to further reduce the potential reactogenicity of GMMA [212], it has been shown that Alhydrogel does not enhance the humoral immune response induced by GMMA [213]. Here, the four-component GMMA and glycoconjugate formulations were evaluated both with and without Alhydrogel, aiming at further investigating the role that this adjuvant can have on the immune response elicited by GMMA and glycoconjugates.

The results of this work contributed to a better understanding of the potential differences between traditional glycoconjugates and GMMA as delivery systems for *Shigella* OAg.

3.2. MATERIALS AND METHODS

Preparation and characterization of GMMA

Shigella GMMA were obtained from GVGH. They were produced from the following strains: *S. sonnei* 53G ΔtolR::kan ΔvirG::nadAB ΔmsbB2::cat ΔmsbB::erm, *S. flexneri* 1b Stansfield ΔtolR::frt ΔmsbB1a::frt ΔmsbB1b::frt, *S. flexneri* 2a 2457T ΔtolR::kan, ΔmsbB::cat, and *S. flexneri* 3a 6885 ΔtolR::kan, ΔmsbB::cat, and purified as previously described [78].

Purified GMMA were characterized for total protein content by micro Bicinchoninic acid assay BCA (Thermo Scientific, Waltham, MA, USA) according to the manufacturer's instructions, total OAg amount by high-performance anion-exchange chromatography with pulsed amperometric detection (HPAEC-PAD) after performing acid hydrolysis directly on GMMA, and OAg to protein ratio was calculated. GMMA size was estimated by dynamic light scattering (DLS), OAg molecular size was determined by size exclusion-high-performance liquid chromatography (HPLC-SEC) after acetic acid extraction [214].

HPAEC-PAD of *S. flexneri* 1b, 2a and 3a OAg

To quantify the *S. flexneri* 1b, 2a, and 3a OAg on GMMA, the neutral sugars HPAEC-PAD was employed [215]. Rhamnose (Rha) was used to construct the calibration curve, while other common monosaccharides for this analysis include galactose (Gal), glucose (Glc), mannose (Man), and *N*-acetylglucosamine (GlcNAc); calibration curves were generated using commercial monomer sugars.

The GMMA samples were diluted to have the rhamnose content corresponding to the OAg within the 0.5–10 μg/mL range, and then hydrolyzed at 100 °C for 4 hours in 2 M trifluoroacetic acid (TFA). This hydrolysis condition was found to optimally release all monosaccharides constituting the repeating units of the *S. flexneri* OAg without degradation. After hydrolysis, the vial contents were evaporated to dryness using a centrifugal evaporator. Each dried sample was then re-dissolved in 450 μL of water and mixed thoroughly by vortexing. The reconstituted sample was transferred into an AcroPrep Advance 96 Filter Plate (0.2 μm, Pall, Port Washington, NY, USA), positioned over a 96 conical BTM plate (Thermo, Waltham, MA, USA), and centrifuged at 524 rcf for 2 minutes using an Allegra X-15 with an SX4750 swinging-bucket rotor and 393070 microplate carrier (Beckman-Coulter, Brea, CA, USA) to collect the filtered samples. The plate containing the filtered sample or standard solutions was then covered with a Pre-Slit Well Cap for a 96-well PP Plate (Thermo, Waltham, MA, USA) and loaded into the HPAEC-PAD autosampler compartment.

Chromatographic runs were performed on an ICS-6000, ICS-5000, or ICS-3000 system equipped with Chromeleon 7.2 (Thermo, Waltham, MA, USA) in pulsed amperometric mode, utilizing a gold working electrode and an Ag/AgCl reference electrode with a standard quad carbohydrate waveform. Separation was achieved using a Thermo CarboPac PA10 column (4 × 250 mm) with a PA10 guard column (4 × 50 mm) at a flow rate of 1 mL/min. The sugars were eluted with a gradient from 10 to 18 mM NaOH over 20 minutes, followed by a 20-minute wash with 100 mM AcONa in 28 mM NaOH and a 20-minute reequilibration with 10 mM NaOH.

Calibration curves were established for each sugar monomer in the 0.5–10 μg/mL range, with the standards undergoing the same hydrolysis and analysis as the samples. Note that GlcNAc (hydrolyzed to glucosamine, the monomer detected by HPAEC-PAD) was not used for quantification because the optimal hydrolysis conditions for GlcNAc require heating at 100 °C for 6 hours in 1 M TFA.

HPAEC-PAD of *S. sonnei* OAg

To quantify the *S. sonnei* OAg on GMMA, the amino uronic acid HPAEC-PAD method was employed [216]. A standard of *S. sonnei* OAg was used to construct the calibration curve. First, a TFA–HCl mixture was prepared by mixing TFA and HCl in a 2:13 v/v ratio in a glass bottle. Using an Eppendorf Xstream Electronic Pipettor, 1 mL of this mixture was added to 300 μL of a sample or standard solution in a 2 mL screw-capped vial. The vial was sealed and vortexed to ensure thorough mixing. The vials were then placed in a SBH130D/3 Stuart Thermoblock, equipped with three preheated SHT1 12 33 Stuart aluminum blocks, and incubated at 80 °C for 4.5 hours for hydrolysis. After cooling to room temperature, the contents were evaporated to dryness under a nitrogen flush using a Techne sample concentrator FSC400D with PTFE-coated needles (FSC4NCS). The dried residue in each vial was reconstituted in 300 μL of water and mixed thoroughly by vortexing. Next, the reconstituted solutions were transferred into a 0.2 μm filtration 96-well plate placed over a 96-conical BTM plate, then centrifuged at 524 rcf for 1 minute using a Beckmann Allegra X-15 with an SX4750 swinging-bucket rotor and a 393070 microplate carrier to collect the filtered samples. The plate containing the filtered sample and standard solutions was covered with a preslit 96-well cap and loaded into the HPAEC-PAD autosampler compartment.

Chromatographic runs were performed on an ICS-6000, ICS-5000, or ICS-3000 system equipped with Chromeleon 7.2 (Thermo, Waltham, MA, USA) in pulsed amperometric mode, utilizing a gold working electrode and an Ag/AgCl reference electrode with a standard quad carbohydrate waveform. A Thermo CarboPac PA1 analytical column (4 × 250 mm) equipped with a Thermo CarboPac PA1 guard column (4 × 50 mm) was used. The column and detector compartments were maintained at 25

°C, while the sample compartment was kept at 10 °C. Before analysis, a system suitability test was conducted by injecting a solution of glucuronic acid and galacturonic acid (5 µg/mL each) three times to check the plate count and peak asymmetry. Chromatographic conditions included a 25 µL injection volume, a total run time of 15 minutes, and isocratic elution with 400 mM NaOH at a flow rate of 1.5 mL/min without an intervening washing step. After the analysis, the column was washed with 500 mM NaOH at a flow rate of 1 mL/min for 20 minutes and then stored in 200 mM NaOH.

Calibration curves were constructed for the *S. sonnei* OAg repeating unit in the 0.16–2.56 µg/mL range, with the standards undergoing the same hydrolysis and analysis procedures as the samples.

DLS

The mean hydrodynamic (Z-average) diameter and the polydispersity index (PDI) of GMMA were determined. The analysis was carried out on a Zetasizer Nano ZS (Malvern Panalytical, UK) under the following conditions: the measurement type was set to "Size," with the "Material" defined as "Protein" and the "Dispersant" being the buffer in which the sample was diluted. The "General options" used the default Mark-Houwink parameters, while the temperature was maintained at 25 °C with an equilibration time of 120 seconds. Measurements were taken at a 173° backscatter angle (NIBS default) with an automatic measurement duration, performing three measurements with a 30-second delay between each. Data processing was executed using the General Purpose analysis model (normal resolution).

HPLC-SEC of extracted OAg from GMMA

GMMA treatment at low pH and high temperature resulted in the cleavage of the labile bond between 3-Deoxy-D-manno-oct-2-ulosonic acid (KDO), located at the proximal end of the core oligosaccharide, and lipid A. This process released the OAg-core chains or the core alone into the supernatant, while causing GMMA proteins and lipids to precipitate. The extracted sugars reflected the composition of the LPS molecules on GMMA. Hydrolysis was performed in 1% acetic acid, at 100 °C for 2 hours. The entire content of the vial was then transferred to an Eppendorf tube and centrifuged at 14,000 × g for 30 minutes. The supernatant, which contained the extracted OAg, was recovered and dried for further analysis without any desalting step.

OAg samples were subsequently analyzed by HPLC-SEC using a Waters Acquity UPLC H-Class PLUS Bio System. They were diluted with water to a concentration of 100–200 µg/mL OAg. A refractive index detector was used to estimate their apparent molecular size. Calibration was performed using dextrans in the range 5–150 kDa with a Gel Permeation Chromatography (GPC)

software, performing a linear regression between log(MW) and retention time. Data are reported as Mp (the mode of the molecular weight distribution). The analysis employed a TSK gel G3000 PWXL column connected in series with a TSK gel PWXL guard column (Tosoh, King of Prussia, PA, USA), with the column compartment set at 30 °C and the autosampler compartment at 4 °C. The samples and standards were injected with 80 µL volume at a flow rate of 0.5 mL/min over a 35-minute run under isocratic conditions, using an eluent composed of 0.1 M NaCl, 0.1 M NaH_2PO_4, 5% ACN at pH 7.2. After the final chromatographic run, the system was stored in a 0.02% NaN_3 preservative solution.

Preparation and characterization of glycoconjugates

Purified OAg, extracted from *S. sonnei* (S. sonnei 53G ΔtolR::kan ΔvirG::nadAB), *S. flexneri* 1b (strain *S. flexneri* 1b Stansfield ΔtolR::frt ΔmsbB1a::frt ΔmsbB1b::frt), 2a (strain *S. flexneri* 2a 2457T ΔtolR::kan, ΔmsbB::cat), 3a (strain *S. flexneri* 3a 6885 ΔtolR::kan) GMMA, were obtained from GVGH [217].

The OAg were independently activated with 1-cyano-4-dimethylaminopyridine tetrafluoroborate (CDAP) using the following procedure [218]: 100 mg/mL CDAP in acetonitrile was added to 9 mg/mL OAg in 2M NaCl to reach a final 1.5:1 weight ratio CDAP/OAg. Soon after, 0.3M NaOH was added to reach pH 9. After 3 minutes, CRM_{197} was added to the solution in a CRM_{197}/OAg 1:1 weight ratio with final concentration of 5 mg/mL. The reaction was mixed for 2 h at room temperature maintaining the pH at 9 by adding 0.3 M NaOH. At the end, 2M glycine at pH 9 was added in a weigth ratio of 7.5:1 glycine/OAg to quench the reaction. The solution was mildly mixed over night at room temperature.

S. sonnei OAg conjugate was purified by size exclusion chromatography on a 1.6 cm x 60 cm Sephacryl S-300 column (Cytiva Life Sciences, Marlborough, MA, USA; formerly GE Healthcare Life Sciences) eluted at 0.5 mL/min in Phosphate Buffer Saline (PBS). Fractions at higher molecular weight that did not overlap with free OAg and free CRM_{197} were collected. *S flexneri* OAg conjugates were purified by hydrophobic interaction chromatography (HIC) on a Phenyl HP column (Cytiva Life Sciences, Marlborough, MA, USA; formerly GE Healthcare Life Sciences), loaded in 20mM NaH_2PO_4 3M NaCl at pH 7.2. The purified conjugates were eluted in 20mM NaH_2PO_4 at pH 7.2 and the collected fractions were exhanged against PBS by Amicon Ultra (Merck, Darmstadt, Germany) 30 kDa cut-off.

Purified conjugates were characterized by micro BCA and HPAEC-PAD [215, 216]—using the same methods reported above for GMMA samples—for total protein and total OAg content respectively,

and the OAg to protein ratio was calculated. Free polysaccharide was separated through reverse phase-solid phase extraction (SPE) using Vydac C4 SPE cartridges and quantified by HPAEC-PAD [219]. Conjugates formation was verified by HPLC-SEC, comparing the conjugates with unconjugated CRM_{197} [220].

Free saccharide quantification via SPE

One mL of each conjugate, diluted to 100 µg/mL (protein based) in 5 mM sodium phosphate (pH 7.2) containing 150 mM NaCl and 0.005% Tween 20, was loaded onto a C4 solid-phase extraction disposable column (Vydac Bioselect C4, 100 mg/3 mL, Grace, Columbia, MD, USA). The solution was eluted by applying positive air pressure over the liquid phase, and the flow-through was collected. Then, 1 mL of 20% ACN in water with 0.05% TFA was applied to the cartridge to maximize the recovery of free OAg, and the resulting eluate was combined with the initial flow-through. The total 2 mL volume was dried using a centrifugal evaporator and subsequently resuspended in an appropriate volume of water for quantifying the free saccharide by HPAEC-PAD, using the methods described above for GMMA samples.

HPLC-SEC of the conjugates

Conjugates were analyzed via HPLC-SEC with an 80 µL injection on a Waters Acquity UPLC H-Class PLUS Bio System. The analysis used a Tosoh TSKgel 5000 PW column (King of Prussia, PA, USA) connected in series with a Tosoh TSKgel PW guard column and an eluent composed of 0.1 M NaCl, 0.1 M NaH_2PO_4, 5% ACN at pH 7.2, with a flow rate of 0.5 mL/min. The column compartment was maintained at 30 °C while the autosampler compartment was kept at 4 °C. Molecular weight determination was carried out in a refractive index detector, using a dextran MW standard calibration curve (standards at 50, 80, 150, 270, 410, and 670 KDa, Sigma-Aldrich) by performing a linear regression between log(MW) and retention time. Data were reported as Mp, the mode of the molecular weight distribution.

GMMA and glycoconjugates formulation

Formulations and related activities were performed under a sterile hood in aseptic conditions.

Four-component GMMA with Alhydrogel formulation was prepared by adsorbing *S. sonnei* and *S. flexneri* 1b, 2a and 3a GMMA in NaCl 154 mM NaH_2PO_4 10 mM pH 6.5 on 0.7 mg/mL (Al^{3+}) Alhydrogel at the final concentration of 120 µg/mL total OAg (30 µg/mL each OAg). Further dilutions for immunogenicity studies were performed with Alhydrogel diluent (0.7 mg/mL Al^{3+} in NaCl 154 mM NaH_2PO_4 10 mM pH 6.5). Four-component GMMA without Alhydrogel formulation

was prepared by diluting *S. sonnei* and *S. flexneri* 1b, 2a and 3a GMMA in NaCl 154 mM NaH_2PO_4 10 mM pH 6.5 at the final concentration of 12 µg/mL total OAg (3 µg/mL each OAg). Further dilutions were performed with NaCl 154 mM NaH_2PO_4 10 mM pH 6.5.

S. sonnei and *S. flexneri* 1b, 2a and 3a glycoconjugates were first diluted in NaCl 154 mM at the final concentration of 12 µg/mL total OAg (3 µg/mL each OAg). Further dilutions were performed with NaCl 154 mM (formulations without Alhydrogel) or 0.7 mg/mL Al^{3+} in NaCl 154 mM (formulations with Alhydrogel).

***In-vivo* Studies**

Mouse and rabbit studies were performed at the GSK Animal Facility (Siena, Italy), in compliance with the relevant legislation (Italian D.Lgs. n. 26/2014 and European Directive 2010/63/UE) and the institutional animal welfare policies of GSK. The facility is AAALAC-accredited. The animal protocols were approved by the Italian Ministry of Health (project No. 1140/2020-PR, approval date 18/11/2020).

GSK is committed to the Replacement, Reduction and Refinement of animal studies (3Rs). Non-animal models and alternative technologies are part of our strategy and employed where possible. When animals are required, application of robust study design principles and peer review minimises animal use, reduces harm and improves benefit in studies.

Female, 5 weeks old CD1 mice (8 per group) were vaccinated intraperitoneally (i.p.) with 200 µL of formulated antigens at study day 0 and 28. Approximately 100 µL bleeds (50 µL serum) were collected at day -1 (pooled sera) and at day 27 (individual sera), with final bleed at day 42 (**Figure 3.1(A)**).

Female New Zealand White rabbits Crl:KBL(NZW) (8 per group) were vaccinated intramuscularly (i.m.) with 500 µL of formulated antigens at study day 0 and 28 or 0 and 84. Sera were collected on study days -1 (pooled), 27, 42, 83 (all animals) and 98 (animals who only received immunization at day 84) (**Figure 3.1(B,C)**). Maximum volume of blood was sampled according to animal welfare's good practices.

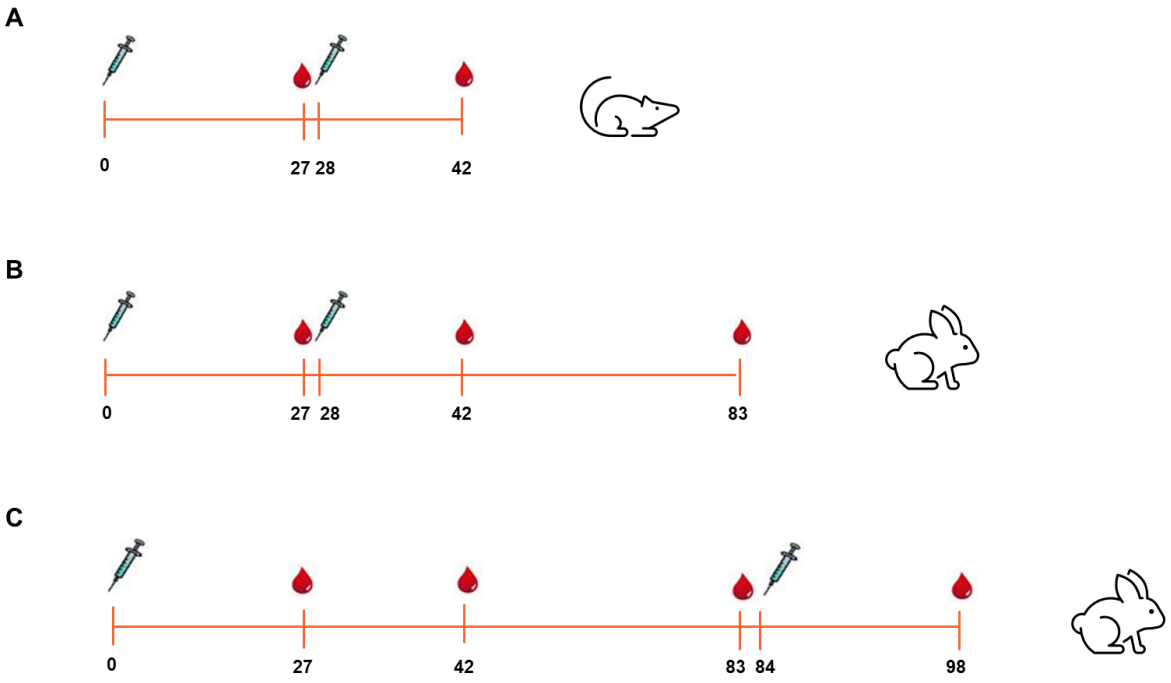

Figure 3.1. Immunization schemes used for studies in mice (A) and rabbits (B,C).

Sera analyses

ELISA

Sera collected at different time points were analysed by enzyme-linked immunosorbent assay (ELISA). ELISA plates were coated, over night at 2–8°C, as follow: *S. sonnei* LPS at the concentration of 0.5 µg/mL in PBS, *S. flexneri* 1b OAg at the concentration of 2 µg/mL in Carbonate Buffer, *S. flexneri* 2a OAg at the concentration of 5 µg/mL in Carbonate Buffer, *S. flexneri* 3a OAg at the concentration of 1 µg/mL in PBS.

Plates were blocked 1 h at 25°C with PBS milk 5% and subsequently incubated for 2 h at 25°C with the sera diluted 1:100, 1:4,000 and 1:160,000 in PBS-Tween 0.05% 0.1% BSA (for mouse sera) or PBS milk 5% (for rabbit sera). Bound antibodies were then detected after 1 h incubation at 25°C with an enzyme-labelled secondary antibody (anti-mouse or anti-rabbit IgG-alkaline phosphatase, anti-mouse IgG1, IgG2a, IgG2b, IgG3 or IgM-alkaline phosphatase) in PBS-Tween 0.05% 0.1% BSA.

The presence of immunoreacting anti-*S. sonnei* LPS / *S. flexneri* 1b, 2a, 3a OAg antibodies was detected, after 1 h incubation at 25°C with p-nitrophenyl phosphate substrate (Sigma-Aldrich) solution, through formation of a yellow color detected by absorbance at 405 nm subtracted by the

absorbance at 490 nm. The samples were tested in comparison to calibrated mouse or rabbit anti-antigens specific reference standard sera using a sigmoidal five parameter logistic (5 PL) interpolation of sample on the standard curve. Results were expressed in ELISA units/mL determined relative to the reference serum. One ELISA unit equals the reciprocal of the dilution of the reference serum that yields an OD of 1 in the assay.

L-SBA

Individual serum samples collected at day 42 (mice and rabbits), 83 and 98 (rabbits) were tested against bacterial strains (*S. sonnei* 53G virG::cat [221], *S. flexneri* 1b, Stansfield NTCT 5 strain; *S. flexneri* 2a, 2457T strain and *S. flexneri* 3a, 6885 strain) in serum bactericidal activity (SBA) assay based on luminescent readout (L-SBA) as previously described [222, 223]. Briefly, heat-inactivated sera, baby rabbit complement (BRC) from Cedarlane (Euroclone)—used as an exogenous complement source—and diluted bacteria were mixed and incubated for 180 min at 37 °C in a 96-well Corning plate. Note that an additional well containing buffer only was also added as negative control and was used for fitting purposes. Furthermore, ratio of luminescence detected after 180 min in wells containing buffer and BRC only and luminescence at time 0 is used to evaluate the optimal growth in the assay and as quality control to validate the assay. At the end of the incubation, the plate containing the assay reaction was centrifuged at 25 °C (room temperature, RT) for 10 min at 4000 × g. The supernatant was discarded to remove bacterial debris, dead bacteria and the other SBA reagents; the bacterial pellet was resuspended in PBS, transferred to white round-bottom 96-well plates (Greiner Bio-One, Kremsmünster, Austria) and mixed 1:1 (v:v) with BacTiter-Glo Reagent (Promega, Madison, WI, USA). After 5 min of incubation at RT on an orbital shaker, the luminescence signal was measured by a luminometer (Synergy Biotek, Winooski, VT, USA).

Baby rabbit complement (BRC) was used 20% in the case of *S. sonnei*, 15% in the case of *S. flexneri* 1b and 3a, 7.5% in the case of *S. flexneri* 2a. Phosphate-buffered saline (PBS) and LB medium (only in the case of *S. flexneri* 1b strain) were used for serum and bacteria dilutions for preparation of the reaction mix.

Results of the assay were expressed as the IC50, the reciprocal serum dilution that resulted in a 50% reduction of luminescence and thus corresponding to 50% growth inhibition of the bacteria present in the assay. For data analysis, a 4-parameter non-linear regression was applied to raw luminescence data obtained at different dilutions tested for each serum sample. Fitting was performed by weighting the data for the inverse of luminescence^2. A titer equal to half of the first dilution of sera tested was assigned to titers below the minimum measurable signal (i.e., 50).

Statistics

Statistical analysis was performed using GraphPad Prism 7. Mann-Whitney two-tailed test was used to compare the immune response elicited by two different formulations compared at same antigen dose. Wilcoxon test matched-pairs signed rank two-tailed test was performed to compare the response induced by the same formulation at different timepoints. Significance is set with a p of 0.05.

3.3. RESULTS

3.3.1. Characterization of GMMA and glycoconjugates

With the intent of comparing GMMA and glycoconjugation approaches for an OAg-based vaccine against *Shigella* in animal models, OAg glycoconjugates were produced using CRM_{197}, one of the most extensively used carrier proteins in licensed vaccines [79]. GMMA were produced and purified as previously reported [78].

OAg from *S. sonnei*, *S. flexneri* 1b, 2a and 3a were extracted from the corresponding GMMA [217] and independently linked to CRM_{197}. The molecular size distribution of OAg used for conjugation and OAg populations present on corresponding GMMA are reported in **Table 3.1**. Notably, only *S. sonnei* GMMA had an additional population at higher molecular weight compared to the OAg used for conjugation, corresponding to the group 4 capsule (G4C) [224]. It is also noteworthy that GMMA present lipooligosaccharide chains at around 2 kDa, with core only or core plus few OAg repeating units, which were removed during OAg purification for glycoconjugates production. Hydroxyl groups along the OAg chain were randomly activated using the CDAP cyanilating agent, followed by conjugation with lysine residues on CRM_{197} through the formation of isourea linkages [218] (**Figure 3.2**). Conjugates formation was verified by HPLC-SEC, revealing the presence of higher molecular weight peaks compared to the protein alone, with no detectable unreacted CRM_{197}. The *S. sonnei* OAg conjugate was purified by size exclusion chromatography, while *S. flexneri* conjugates were purified by HIC. All conjugates were characterized by an OAg to protein weight ratio in the range of 0.37-0.5, with < 25% free saccharide. It should be noted that OAg to protein ratio was similar for *S. sonnei* GMMA (0.29), but higher and close to 1 for all *S. flexneri* GMMA (**Table 3.1**). GMMA had a particulate size in the range 82.5 – 160.4 nm as verified by DLS analysis, while glycoconjugates size was estimated in the range 47.3 – 329.5 kDa by HPLC-SEC using dextrans as standards (**Table 3.1**).

Table 3.1. Main characteristics of GMMA and glycoconjugates tested in animal studies.

	Total OAg/protein w/w ratio		**OAg molecular size distribution**		**Size**	
	GMMA	**Glyco-conjugate**	**GMMA**	**Glyco-conjugate**	**GMMA**	**Glyco-conjugate**
S. sonnei	0.29	0.38	234 kDa (G4C); 19.2 kDa; 2.2 kDa	19.3 kDa	160.4 nm (0.16 PdI)	47.3 kDa
S. flexneri 1b	1.18	0.37	13.8 kDa; 1.7 kDa	13.6 kDa	108.9 nm (0.18 PdI)	82.1 kDa
S. flexneri 2a	1.11	0.41	47.1 kDa; 14.2 kDa; 1.8 kDa	35.8 kDa; 14.4 kDa	109.7 nm (0.14 PdI)	209.3 kDa
S. flexneri 3a	1.17	0.50	15.5 kDa; 1.8 kDa	15.2 kDa with 70.1 kDa shoulder	82.5 nm (0.17 PdI)	329.5 kDa

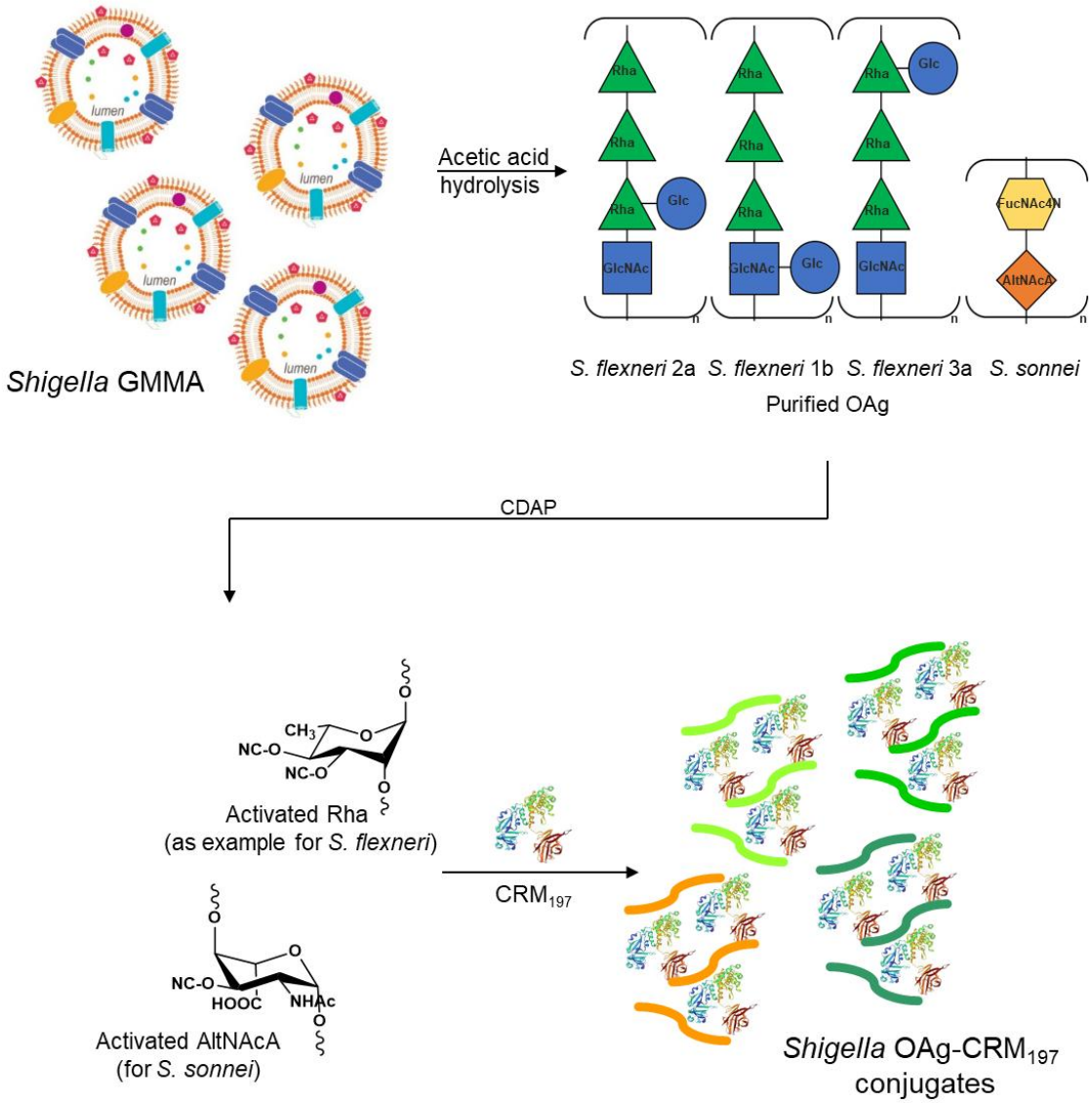

Figure 3.2. Purified *S. sonnei*, *S. flexneri* 1b, 2a and 3a OAg extracted from GMMA by acetic acid hydrolysis were conjugated to CRM_{197} through random activation of hydroxyl groups along the polysaccharide chain using the cyanilating agent CDAP, followed by linkage with lysines on the carrier protein.

3.3.2. GMMA and glycoconjugates comparison in mice

GMMA and glycoconjugates were formulated, without and with Alhydrogel, in corresponding four-component formulations and tested in mice at four different OAg doses, ranging from 9.4 to 600 ng of total OAg (2.3 to 150 ng of each OAg).

Without Alhydrogel, GMMA elicited significantly higher IgG antibodies than glycoconjugates at all tested doses, both 27 days after first injection and 14 days after the second injection, which was given at day 28. Results reported in **Figure 3.3(A)** are from the selected dose of 150 ng total OAg, representative of what observed at all the doses tested. The reduced OAg-specific IgG response observed for glycoconjugates compared to GMMA was associated to lower bactericidal activity against all the *Shigella* serotypes (**Figure 3.3(B)**).

When adsorbed on Alhydrogel, 27 days after the first injection, a higher anti-OAg IgG response was observed against *S. flexneri* 2a in mice immunized with GMMA *vs* glycoconjugates, while comparable responses were induced against *S. sonnei*, *S. flexneri* 1b and 3a and post 2 against all *Shigella* serotypes (**Figure 3.3(C)**). However, regarding sera functionality, GMMA induced statistically significantly higher SBA titers against all *Shigella* serotypes compared to glycoconjugates (**Figure 3.3(D)**). Upon second immunization, GMMA boosted the response either when adsorbed on Alhydrogel or not, while glycoconjugates only when Alhydrogel-adjuvanted.

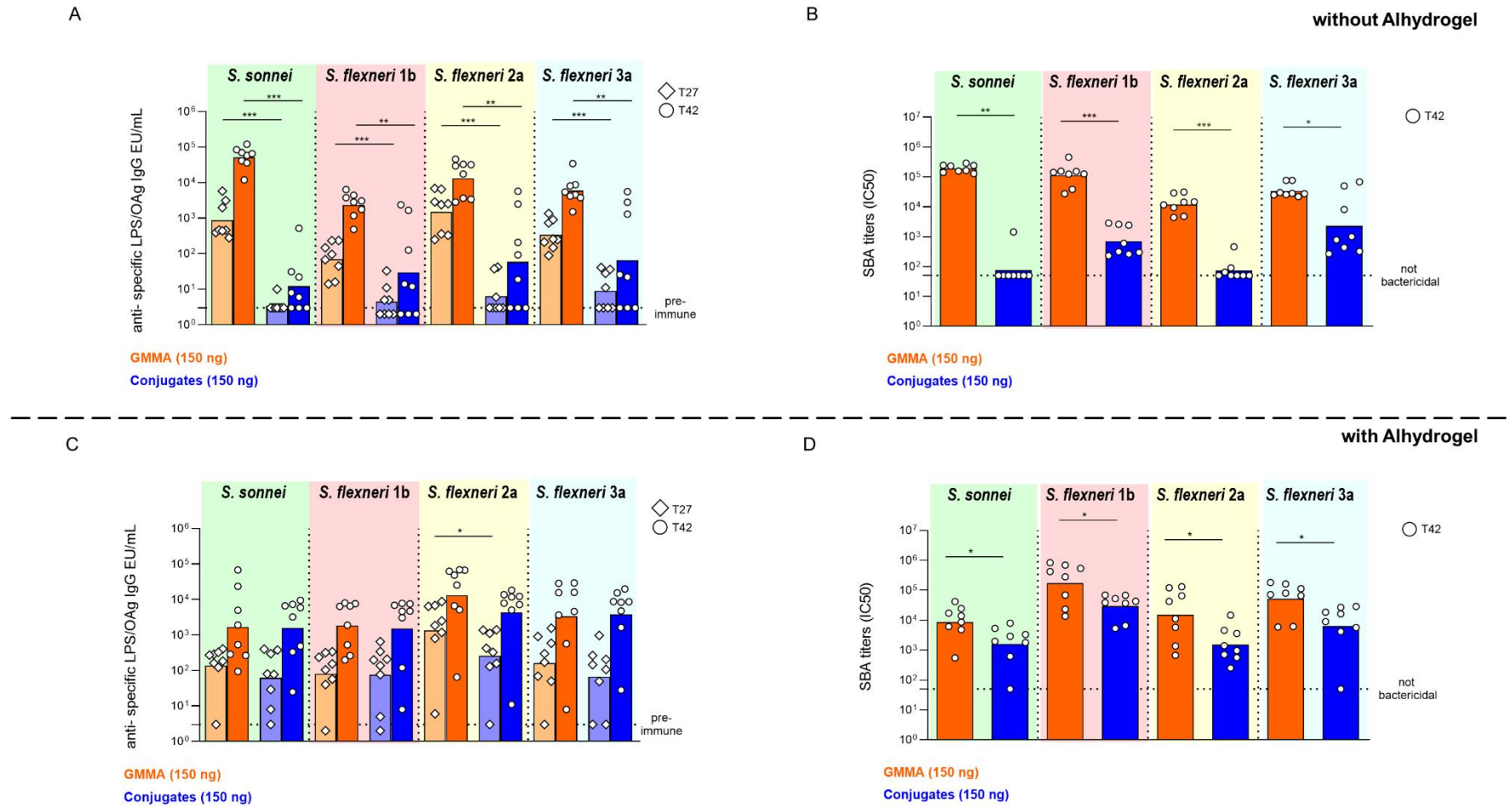

Figure 3.3. Comparison of GMMA and glycoconjugate 4-component formulations in mice in the absence **(A,B)** or presence **(C,D)** of Alhydrogel. CD1 mice were immunized intraperitoneally (i.p.) at day 0 and 28 with 9 ng, 37 ng, 150 ng and 600 ng total OAg dose. If present, concentration of Alhydrogel was 0.7 mg/mL (Al^{3+}). Results at 150 ng total OAg dose are reported here as representative of the other doses. Sera were analyzed by **(A,C)** ELISA for LPS-specific (*S. sonnei*) or OAg-specific (*S. flexneri*) total IgG (EU/mL) and **(B,D)** serum bactericidal activity (SBA) assay for bactericidal titers expressed as IC50. Summary graphs of geometric mean units (bars) and individual levels (dots) are reported. * $p < 0.05$; ** $p < 0.01$; *** $p < 0.001$.

To further assess the differences between the immune responses elicited by GMMA and glycoconjugate 4-component formulations, a detailed characterization of the quality of the humoral response was conducted. This included analysis of IgG subclasses and IgM, in sera from immunizations with 150 ng total OAg per dose.

In the absence of Alhydrogel, GMMA induced significantly higher levels of IgG1, IgG2, IgG3 and IgM across all serotypes compared to glycoconjugates. When Alhydrogel was present, GMMA and glycoconjugates elicited comparable levels of IgG1. Additionally, IgG2a, IgG2b, and IgM levels induced by *S. sonnei*, *S. flexneri* 1b, and 3a GMMA were comparable to those elicited by glycoconjugates, whereas *S. flexneri* 2a GMMA induced higher levels than the corresponding glycoconjugates. IgG3 levels induced by GMMA were consistently higher than those elicited by glycoconjugates, except for *S. flexneri* 1b formulations, which elicited a similar response (**Figure 3.4**, **Table 3.2**). Overall, glycoconjugates predominantly elicited IgG1, whereas GMMA induced a broader range of IgG subclasses (**Figure 3.5**).

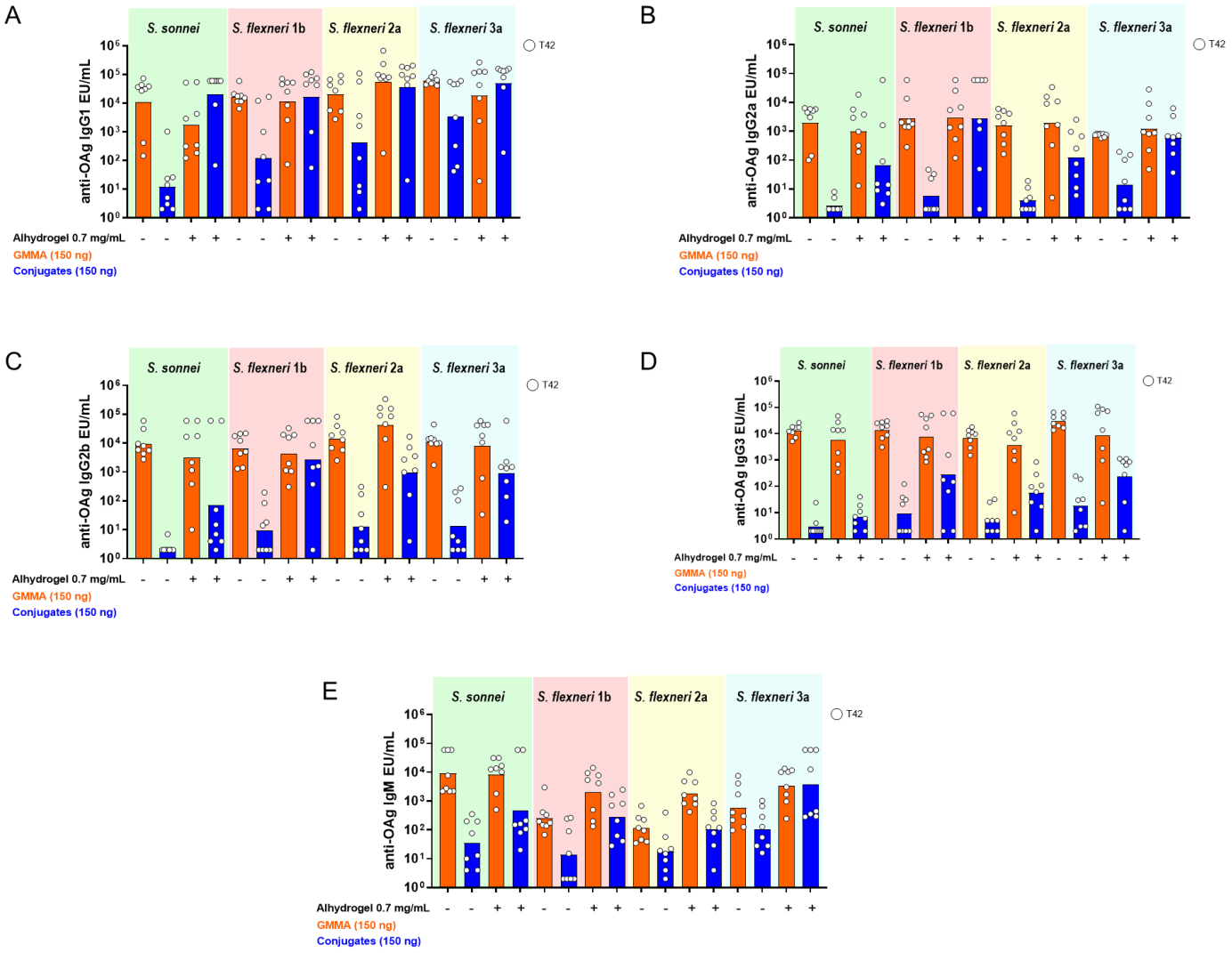

Figure 3.4. Characterization of the quality of the humoral response elicited by GMMA and glycoconjugates in mice. CD1 mice were immunized i.p. at day 0 and 28 with 150 ng total OAg per dose in absence or presence of Alhydrogel. **(A-D)** Anti-OAg-specific IgG subclasses and **(E)** IgM were evaluated at day 42. Summary graphs of geometric mean units (bars) and individual levels (dots) are reported.

Table 3.2. Comparison of GMMA and glycoconjugates 4-component formulations in mice. CD1 mice were immunized i.p. at day 0 and 28 with 150 ng total OAg dose in absence or presence of 0.7 mg/mL of Alhydrogel (Al^{3+}). Mann-Whitney two-tailed test was performed on IgG subclasses and IgM ELISA results at day 42: ns (not significant) $p > 0.05$, * $p < 0.05$; ** $p < 0.01$; *** $p < 0.001$.

GMMA *vs* Conjugates without Alhydrogel		**IgG1**	**IgG2a**	**IgG2b**	**IgG3**	**IgM**
S. sonnei	Day 42 p value	***	***	***	***	***
***S. flexneri* 1b**	Day 42 p value	**	***	***	***	*
***S. flexneri* 2a**	Day 42 p value	ns	***	***	***	*
***S. flexneri* 3a**	Day 42 p value	*	***	***	***	ns
GMMA *vs* Conjugates with Alhydrogel		**IgG1**	**IgG2a**	**IgG2b**	**IgG3**	**IgM**
S. sonnei	Day 42 p value	*	ns	ns	***	ns
***S. flexneri* 1b**	Day 42 p value	ns	ns	ns	ns	ns
***S. flexneri* 2a**	Day 42 p value	ns	*	**	**	**
***S. flexneri* 3a**	Day 42 p value	ns	ns	ns	*	ns

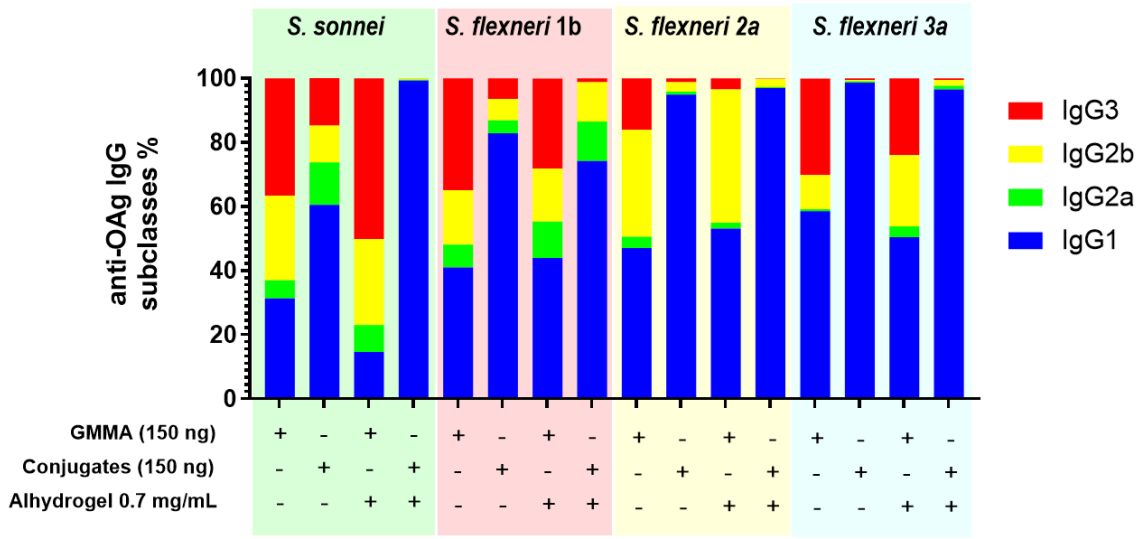

Figure 3.5. Characterization of the quality of the humoral response elicited by GMMA and glycoconjugates in mice. CD1 mice were immunized i.p. at day 0 and 28 with 150 ng total OAg dose in absence or presence of Alhydrogel. Anti-OAg-specific IgG subclasses have been evaluated at day 42. Relative percentage of each specific IgG subclass with respect to total IgG (ratio of geometric means) is reported in different colors in the bar plot for each formulation tested.

3.3.3. GMMA and glycoconjugates comparison in rabbits

The same GMMA and glycoconjugate formulations were also compared in rabbits, at the dose of 600 ng of total OAg (150 ng of each OAg). The same immunization scheme already used with mice was tested, but with intramuscular injection.

A stronger *S. sonnei* LPS-specific total IgG response was elicited by GMMA with respect to glycoconjugates at all time points investigated, both without and with Alhydrogel (**Figure 3.6(A,C)**). SBA titers paralleled the IgG response (**Figure 3.6(B,D)**).

For all *S. flexneri* serotypes, the anti-OAg IgG response elicited by GMMA was significantly higher than that promoted by glycoconjugates only after the first injection (post 1) and in the absence of Alhydrogel (**Figure 3.6(A)**). At day 42 (after the second injection, post 2), the responses induced were similar, with the exception of a higher anti-*S. flexneri* 2a OAg IgG response elicited by glycoconjugates compared to GMMA in the presence of Alhydrogel (**Figure 3.6(C)**). No differences were observed in terms of bactericidal titers, evaluated at day 42, without or with Alhydrogel, for all serotypes (**Figure 3.6(B,D)**).

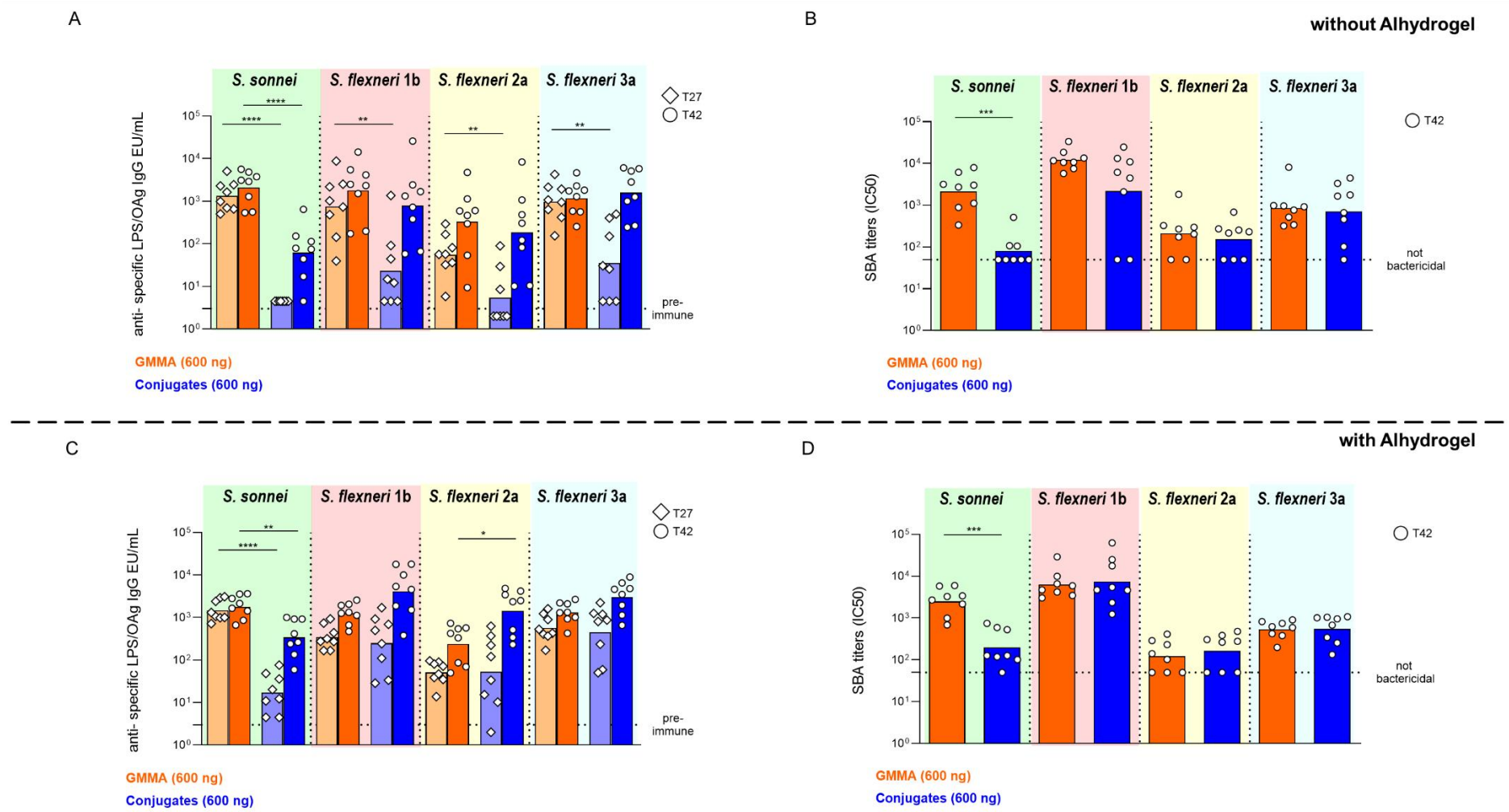

Figure 3.6. Comparison of GMMA and glycoconjugates 4-component formulations in rabbits in the absence **(A,B)** or presence **(C,D)** of Alhydrogel. New Zealand rabbits were immunized intramuscularly (i.m.) at day 0 and 28 with 600 ng total OAg per dose. If present, concentration of Alhydrogel was 0.7 mg/mL (Al^{3+}). Sera were analyzed by **(A,C)** ELISA for LPS-specific (*S. sonnei*) or OAg-specific (*S. flexneri*) total IgG (EU/mL) and **(B,D)** SBA for bactericidal titers expressed as IC50. Summary graphs of geometric mean units (bars) and individual levels (dots) are reported. * $p < 0.05$; ** $p < 0.01$; *** $p < 0.001$.

3.3.4. Different immunization schedules in rabbits

Two different immunization schedules were compared in rabbits with GMMA and glycoconjugates formulated on Alhydrogel. Animals were immunized at day 0 and 1 month (day 28) or 3 months (day 84) later.

Before the second vaccination, the anti-OAg-specific IgG responses elicited by GMMA were consistent across all serotypes at both day 27 (before the second immunization on day 28) and day 83 (before the second vaccination on day 84), except for *S. flexneri* 1b, with higher IgG titers at day 83 compared to day 27. After the second injection, there was significant increase of the IgG responses against the *S. flexneri* serotypes only when rabbits were immunized one month after primary injection. No booster was observed for *S. sonnei*, either with 1 month or 3 months interval schedule. Comparing the responses elicited by GMMA post second dose, total IgG were higher with the 0-1 month schedule for all *Shigella* serotypes but *S. flexneri* 2a, for which IgG responses were similar (**Figure 3.7(A)**). SBA titers analysed in post 2 sera paralleled IgG responses, with exception of titers against *S. flexneri* 2a that were significantly higher at day 98 *vs* day 42 (**Figure 3.7(B)**).

As observed with GMMA, glycoconjugates induced similar anti-OAg-specific IgG responses among all serotypes at both day 27 (prior to the second immunization on day 28) and day 83 (prior to the second vaccination on day 84), except for *S. sonnei*, with higher IgG titers at day 27. Second immunization with glycoconjugates always boosted the total IgG response irrespectively of the immunization scheme used, except for *S. flexneri* 2a with the 0-3 months protocol. Comparing the responses elicited by glycoconjugates after the second dose, total IgG were similar with the 0-1 or 0-3 month schedule for all *Shigella* serotypes but *S. flexneri* 2a, for which IgG response was higher at day 42 (**Figure 3.7(C)**). However, antibody titers were not bactericidal against the *S. flexneri* serotypes when the second immunization was done 3 months after the first one (**Figure 3.7(D)**).

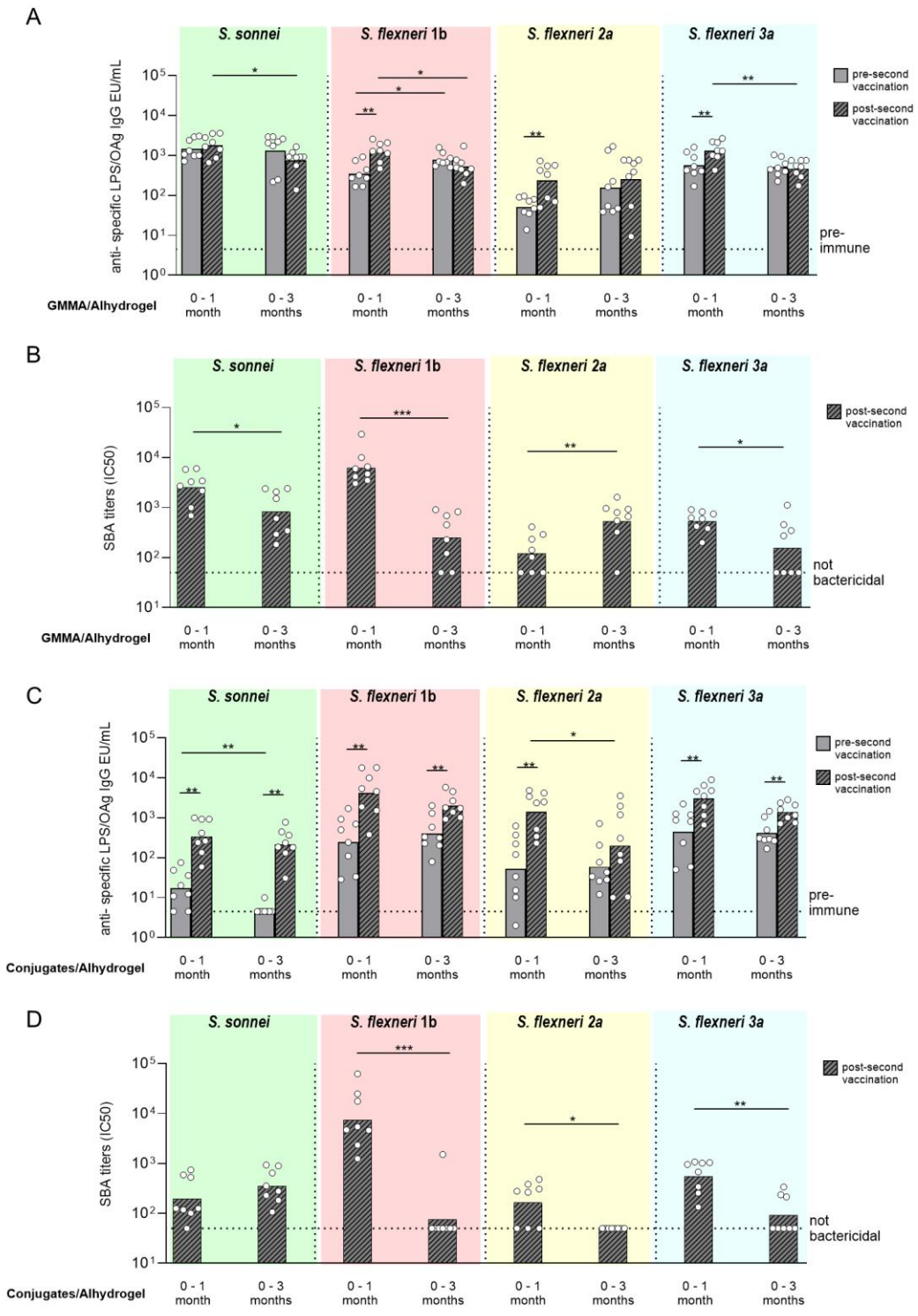

Figure 3.7. Comparison of two different immunization schemes for GMMA and glycoconjugate 4-component formulations in rabbits. New Zealand rabbits were immunized i.m. at day 0 and 28 (0-1 month) or 0 and 84 (0-3 months) with 600 ng total OAg per dose in presence of 0.7 mg/mL of Alhydrogel (Al^{3+}). Sera were analyzed by **(A,C)** ELISA for LPS-specific (*S. sonnei*) or OAg-specific (*S. flexneri*) total IgG (EU/mL) pre second vaccination (at day 27 or 83) and post second vaccination (at day 42 or 98) and by **(B,D)** SBA for bactericidal titers expressed as IC50 post second vaccination only. Summary graphs of geometric mean units (bars) and individual levels (dots) are reported. * $p < 0.05$; ** $p < 0.01$; *** $p < 0.001$.

3.3.5. Role of Alhydrogel on the immunogenity induced by GMMA and glycoconjugates

To further elucidate the role of Alhydrogel on the immune response elicited by GMMA, 4-component GMMA formulations with and without the adjuvant were compared. We aimed to determine whether Alhydrogel could enhance the humoral response induced by the combination of *S. sonnei*, *S. flexneri* 1b, 2a, and 3a GMMA. A similar assessment was also conducted for the 4-component combination of glycoconjugates.

In mice, use of Alhydrogel was detrimental, both for GMMA and glycoconjugates, to the levels of total IgG and serum bactericidal activity against *S. sonnei*, in line with what has been observed with *S. sonnei* GMMA alone [213]. No differences were instead evidenced against the *S. flexneri* serotypes (**Figure 3.8(A,B)**).

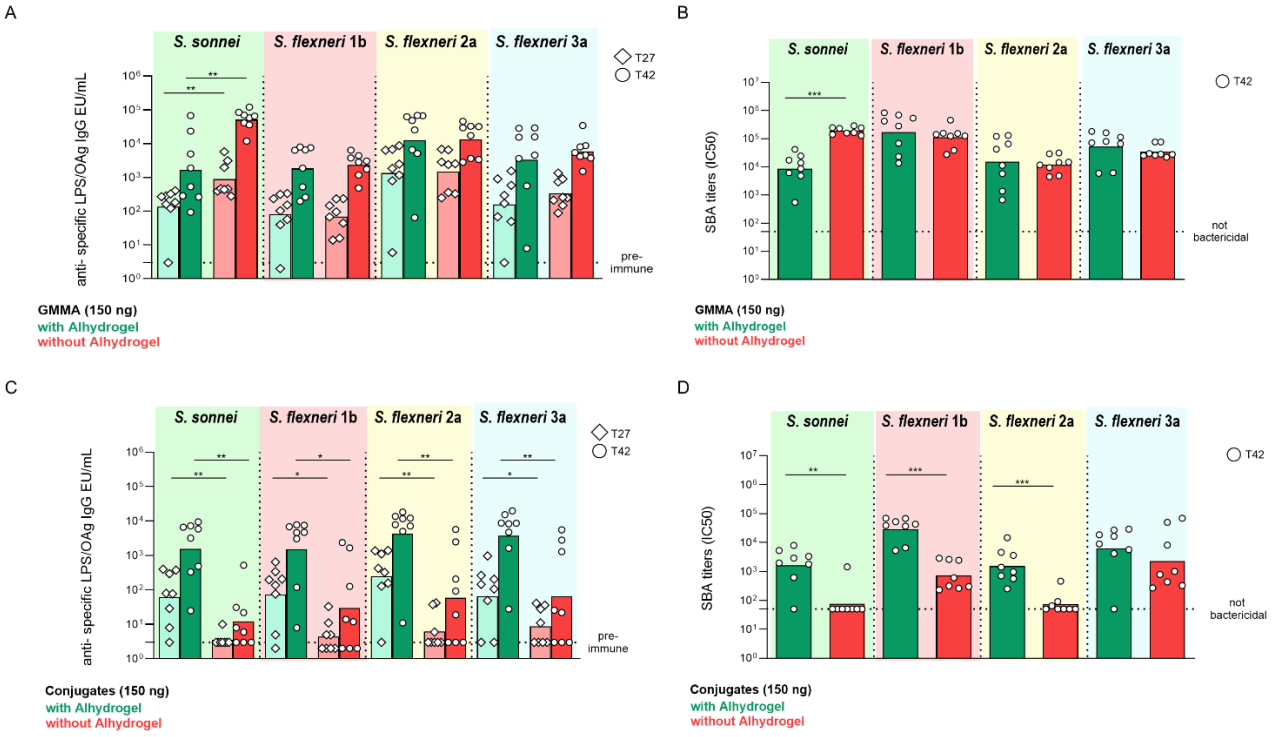

Figure 3.8. Impact of Alhydrogel on the immunogenity induced by GMMA and glycoconjugates in mice. CD1 mice were immunized i.p. at day 0 and 28 with 9 ng, 37 ng, 150 ng and 600 ng total OAg dose. Results at 150 ng total OAg dose are reported as representative of the other doses. Sera were analyzed by **(A,C)** ELISA for LPS-specific (*S. sonnei*) or OAg-specific (*S. flexneri*) total IgG (EU/mL) and **(B,D)** SBA for bactericidal titers expressed as IC_{50}. Summary graphs of geometric mean units (bars) and individual levels (dots) are reported. * $p < 0.05$; ** $p < 0.01$; *** $p < 0.001$.

On the contrary, Alhydrogel worked as good adjuvant for glycoconjugates, resulting in stronger IgG response and SBA titers against all the *Shigella* serotypes, with the exception of *S. flexneri* 3a in SBA only at the dose shown and at the higher one (600 ng) (**Figure 3.8(C,D)**).

In rabbits, Alhydrogel did not enhance the immunogenicity elicited by *Shigella* GMMA. Total IgG responses against all *Shigella* serotypes were not significantly different, regardless of the presence of Alhydrogel, either 27 days after the first injection or 14 days after the second injection (**Figure 3.9(A)**). Additionally, similar SBA titers were elicited, except at the day 42 timepoint, in which the 4-component GMMA without Alhydrogel induced higher SBA titers against *S. flexneri* 1b compared to the adjuvanted GMMA (**Figure 3.9(B)**).

For glycoconjugates, the presence of Alhydrogel consistently resulted in an increased total IgG response after the first dose, and after the second dose only against *S. sonnei* (**Figure 3.9(C)**). The sera bactericidal activity at day 42 mirrored the IgG response (**Figure 3.9(D)**).

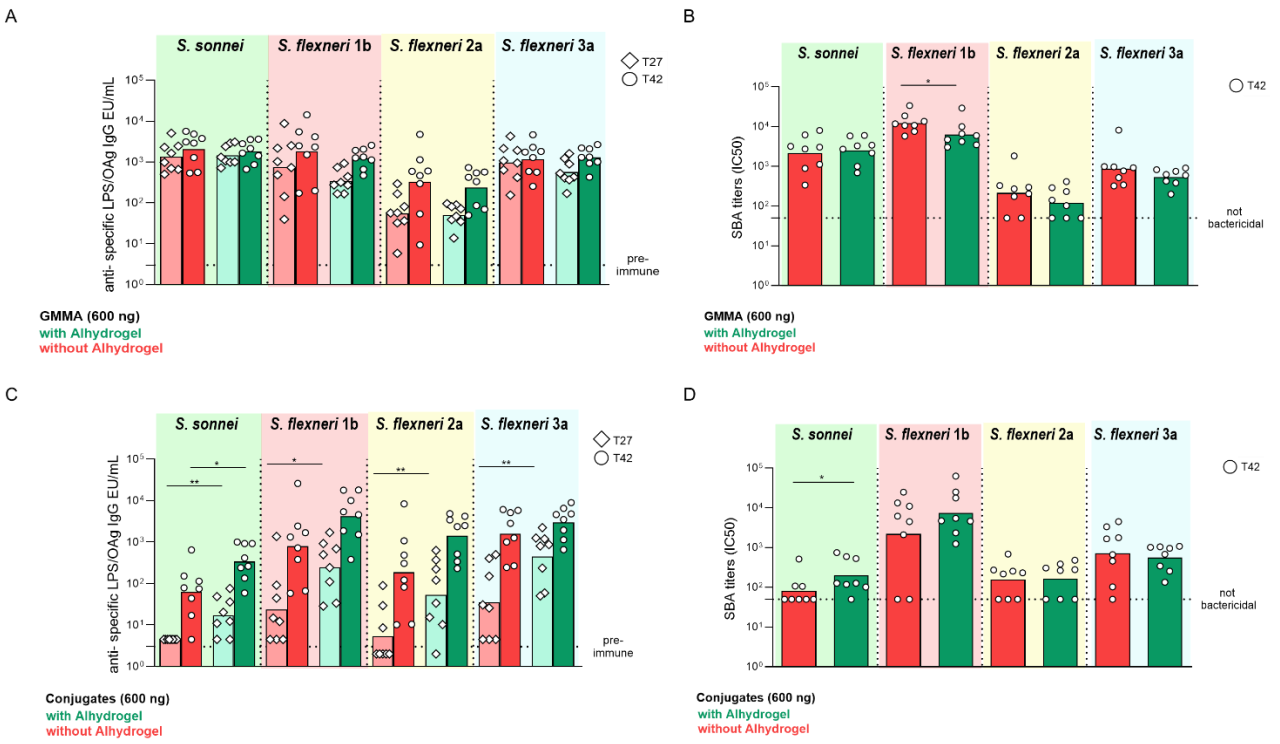

Figure 3.9. Impact of Alhydrogel on the immunogenity induced by GMMA and glycoconjugates in rabbits. New Zealand rabbits were immunized i.m. at day 0 and 28 with 600 ng total OAg per dose. If present, concentration of Alhydrogel was 0.7 mg/mL (Al^{3+}). Sera were analyzed by **(A,C)** ELISA for LPS-specific (*S. sonnei*) or OAg-specific (*S. flexneri*) total IgG (EU/mL) and **(B,D)** SBA for bactericidal titers expressed as IC50. Summary graphs of geometric mean units (bars) and individual levels (dots) are reported. * $p < 0.05$; ** $p < 0.01$; *** $p < 0.001$.

3.4. DISCUSSION

Shigella is the leading bacterial cause of diarrheal disease, frequently associated with AMR [196] and listed by the WHO as a priority pathogen for which new interventions are urgently needed [15]. Currently, no widely available vaccines exist against *Shigella*, although various OAg-based candidates are under clinical evaluation. The diverse distribution of *Shigella* serotypes across countries and over time, driven by OAg structural features, necessitates the development of multi-component vaccines to address the burden of shigellosis [138].

In this work, GMMA and the traditional glycoconjugation approach have been compared for a multi-component OAg-based vaccine against *Shigella*.

Sugar length and polysaccharide to protein ratio are two well-known factors that can influence the immunogenicity of glycoconjugates [225]. In previous work, both for *Shigella* glycoconjugates [226] and GMMA [224, 226], it was demonstrated that OAg length did not significantly affect the ability to induce functional anti-OAg IgG antibodies in mice. Here, the OAg populations used for conjugation to CRM_{197}, a carrier protein commonly used in glycoconjugates [79], were similar in size to those displayed on GMMA. Major difference remained for *S. sonnei*, as GMMA also present a very long group 4 capsule (G4C) polysaccharide not used for conjugation.

Additionally, *S. sonnei* GMMA and the corresponding glycoconjugate had a similar OAg to total protein ratio, whereas the ratio was higher for *S. flexneri* GMMA than corresponding glycoconjugates. In a previous study, the impact of the OAg density on particle surface has been tested with *S. sonnei* GMMA only, revealing that GMMA with different numbers of sugar chains per total protein elicited a similar anti-OAg specific IgG bactericidal response when compared at the same OAg dose [78]. However, the OAg to protein ratio could be critical for the immunogenicity of *Shigella* glycoconjugates [225]. It must be also considered that GMMA have a nanoparticle size and not only provide T-cell help to the OAg chains [224, 226, 227], but also favor the presentation of multiple OAg copies in their native bacterial environment. Furthermore, GMMA possess pathogen-associated molecular patterns, such as lipopolysaccharide and lipoproteins, that can provide self-adjuvanticity [108, 227]. For this reason, GMMA and glycoconjugates were compared in this study with and without Alhydrogel.

Comparison between GMMA and glycoconjugates was based on anti-OAg specific IgG response and bactericidal titers. Numerous studies have demonstrated an association between anti-OAg IgG titers and protection [145]. Furthermore, a threshold level of serum IgG antibodies against *Shigella sonnei* LPS has been proposed as a correlate of protection, based on serological and efficacy data from two

randomized, vaccine-controlled trials of a *S. sonnei* conjugate vaccine conducted in young adults and children aged 1–4 years in Israel [144]. Serum bactericidal activity has also been proposed as an important readout for *Shigella* vaccines [228].

In the absence of Alhydrogel, GMMA elicited significantly higher IgG antibodies than glycoconjugates, both after first and second vaccination in mice. Moreover, the bactericidal activity of sera elicited by GMMA was higher in comparison to glycoconjugates. When adsorbed on Alhydrogel, serotype-specific IgG responses became comparable, but GMMA continued to elicit significantly higher SBA titers than glycoconjugates. The higher functionality could be linked to a broader IgG isotype switch observed with GMMA [229]. These results are consistent with previous observations comparing *Salmonella* GMMA and glycoconjugates in mice [112].

Here, GMMA and glycoconjugate technologies were compared for the first time in rabbits. Results obtained confirmed improved immune response elicited by *S. sonnei* GMMA with respect to corresponding glycoconjugate, regardless of the presence of Alhydrogel. However, unlike the results observed in mice, *S. flexneri* GMMA and glycoconjugates elicited comparable immune responses in rabbits.

It is important to note that ELISA against *S. sonnei* was performed using LPS as coating antigen. Therefore, it cannot be excluded that higher levels of antibodies against core or lipid A from GMMA were quantified compared to those from glycoconjugate immunization. Nevertheless, previous immunizations with OAg-negative GMMA have confirmed that these antibodies are not bactericidal [230].

Alhydrogel has been used in clinical settings to further reduce potential GMMA reactogenicity [202]. Our results suggest no need of Alhydrogel to increase GMMA immunogenicity, in both mice and rabbits. This could be expected due to the self-adjuvanting nature of GMMA, and adding an adjuvant to already highly immunogenic GMMA might even be detrimental to the optimal immune response. Conversely, Alhydrogel serves as adjuvant for the immunogenicity of glycoconjugates only in mice.

When *Shigella sonnei* and *S. flexneri* 2a glycoconjugates and *S. sonnei* GMMA have been tested as monovalent formulations in adults, no increase in the anti-LPS IgG response has been observed after a second injection with an interval of 4-6 weeks post first vaccination [199, 202]. Here, two different schedules in rabbits were compared, with the second vaccination administered either 1 or 3 months after the first, to evaluate if a longer interval could result in improved booster and higher post-second vaccination responses. Both GMMA and glycoconjugates were able to elicit serotype specific antibodies that persisted up to 3 months post vaccination. Glycoconjugates boosted the response after

both 1 or 3 months for all serotypes, but antibodies were not functional when the second vaccination was given with a 0-3 month schedule. This could be related to a different quality and functionality of antibodies persisting at 3 months *vs* 1 month post primary vaccination. Similarly to observations in adults, no booster was observed for *S. sonnei* GMMA, regardless of the immunization schedule used. An interval of 1 month resulted instead in increased response for *S. flexneri* GMMA after the second injection. Overall, a longer interval of 3 months between vaccinations did not result in improved immunogenicity: all GMMA, but *S. flexneri* 2a, induced stronger functional IgG post second vaccination with a 1 month interval compared to a 3 months interval.

In conclusion, two different approaches for the development of a multi-component OAg based vaccine against *Shigella* were compared, in both mice and rabbits. Since results obtained in the two animal models were different, it will be interesting to examine clinical data that will become available in the near future from various OAg-based vaccines and in different age group populations to determine if and how preclinical data can be predictive for humans.

4. Development of a multivalent vaccine against *Shigella* and *Salmonella* infections

4.1. INTRODUCTION

As already described in Chapter 3, *Shigella* is the leading cause of diarrheal disease, especially in LMICs [121, 130], increasingly associated to AMR [133, 138, 196].

A well-considered and feasible clinical development pathway is in place to support the licensure of a *Shigella* vaccine [231]. However, even a highly efficacious vaccine may not be recommended, prioritized, purchased, or widely adopted in LMICs, due to increasingly crowded and costly childhood immunization programs, the continuing declines in overall diarrheal disease mortality rates and the recent introduction of other high-priority vaccines [77, 232]. For this reason, combination of a *Shigella* vaccine with another infant vaccine would increase its attractiveness, as recommended by GAVI in the last Vaccine Investment Strategy (VIS) 2024 [233].

Different serovars of *Salmonella enterica* cause systemic diseases in humans. Among these, *S.* Typhi and *S.* Paratyphi A are responsible for typhoid and paratyphoid fever, respectively, and have a high incidence especially in South and Southeast Asia [156]. Antibiotics are widely used, but increasing levels of AMR are limiting their effectiveness [75, 160]. Just like *Shigella*, *Salmonella* serovars are also included in the WHO high priority list of AMR pathogens [234]. While several licensed and WHO–prequalified vaccines are available for typhoid fever, no vaccine currently exists against *S.* Paratyphi A. However, bivalent candidates targeting both diseases are in development [75].

In my PhD project, for the first time, the tetravalent GMMA-based *Shigella* vaccine altSonflex1-2-3 [78] has been combined with a bivalent *Salmonella* vaccine, consisting of the licensed typhoid conjugate vaccine (Vi-CRM_{197}, TCV) and the *S.* Paratyphi A O:2-CRM_{197} glycoconjugate [178]. After promising results in phase 1, altSonflex1-2-3 (see also Chapter 3) is currently being tested in phase 2 clinical trials in 9-months infants in Kenya, where shigellosis is endemic (clinical trials NCT05073003 and NCT06663436) [119]. On the other hand, the bivalent *Salmonella* conjugate vaccine [Alfini R. et al., submitted] has recently been tested in a phase 1 clinical trial in European adults (clinical trial NCT05613205), showing very strong immune response for both components.

This novel hexavalent vaccine has been formulated and tested in different animal models to evaluate its immunogenicity and possible immuno-interference occurring among the different PS components.

A multivalent vaccine tackling *Shigella* and *Salmonella* simultaneously could address a significant unmet need. As these two pathogens coexist in many geographical areas, combining them into a single infant vaccine could substantially contribute to AMR reduction, increase commercial attractiveness through reduced cost of goods, and improve acceptance among end users and health-care providers, ultimately leading to higher and more equitable vaccination coverage.

4.2. MATERIALS AND METHODS

Preparation and characterization of *Shigella* GMMA

Shigella GMMA were obtained from GVGH. They were produced from the following strains: *S. sonnei* 53G ΔtolR::kan ΔvirG::nadAB ΔmsbB2::cat ΔmsbB::erm, *S. flexneri* 1b Stansfield ΔtolR::frt ΔmsbB1a::frt ΔmsbB1b::frt, *S. flexneri* 2a 2457T ΔtolR::kan, ΔmsbB::cat, and *S. flexneri* 3a 6885 ΔtolR::kan, ΔmsbB::cat, and purified as previously described [78].

GMMA were characterized as described in Chapter 3. In addition, lipid A on GMMA was quantified by Reversed Phase-High Performance Liquid Chromatography coupled with Mass Spectometry (HPLC-RP MS) analysis, as reported below [214].

HPLC-RP MS for lipid A quantification

The lipid A in the GMMA samples was quantified via its 3-hydroxymyristic acid content, which is present as a primary ester in its structure. The process began with hydrolysis in which the ester bonds between the glucosamine and the 3-hydroxy fatty acid were quantitatively cleaved, releasing the 3-hydroxy fatty acid. This released acid was then separated by reversed-phase HPLC and quantified using an MS detector. Both samples and standards were processed through an on-line SPE hydrophobic cartridge (Strata-X 25 µm On-Line Extraction, Cartridge 20 × 2.0 mm, Phenomenex, Torrance, CA, USA), which served to concentrate and desalt the analytes prior to analysis on a Thermo Quantum Access triple quadrupole system.

Reversed-phase separation was achieved on a Luna 3u C8(2) column, 50 × 2 mm, 100A, (Phenomenex) with an injection volume of 1 µL. The elution was carried out at the flow of 0.25 mL/min, using 100% eluent B (70% ACN, 0.05% formic acid), while eluent A (40% methanol, 0.05% formic acid) was used to wash and re-equilibrate the SPE cartridge.

The mass spectrometer was operated in negative ion mode with the following key settings: ESI spray voltage of 4000 V, sheath gas pressure of 25, auxiliary gas pressure of 10, capillary temperature of 300 °C, tube lens offset of −70, and skimmer offset of 10. The collision cell was filled with argon at 1 mTorr, with a collision energy set at 16 V. The MS scan event was programmed for a time segment of 0–10 minutes with Q1 set to 243 ± 0.02 *m/z* for 3-hydroxymyristic acid and Q3 to 59 ± 0.02 *m/z* as the diagnostic product ion, using a scan time of 0.5 seconds.

Sample preparation involved diluting the samples in low-bind tubes with 50% isopropyl alcohol (IPA), treating them with 0.25 M NaOH, incubating at 40 °C for 2 hours, cooling to 4 °C, and transferring into HPLC low-bind vials.

A linear regression was established from the 3-hydroxy fatty acid standard, correlating peak areas to concentrations, to calculate the analyte concentration in the samples, considering that each lipid A molecule contains two 3-hydroxy fatty acid ester groups.

Preparation and characterization of *Salmonella* glycoconjugates

S. Paratyphi A OAg (O:2)—extracted from the ED199 ΔtolR strain as previously described [217]—and the Vi PS—purified from *Citrobacter freundii* NVGH 328 [235] and fragmented as reported in [236]—were obtained from GVGH.

The O:2-CRM_{197} glycoconjugate was produced using the procedure reported in [237]. Briefly, O:2 at 4.5 mg/mL in 0.5 M NaCl and 50 mM 1,4-diazabicyclo[2.2.2]octane (DABCO) pH 9 was activated with a solution of CDAP in acetonitrile using a 0.2:1 weight ratio CDAP/OAg. After 15 minutes in ice bath, CRM_{197} was added to the solution in a CRM_{197}/OAg 1:1 weight ratio with final concentration of 3.8 mg/mL. The reaction was mixed for 2 h at room temperature (RT). At the end, 1M glycine at pH 9 was added (1:1 v/v with respect to the reaction mixture) to quench the reaction. The solution was mildly mixed over night at RT.

The Vi-CRM_{197} glycoconjugate was synthesized as described in [236]. Fragmented Vi was solubilized in 100 mM MES pH 6 at a concentration of 50 mg/mL. N-Hydroxysuccinimide (NHS) and then 1-Ethyl-3-(3-dimethylaminopropyl)carbodiimide (EDAC) were added to have 0.33 M NHS and EDAC/Vi repeating units molar ratio of 5. The reaction was mixed at room temperature (RT) for 1h and then the protein, previously derivatized with ADH [235], was added in a Vi:CRM_{197} w/w ratio of 1:1 to give a Vi concentration of 5.0 mg/mL in 20 mM MES pH 6 and mixed at RT for 2h.

The conjugates were purified by hydrophobic interaction chromatography (HIC) on a Phenyl HP column (Cytiva Life Sciences, Marlborough, MA, USA), loaded in 20 mM NaH_2PO_4 3 M NaCl at pH 7.2. The purified conjugate was eluted in 20 mM NaH_2PO_4 at pH 7.2 and the collected fractions were exhanged against Phosphate-buffered saline (PBS) by Amicon Ultra (Merck, Darmstadt, Germany) 30 kDa cut-off.

Purified conjugates were characterized by micro BCA (Thermo Scientific, Waltham, MA, USA) and HPAEC-PAD [216, 217] for total protein and total PS content respectively and the PS to protein ratio was calculated. The HPAEC-PAD method for Vi quantification is reported below, while the method

for O:2 quantification was developed in the context of this PhD project and will be described in depth in Chapter 5. Free O:2 was separated through reverse phase-solid phase extraction (SPE) using Vydac C4 SPE cartridges [178], as described in Chapter 3, and quantified by HPAEC-PAD (Chapter 5), while for free Vi the unconjugated saccharide was estimated by HPAEC-PAD method [216] after conjugate coprecipitation with deoxycholate [217, 238]. Conjugates formation was verified by HPLC-SEC, comparing the conjugates with unconjugated CRM_{197} [220].

HPAEC-PAD of Vi

To quantify the Vi PS, the same amino uronic acid HPAEC-PAD method already described in Chapter 3 for *S. sonnei* OAg was employed [216]. A standard of Vi PS was used to construct the calibration curve in the 0.16–5 µg/mL range, with the standards undergoing the same hydrolysis and analysis procedures as the samples.

Free saccharide quantification via DOC

The Vi glycoconjugate samples were diluted to 100 µg/mL (protein based) in 0.1 M NaCl and then processed as follows. A 1.5 mL aliquot of the solution was chilled on ice for 30 minutes before adding 0.15 mL of a 1% deoxycholate sodium salt solution; the mixture was returned to ice for an additional 30 minutes. Next, 75 µL of a chilled 1 M HCl solution was added, and after vortexing, the mixture was centrifuged at 12,000 × g for 30 minutes at 4 °C. The resulting supernatant was dried using a centrifugal evaporator and then resuspended in an appropriate volume of water for the quantification of free saccharide by HPAEC-PAD, according to the method described above. In parallel, a sample spiked with a known amount of free OAg was processed each time to verify the procedure, with spike recoveries expected to be in the 80–120% range.

HPLC-SEC

Conjugates were analyzed via HPLC-SEC with an 80 µL injection on a Waters Acquity UPLC H-Class PLUS Bio System. The analysis used a Tosoh TSK gel 6000 PW column connected in series with a Tosoh TSK gel 5000 PW column and a Tosoh TSK gel PWH guard column (Tosoh, King of Prussia, PA, USA). The eluent was composed of 0.1 M NaCl, 0.1 M NaH_2PO_4, 5% ACN at pH 7.2, with a flow rate of 0.5 mL/min. The column compartment was maintained at 30 °C while the autosampler compartment was kept at 4 °C. The peaks corresponding to the saccharide are detected by differential refractive index (dRI), while UV detection at 214 nm and 280 nm are used for free protein and conjugate detection. Protein and conjugate peaks are also detected using tryptophan fluorescence (emission spectrum at 336 nm, with excitation wavelength at 280 nm).

Preparation and characterization of multivalent formulations

Formulations and related activities were performed under a sterile hood in aseptic conditions.

All the formulation conditions tested, named Conditions 1, 2 and 3, are summarized in **Scheme 4.1**.

Hexavalent formulations trials

For Conditions 1 and 2, firstly, *S. sonnei* and *S. flexneri* 1b, 2a and 3a GMMA were adsorbed on Alhydrogel to reach the final concentrations of 120 µg/mL total OAg (30 µg/mL each OAg) and 0.7 mg/mL Al^{3+}, under continuous stirring for 2 hours. Then, NaH_2PO_4 100 mM pH 6.5 (final concentration of 5 to 20 mM for Condition 1, and 20 to 50 mM for Condition 2) and NaCl solution 1540 mM (154 mM in the final formulations) were added, followed by continuous stirring for 30 min.

After this step, two alternative options were selected for the addition of the glycoconjugates.

In Condition 1, a previously prepared solution of the conjugates in 154 mM NaCl was added to the adsorbed GMMA in a 1:1 v/v conjugates:GMMA. The final concentration of each PS was of 50 µg/mL. After this addition, the formulations were stirred for 15 h ± 4 h.

In Condition 2, the Vi-CRM_{197} (50 µg/mL Vi final concentration) was first added and the suspension mixed for 1 hour. Finally, O:2-CRM_{197} (50 µg/mL OAg final concentration) was added, followed by continuous stirring for 15 h ± 4 h.

Condition 3, which was the procedure selected for animal studies, is described in the following paragraph.

Formulations for animal studies

Hexavalent formulation Condition 3: Hexavalent vaccine formulations with Alhydrogel were prepared by firstly adsorbing, under continuous stirring, *S. sonnei* and *S. flexneri* 1b, 2a and 3a GMMA on Alhydrogel to reach the final concentrations of 120 µg/mL total OAg (30 µg/mL each OAg) and 0.7 mg/mL Al^{3+}. After 2 hours, O:2-CRM_{197} (50 µg/mL OAg final concentration) was added and the suspension was mixed for 1 hour. Then, NaH_2PO_4 100 mM pH 6.5 (5 to 50 mM in the final formulations) and NaCl solution 1540 mM (154 mM in the final formulations) were added, followed by continuous stirring for 15 min. Finally, Vi-CRM_{197} (50 µg/mL Vi final concentration) was added, followed by continuous stirring for 15 h ± 4 h. Further dilutions for immunogenicity studies were performed with Alhydrogel diluent (0.7 mg/mL Al^{3+} in NaCl 154 mM NaH_2PO_4 20 mM pH 6.5).

Four-component *Shigella* GMMA formulation with Alhydrogel was prepared as reported in Chapter 3 [78].

Bivalent O:2-CRM_{197} + Vi-CRM_{197} with Alhydrogel formulation was prepared by firstly adsorbing, under continuous stirring, O:2-CRM_{197} (50 µg/mL OAg final concentration) on Alhydrogel (0.7 mg/mL Al^{3+} final concentration). After 2 hours, NaH_2PO_4 100 mM pH 6.5 and NaCl solution 1540 mM were added to reach, respectively, 20 mM and 154 mM in the final formulation, followed by continuous stirring for 30 min. Finally, Vi-CRM_{197} (50 µg/mL Vi final concentration) was added, followed by continuous stirring for 15 h ± 4 h. Further dilutions for immunogenicity studies were performed with Alhydrogel diluent (0.7 mg/mL Al^{3+} in NaCl 154 mM NaH_2PO_4 20 mM pH 6.5).

All the formulations without Alhydrogel were prepared by diluting antigens in NaCl 154 mM NaH_2PO_4 20 mM pH 6.5.

Formulations characterization

All formulations with Alhydrogel were characterized in terms of not adsorbed antigens. The supernatants collected after 0.2 µm centrifugal filtration by nanosep were analysed by HPLC-RP MS [214] to quantify unabsorbed lipid A GMMA content using the method described above. Alternatively, the % of not adsorbed GMMA was measured via HPAEC-PAD using the methods described in Chapter 3 for *S. sonnei* OAg and total *S. flexneri* OAg. Furthermore, the same supernatants were analysed via HPAEC-PAD [216, 217] for free O:2 and Vi content, using the method described above for Vi and the one reported in Chapter 5 for O:2.

Scheme 4.1. Formulation conditions 1, 2 and 3 tested for obtaining hexavalent *Shigella-Salmonella* combinations.

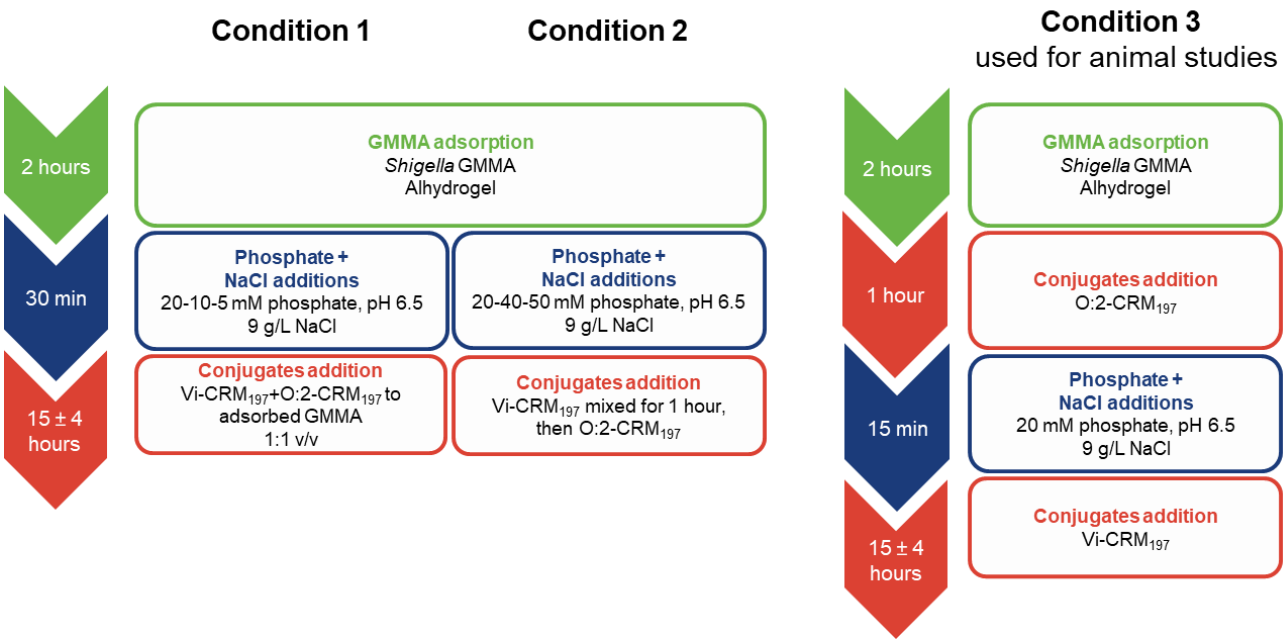

In vivo Studies

Mouse, rabbit and rat studies were performed at the GSK Animal Facility (Siena, Italy), in compliance with the relevant legislation (Italian D.Lgs. n. 26/2014 and European Directive 2010/63/UE) and the institutional animal welfare policies of GSK. The facility is AAALAC-accredited. The animal protocols were approved by the Italian Ministry of Health (projects No.: 643/2021-PR with approval date 12/08/2021; 817/2024-PR with approval date 29/08/2024).

GSK is committed to the Replacement, Reduction and Refinement of animal studies (3Rs). Non-animal models and alternative technologies are part of our strategy and employed where possible. When animals are required, application of robust study design principles and peer review minimises animal use, reduces harm and improves benefit in studies.

Female, 5 weeks old, CD1 mice (10 per group) were vaccinated intraperitoneally (i.p.) with 200 µL of formulated antigens at study day 0 and 28. Individual sera were collected at days 27 and 42.

Female New Zealand White rabbits Crl:KBL(NZW) (6 per group) were vaccinated intramuscularly (i.m.) with 500 µL of formulated antigens at study day 0 and 28. Single sera were collected on study days 27 and 42. Maximum volume of blood was sampled according to animal welfare's good practices.

Female, 8 weeks old, Sprague Dawley rats (8 per group) were vaccinated i.m. with 200 µL of formulated antigens at study day 0 and 28. Individual sera were collected at days 27 and 42.

Sera analyses

Sera collected at different time points were analysed by ELISA according to the procedure described in Chapter 3 [178, 194, 239], using as ELISA coating antigens: *S. sonnei* LPS at the concentration of 0.5 µg/mL in PBS, *S. flexneri* 1b OAg at the concentration of 2 µg/mL in Carbonate Buffer, *S. flexneri* 2a OAg at the concentration of 5 µg/mL in Carbonate Buffer, *S. flexneri* 3a OAg at the concentration of 1 µg/mL in PBS, *Salmonella* Paratyphi A OAg at the concentration of 2 µg/mL in Carbonate Buffer, Vi PS at the concentration of 1 µg /mL in phosphate buffer.

Individual serum samples collected at day 42 were also tested against bacterial strains (*S. sonnei* 53G virG::cat [221], *S. flexneri* 1b, Stansfield NTCT 5 strain; *S. flexneri* 2a, 2457T strain and *S. flexneri* 3a, NCTC9989 strain; *S.* Paratyphi A ED199 strain) in SBA based on luminescent readout as described in Chapter 3 [223, 240, 241]. Baby rabbit complement (BRC) was used 20% for *S. sonnei* and *S.* Paratyphi A, 15% in the case of *S. flexneri* 1b and 3a, and 7.5% for *S. flexneri* 2a.

Statistics

Statistical analysis was performed using GraphPad Prism 7 or 10. Mann-Whitney two-tailed test was used to compare the immune response elicited by two different groups. Wilcoxon test matched-pairs signed rank two-tailed test was performed to compare the response induced by the same formulation at different timepoints.

4.3. RESULTS

4.3.1. Hexavalent formulation against both *Shigella* and *Salmonella*

The four *Shigella* GMMA from *S. sonnei*, *S. flexneri* 1b, 2a and 3a were combined with *S.* Typhi Vi-CRM_{197} and *S.* Paratyphi A O:2-CRM_{197} glycoconjugates. The different drug substances, whose main characteristics are reported in **Table 4.1**, were combined at their highest envisaged human dose, corresponding to 15 µg of each *Shigella* OAg and 25 µg of each *Salmonella* PS. The 4-valent *Shigella* vaccine uses Alhydrogel as adsorbent, to contribute in reducing potential residual GMMA endotoxicity, while Vi-CRM_{197} is licensed without any adjuvant. To account for both situations, the vaccine was formulated with and without Alhydrogel.

With Alhydrogel, different formulation tests were performed, in order to have GMMA mainly adsorbed in the final formulation. The addition of the two *Salmonella* glycoconjugates did not decrease the adsorption of GMMA on Alhydrogel, which was >95%, as verified by analysing lipid A content in the supernatant. In all the conditions used, the Vi-CRM_{197} was mainly not adsorbed (55-85% not adsorbed Vi) whereas, by changing the concentrations of the phosphate buffer in the formulation conditions, not adsorbed O:2-CRM_{197} ranged from 8 to 79% (**Table 4.2**). In the following animal studies, the formulation condition used were similar to those adopted for the *Shigella* GMMA vaccine, with 20 mM of phosphate buffer (**Table 4.2**).

Table 4.1. Main characteristics of GMMA and glycoconjugates used to formulate the hexavalent vaccine.

Sample	PS/protein weight ratio	Free PS %	Lipid A/OAg (nmol/µg)	Lipid A/total protein (nmol/µg)	PS molecular size distribution (KDa)	Particle Size Z-average (diameter in nm) PDI
S. sonnei GMMA	0.32	na	0.56	0.18	247.3 18.7 2.2	162.8 0.206
S. flexneri 1b GMMA	1.18	na	0.39	0.46	13.8 1.7	108.9 0.18
S. flexneri 2a GMMA	1.11	na	0.22	0.25	47.1 14.2 1.8	109.7 0.14
S. flexneri 3a GMMA	1.17	na	0.37	0.43	15.5 1.8	82.5 0.1
Vi-CRM_{197}	0.41	10.2	na	na	46.5	na
O:2-CRM_{197}	0.69	4.7	na	na	100 16	na

na: not applicable

Table 4.2. Different hexavalent formulation composition and formulates characterization. All the formulations have the following final composition: 30 µg/mL OAg (each GMMA, corresponding to 46.2 nmol/mL total Lipid A); 50 µg/mL Vi; 50 µg/mL O:2; 0.7 mg/mL Al^{3+}; 154 mM NaCl. The concentration of sodium phosphate (NaPi) is reported, for each formulation, in the first column of the Table.

Formulation	**Formulation procedure**	**Not adsorbed O:2 %**	**Not adsorbed Vi %**	**Not adsorbed Lipid A %**
Hexavalent_ 5 mM NaPi	**Condition 1:** GMMA adsorption on Alum (2 hours), NaPi and NaCl addition (30 minutes), conjugates addition (15 h ± 4 hours)	<18	na	<1
Hexavalent_ 10 mM NaPi		<18	55	<1
Hexavalent_ 20 mM Napi		<18	65	<1
Hexavalent_ 50 mM NaPi		66	70	nd (via HPAEC-PAD)
Hexavalent_ 20 mM NaPi	**Condition 2:** GMMA adsorption on Alum (2 hours), NaPi and NaCl addition (30 minutes), Vi-CRM_{197} addition (1 hour), O:2-CRM_{197} addition (15 h ± 4 hours)	<18	71	<1
Hexavalent_ 40 mM NaPi		37	81	<1
Hexavalent_ 50 mM NaPi		79	85	<1
Hexavalent_ 20 mM NaPi	**Condition 3:** GMMA adsorption on Alum (2 hours), O:2-CRM_{197} addition (1 hour), NaPi and NaCl addition (15 minutes), Vi-CRM_{197} addition (15 h ± 4 hours)	8	77	1

4.3.2. Immunogenicity study of the hexavalent formulation in mice

The hexavalent formulations with and without Alhydrogel were tested in mice. Animals were injected twice i.p., 28 days apart, at 1/200 of the highest expected human dose. The 4-valent *Shigella* GMMA and the bivalent *Salmonella* glycoconjugates, with and without Alhydrogel, were included in the study for comparison.

The hexavalent formulation, irrespective of the presence of Alhydrogel, was able to induce a significant IgG response against all antigens 27 days (T27) after the first injection (**Figure 4.1(A)**). Only for the O:2 component, in the absence of Alhydrogel, the second injection was needed for a significant response. After the second injection (T42), the IgG responses further increased for all components (*P* values < 0.005; T27 *vs* T42 of the hexavalent vaccine against *S.* Paratyphi A, *S.* Typhi *S. flexneri* 1b, 2a, 3a). Only for *S. sonnei* there was a non-statistically significant increase of IgG for the formulation with Alhydrogel (*P* value > 0.005; T27 *vs* T42 of the hexavalent vaccine against *S. sonnei*). All sera, tested after the second injection, showed serum bactericidal activity against *S.* Paratyphi A and *Shigella* serotypes, except for the antibodies against *S.* Paratyphi A elicited by the formulation without Alhydrogel (**Figure 4.1(B)**).

Impact of Alhydrogel on IgG responses induced by the hexavalent formulation was also assessed. Anti-Vi, -O:2, and -*Shigella flexneri* 1b and 3a IgG responses were higher when Alhydrogel was present in the formulation, whereas anti-*S. sonnei* and S. *flexneri* 2a IgG responses were similar with or without it (**Figure 4.1(A)**). Additionally, the hexavalent formulation with Alhydrogel induced higher bactericidal titers against *S.* Paratyphi A, *Shigella flexneri* 1b, 2a and 3a. No difference was observed for *S. sonnei* (**Figure 4.1(B)**).

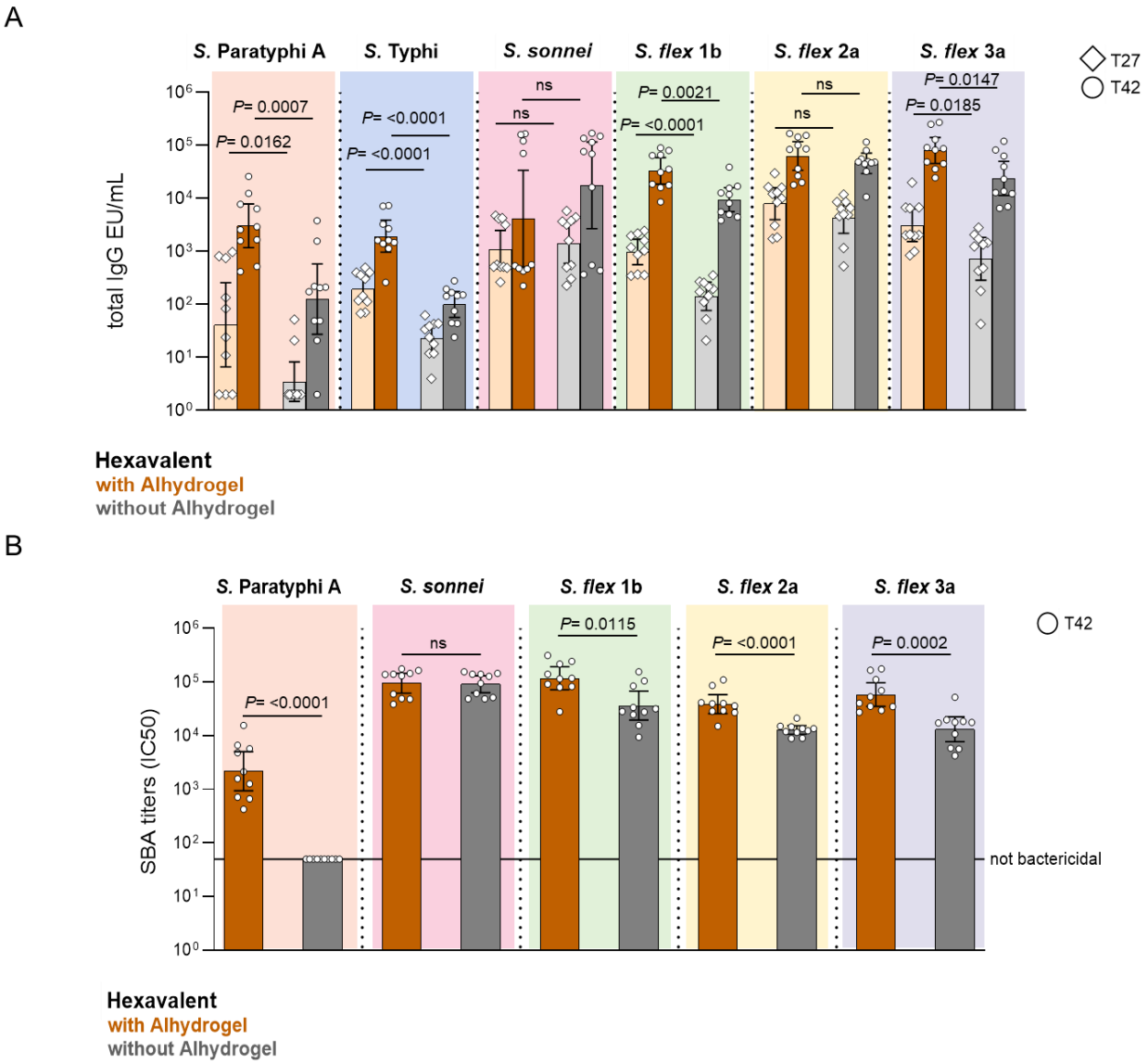

Figure 4.1. Hexavalent formulation tested in mice with and without Alhydrogel. CD1 mice were immunized i.p. at day 0 and 28 with 75 ng/dose of each *Shigella* GMMA OAg and 125 ng/dose of each *Salmonella* glycoconjugate. Concentration of Alhydrogel, if present, was 0.7 mg/mL (Al^{3+}). Sera collected at days 27 (T27) and 42 (T42) were analysed by (A) ELISA for OAg-specific total IgG (*S. sonnei*, *S. flexneri* and *S.* Paratyphi A), or for Vi total IgG expressed as EU/mL. Sera collected at T42 were analysed by (B) SBA for species/serotype-specific bactericidal titers expressed as IC50. Summary graphs of geometric mean units (bars) and individual levels (dots) are reported.

Importantly, when comparing the hexavalent formulation with Alhydrogel to the corresponding bivalent *Salmonella* and 4-valent *Shigella* formulations, no evidence of negative immuno-interference was observed. Similar IgG responses (after both the first and the second injections) and bactericidal titers (after second injection) were induced by all formulations (**Figure 4.2(A-D)**) against all components. The only exception was *S. flexneri* 3a, for which the hexavalent formulation induced lower bactericidal titers compared to the 4-valent *Shigella* GMMA (**Figure 4.2(D)**). For *S.* Typhi and *S.* Paratyphi A, the hexavalent formulation induced more homogeneous responses, both in ELISA and SBA and with a tendency toward a higher response compared to the bivalent formulation (**Figure 4.2(A,C)**).

Interestingly, in the absence of Alhydrogel, the presence of GMMA in the hexavalent formulation led to significantly higher anti-Vi (at both timepoints) and anti-O:2 (at day 42) IgG responses, compared to those induced by the bivalent vaccine (**Figure 4.2(A)**). However, without Alhydrogel, sera against *S.* Paratyphi A were not bactericidal, even in the presence of GMMA (**Figure 4.2(C)**).

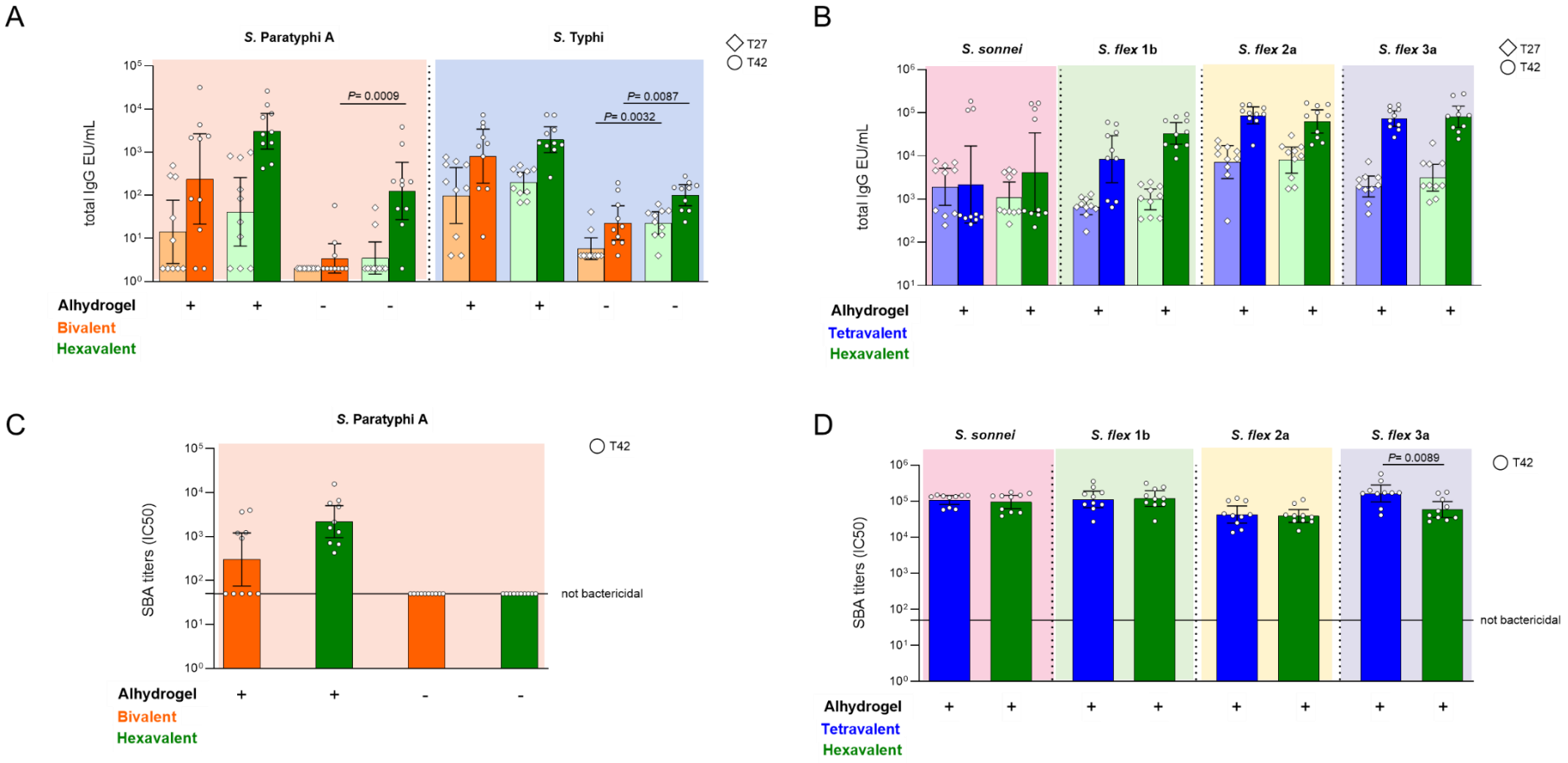

Figure 4.2. Hexavalent formulation tested in mice with and without Alhydrogel in comparison to bivalent *Salmonella* glycoconjugate and *Shigella* tetravalent GMMA vaccines. CD1 mice were immunized intraperitoneally (i.p.) at day 0 and 28 with 75 ng/dose per each *Shigella* GMMA OAg and 125 ng/dose per each *Salmonella* glycoconjugate. Concentration of Alhydrogel, if present, was 0.7 mg/mL (Al^{3+}). Sera collected at days 27 (T27) and 42 (T42) were analysed by (A,B) ELISA for OAg-specific (*S. sonnei*, *S. flexneri* and *S.* Paratyphi A) or Vi total IgG (EU/mL). Sera collected at T42 were analysed by (C,D) SBA for bactericidal titers expressed as IC50. Summary graphs of geometric mean units (bars) and individual levels (dots) are reported.

4.3.3. Immunogenicity study of the hexavalent formulation in rabbits

The hexavalent formulation with Alhydrogel was also tested in rabbits, and compared with the 4-valent *Shigella* GMMA [78, 194] and the bivalent *Salmonella* glycoconjugates [178] [Alfini R. et al., submitted]. Rabbits were injected i.m. at the maximum envisaged human dose of each antigen (15 µg *Shigella* OAg and 25 µg *Salmonella* PS).

Consistent with previous observations in mice, the hexavalent formulation induced significant IgG responses against each component in rabbits 27 days after the first injection, with a further increase following the second dose, except for *S. sonnei* (**Figure 4.3(A)**). Antibodies induced after two immunizations were bactericidal (**Figure 4.3(B)**).

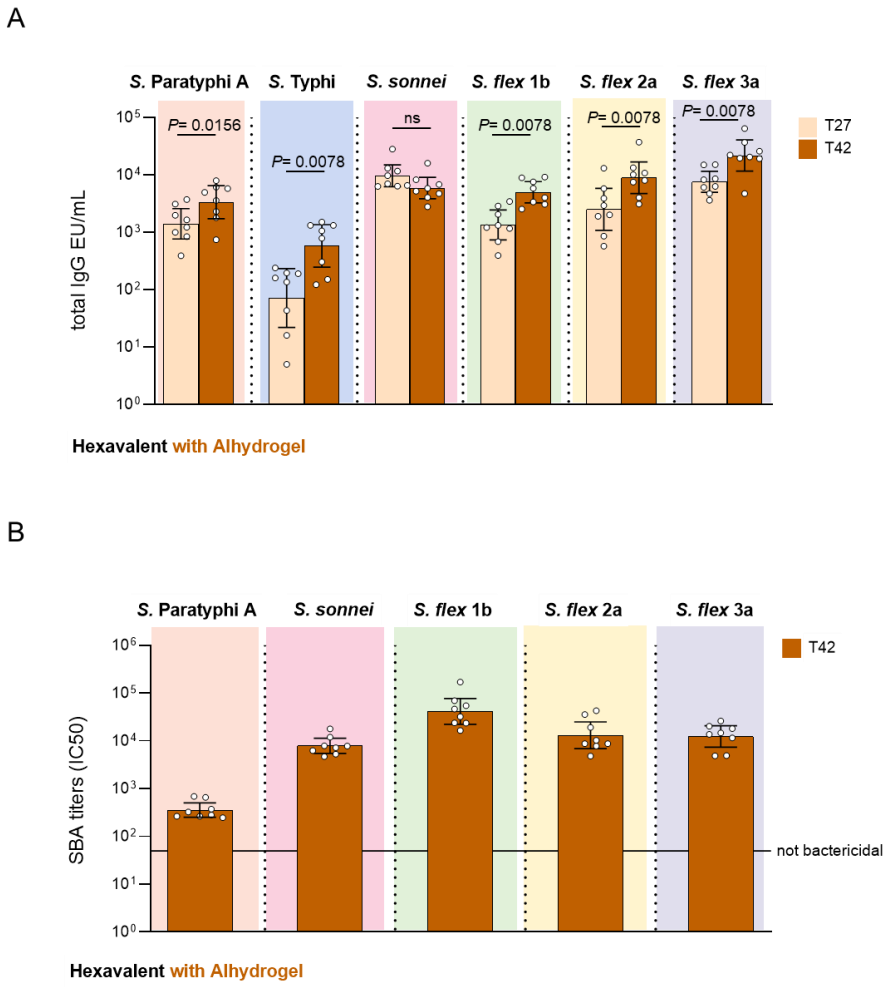

Figure 4.3. Hexavalent formulation tested in rabbits. New Zealand rabbits were immunized intramuscolarly (i.m.) at day 0 and 28 with 15 µg/dose per each *Shigella* GMMA OAg and 25 µg/dose per each *Salmonella* glycoconjugate. Concentration of Alhydrogel was 0.7 mg/mL (Al^{3+}). Sera collected at T27 and T42 were analysed by (A) ELISA for OAg-specific total IgG (*S. sonnei*, *S. flexneri* and *S.* Paratyphi A), or for Vi total IgG expressed as EU/mL. Sera collected at T42 were analysed by (B) SBA for species/serotype-specific bactericidal titers expressed as IC50. Summary graphs of geometric mean units (bars) and individual levels (dots) are reported.

Similarly to mice, no evidence of negative immuno-interference was observed in rabbits. The hexavalent formulation induced comparable responses to the *Salmonella* bivalent and *Shigella* 4-valent formulations (**Figure 4.4(A-D)**). Additionally, as already observed in mice, the presence of GMMA in the hexavalent formulation resulted in a more homogeneous SBA response against *S.* Paratyphi A, with a tendency toward higher response compared to the bivalent formulation (GMR hexavalent/bivalent = 2.17) (**Figure 4.4(C)**).

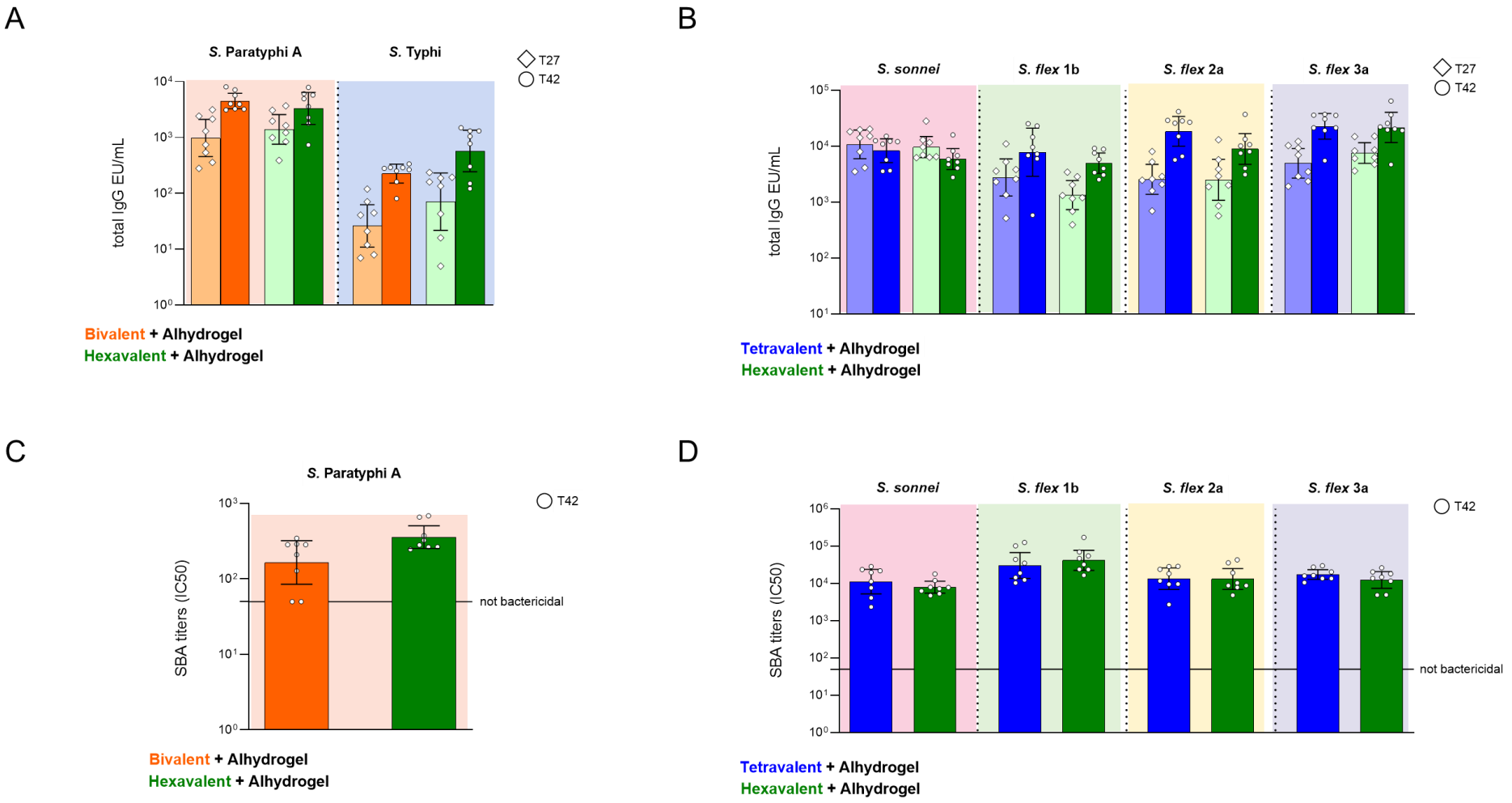

Figure 4.4. Hexavalent formulation tested in rabbits in comparison to bivalent *Salmonella* glycoconjugate and *Shigella* tetravalent GMMA vaccines. New Zealand rabbits were immunized i.m. at day 0 and 28 with 15 µg/dose per each *Shigella* GMMA OAg and 25 µg/dose per each *Salmonella* glycoconjugate. Concentration of Alhydrogel was 0.7 mg/mL (Al^{3+}). Sera collected at T27 and T42 were analysed by (A,B) ELISA for OAg-specific (*S. sonnei*, *S. flexneri* and *S.* Paratyphi A) or Vi total IgG (EU/mL). Sera collected at T42 were analysed by (C,D) SBA for bactericidal titers expressed as IC50. Summary graphs of geometric mean units (bars) and individual levels (dots) are reported.

4.3.4. Immunogenicity study of the hexavalent formulation in rats

The hexavalent formulations, with and without Alhydrogel, were also tested in rats, in comparison with corresponding bivalent and tetravalent control groups, which were similarly formulated with and without Alhydrogel. For *Shigella*, it was verified that the rat model best mimic human responses [Caradonna V. et al., submitted]. Moreover, the rat model is frequently used to evaluate the immunogenicity of multivalent vaccines in which immuno-interference among various antigens may occur [242, 243]. The rats received two i.m. injections 28 days apart, with each dose containing 0.6 µg of OAg per *Shigella* GMMA and 1.0 µg per *Salmonella* glycoconjugate.

Both the hexavalent formulation with Alhydrogel and the one without induced significant IgG responses against all antigens 27 days after the first vaccination; a booster effect was observed after the second injection (*P* values < 0.005; T27 *vs* T42 of the hexavalent vaccine against *S.* Paratyphi A, *S.* Typhi, *S. flexneri* 1b, 2a, 3a, *S. sonnei*). All sera, at day 42, showed serum bactericidal activity against *S.* Paratyphi A and the *Shigella* serotypes (**Figure 4.5(B)**).

The presence of Alhydrogel had a different impact on the specific IgG responses induced by the hexavalent formulation. Anti-Vi (both timepoints), -O:2 (only post 2) and -*Shigella flexneri* 1b OAg (only post 1) IgG responses were higher when Alhydrogel was present in the formulation, whereas anti-*S. sonnei* (post 2) and -*S. flexneri* 2a (post 1) OAg IgG responses were stronger without it. The responses against *S. flexneri* 3a were similar regardless of Alhydrogel (**Figure 4.5(A)**), and no differences were evidenced in SBA (**Figure 4.5(B)**).

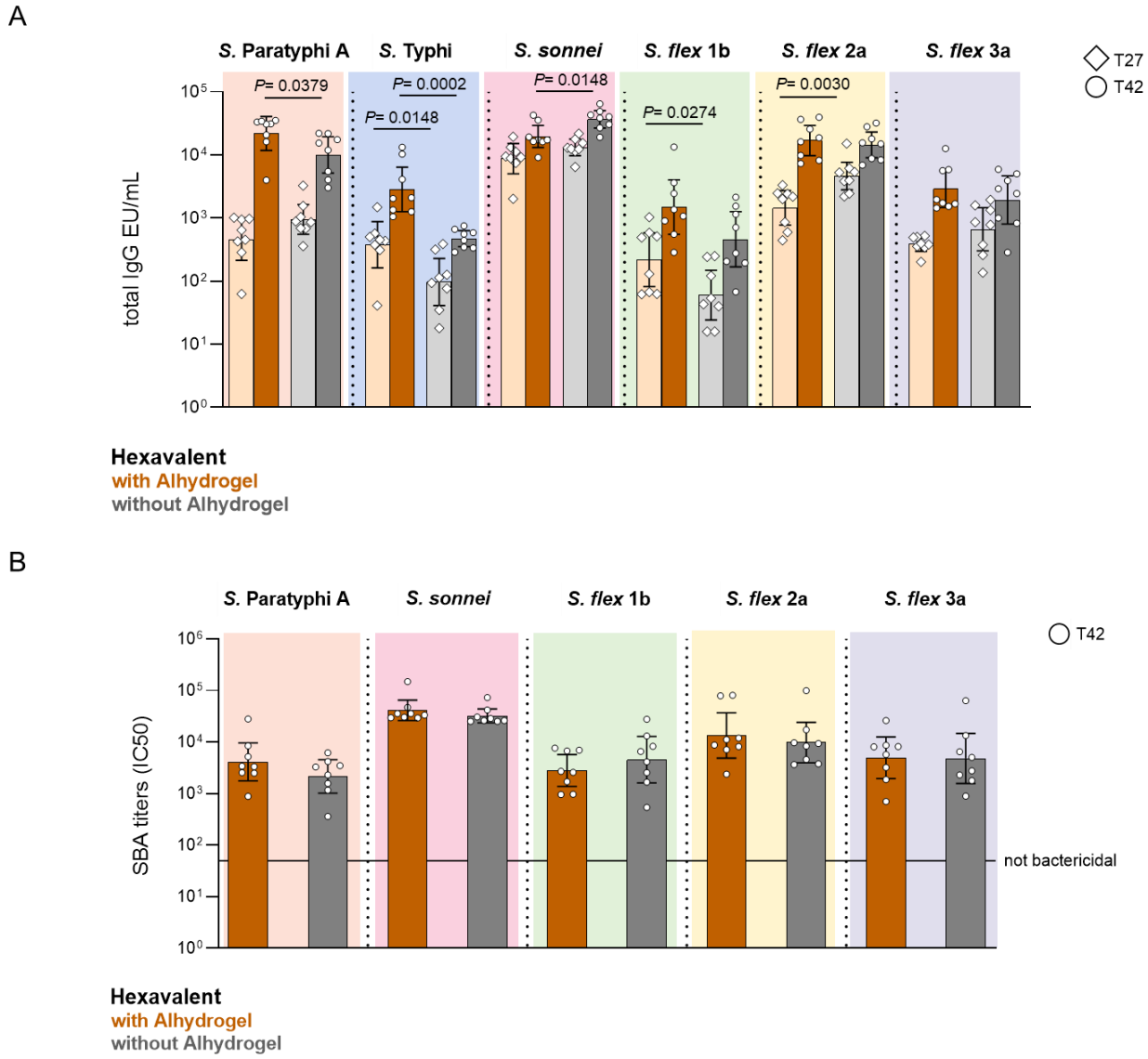

Figure 4.5. Hexavalent formulation tested in rats with and without Alhydrogel. Sprague Dawley rats were immunized i.m. at day 0 and 28 with 0.6 µg/dose of each *Shigella* GMMA OAg and 1 µg/dose of each *Salmonella* glycoconjugate. Concentration of Alhydrogel, if present, was 0.7 mg/mL (Al^{3+}). Sera collected at days 27 (T27) and 42 (T42) were analysed by (A) ELISA for OAg-specific total IgG (*S. sonnei*, *S. flexneri* and *S.* Paratyphi A), or for Vi total IgG expressed as EU/mL. Sera collected at T42 were analysed by (B) SBA for species/serotype-specific bactericidal titers expressed as IC50. Summary graphs of geometric mean units (bars) and individual levels (dots) are reported.

When comparing the hexavalent formulation with Alhydrogel to the corresponding bivalent *Salmonella* formulations, all vaccines induced similar anti-Vi IgG responses after both the first and second injections. Although the hexavalent formulation elicited a higher anti-O:2 IgG response than the bivalent vaccine after the second injection, the bivalent formulation induced higher SBA titers (**Figure 4.6(A,C)**). In the absence of Alhydrogel, no differences were observed in the responses against *S.* Paratyphi A, both IgG and SBA, while the hexavalent formulation elicited a lower anti-Vi IgG response after the first injection compared to the bivalent vaccine (**Figure 4.6(A,C)**).

No evidence of negative immuno-interference was observed in the responses against *Shigella* when comparing the hexavalent formulation to the tetravalent *Shigella* GMMA vaccine, regardless of the presence of Alhydrogel. Similar IgG responses were observed for most components—but for *S. flexneri* 1b, for which the hexavalent formulation induced higher titers than the bivalent vaccine—and comparable bactericidal titers were induced after the second injection by all formulations against all components (**Figure 4.6(B,D)**). However, for *S. flexneri* 3a, in the absence of Alhydrogel, the hexavalent formulation induced lower bactericidal titers compared to the tetravalent *Shigella* GMMA (**Figure 4.6(D)**).

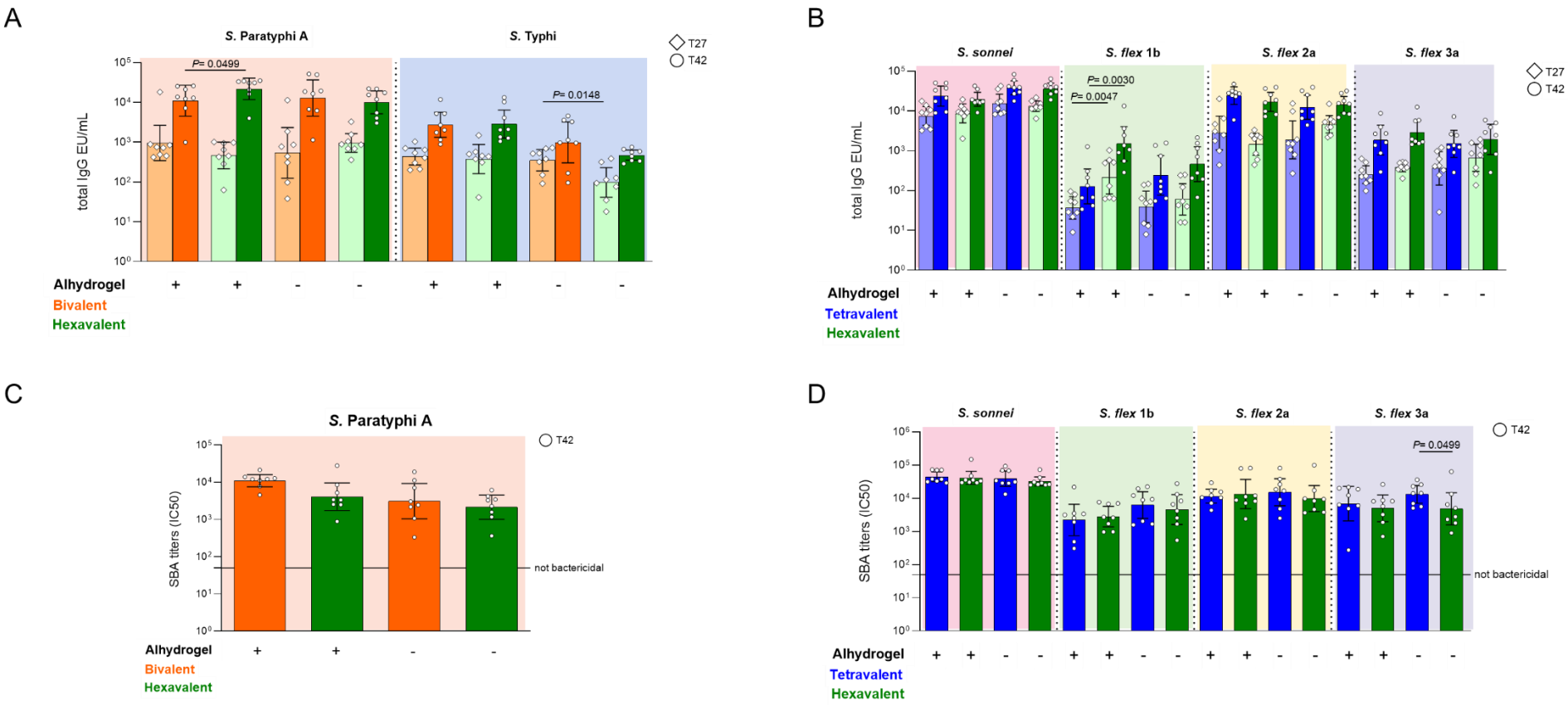

Figure 4.6. Hexavalent formulation tested in rats with and without Alhydrogel in comparison to bivalent *Salmonella* glycoconjugate and *Shigella* tetravalent GMMA vaccines. Sprague Dawley rats were immunized i.m. at day 0 and 28 with 0.6 µg/dose per each *Shigella* GMMA OAg and 1 µg/dose per each *Salmonella* glycoconjugate. Concentration of Alhydrogel, if present, was 0.7 mg/mL (Al^{3+}). Sera collected at days 27 (T27) and 42 (T42) were analysed by (A,B) ELISA for OAg-specific (*S. sonnei*, *S. flexneri* and *S.* Paratyphi A) or Vi total IgG (EU/mL). Sera collected at T42 were analysed by (C,D) SBA for bactericidal titers expressed as IC50. Summary graphs of geometric mean units (bars) and individual levels (dots) are reported.

4.1. DISCUSSION

Shigella is leading bacterial cause of diarrhea-related mortality and is associated with linear growth faltering and stunting [244]. Its resistance to nearly all antimicrobial classes is increasing in prevalence and becoming globally dominant, highlighting the urgent need of new interventions to prevent and treat *Shigella* infections [245]. Several vaccine candidates are approaching phase 3 clinical trials [139] and the pathway for licensure of a standalone vaccine has been defined [231]. However, combination of a *Shigella* vaccine with other infant vaccine candidates could increase its commercial attractiveness and has recently been recommended [233].

Different criteria can drive the selection of an optimal combination vaccine, including technical and clinical feasibility, diseases attributes (burden of disease, geography, target population, etc..), stakeholder interest and speed of development.

Licensed typhoid conjugate vaccines have been considered among the most easily and valuably vaccines to combine with a *Shigella* candidate [77]. Moreover, a licensure pathway to combine TCV with *S.* Paratyphi A is already in place [75].

In my PhD project, for the first time, a multivalent *Shigella* vaccine was successfully combined with a *Salmonella* bivalent formulation, containing both typhoid and paratyphoid conjugate vaccines, demonstrating that a combination of multiple GMMA and glycoconjugates is technically feasible and immunogenic. When choosing the components of the hexavalent formulation, candidate vaccines already advanced in clinic were selected. In particular, the 4-component *Shigella* GMMA vaccine, which is in phase 2 clinical trials in the target population (clinical trials NCT05073003 and NCT06663436), and the bivalent glycoconjugate *Salmonella* vaccine, which has completed phase 1 (clinical trial NCT05613205), were used.

To account for the presence of Alhydrogel as an adsorbent in the tetravalent *Shigella* vaccine [78], formulation conditions to combine GMMA and *Salmonella* glycoconjugates, without impacting their adsorption were identified. However, recent studies suggest no need of Alhydrogel neither to increase GMMA magnitude, quality, or functionality of the antibody response induced [194, 213] nor to reduce their potential residual reactogenicity. *Shigella* GMMA formulated without Alhydrogel were well tolerated in rabbits [213] and analysis by a human monocyte activation test (MAT) showed that GMMA, with or without Alhydrogel, induce a similar level of IL-6 release [213, 246]. For this reason, both formulation with and without Alhydrogel were tested in mice and rats, observing an enhanced antibody response against *S.* Paratyphi A, *Shigella flexneri* 1b, 2a and 3a when Alhydrogel was used,

and no difference for *S. sonnei* in mice; no differences in antibody response was detected in rats. The results in mice are different from what previously observed with GMMA only, in which presence of Alhydrogel did not result in an increased humoral response [194]. We can assume that, in a more complex formulation, the presence of Alhydrogel could favor the response directed against each antigen.

In general, multivalent formulations are quite complex, and there is the need to develop and validate appropriate assays to accurately characterise each component [180]. PS content is one of the critical quality attributes of a PS-based vaccine, and the availability of analytical methods to independently quantify each single PS antigen is fundamental for vaccine release, as well as to monitor its stability and ensure appropriate immune responses.

Methods have been developed to independently quantify the Vi PS, O:2, *S. sonnei* and *S. flexneri* OAg [214, 216, 217] and to check their adsorption on Alhydrogel and they will serve to measure the stability of the single components in the multivalent formulation. In particular, the method for O:2 quantification was developed in the context of this PhD project and will be described in depth in Chapter 5.

In general, combination vaccines may be less effective than vaccines administered separately, as one of the potential risks of multivalent vaccines failure could be due to negative immunological interference [180]. Here, it was shown—in mice, rabbits and rats—the possibility to combine the 6 different antigens with no negative impact on the humoral immune response elicited by each of them. The results obtained in the different animal models are summarized in **Table 4.3**.

Table 4.3. Comparison of hexavalent formulation *vs* bivalent and tetravalent vaccines in animals, in the presence or absence of Alhydrogel.

Alhydrogel	Response	Mice	Rabbits	Rats
+	*S.* Paratyphi A	Similar	Similar	Lower SBA
	S. Typhi	Similar	Similar	Similar
	S. sonnei	Similar	Similar	Similar
	S. flexneri 1b, 2a, 3a	Similar, except lower SBA against 3a	Similar	Similar
-	*S.* Paratyphi A	Similar (no SBA)	Not tested	Similar
	S. Typhi	Higher IgG, both timepoints	Not tested	Lower IgG, post 1
	S. sonnei	Not tested	Not tested	Similar
	S. flexneri 1b, 2a, 3a	Not tested	Not tested	Similar, except lower SBA against 3a

A combined vaccine against *Shigella* and *Salmonella* has the potential to address a huge medical need considering a burden of 148,202 deaths and 10.6 million disability-adjusted life-years (DALYs) caused by *Shigella,* 110,029 deaths and 8.0 million DALYs caused by typhoid fever, 23,337 deaths and 1.6 million DALYs caused by paratyphoid fever, among all ages in 2019 [154]. In addition, *Shigella* and TCV affect same regions in Africa and Asia, and *S.* Paratyphi A mainly affect Asia [154].

The *Shigella* and *Salmonella* vaccines both target infants. A possible obstacle to their combination could be related to the number of doses required and age of the target population. Indeed, TCV is a one-dose vaccine, while 2 doses could be needed for *Shigella* and/or *S*. Paratyphi A. Furthermore, to extend protection, recent data on persistency of antibodies elicited by TCV could suggest the need for a booster dose, ~5 years after their primary dose, or delay in the vaccination [247].

Licensed TCVs are currently administered at the WHO 9-month or 15-month Expanded Programme on Immunization (EPI) time point. This age is compatible with bivalent enteric fever vaccines in development, as paratyphoid A is uncommon in children aged <9 months [75]. For *Shigella,* the peak

of disease is in the second year of life and the current WHO Preferred Product Characteristics (PPC) preference is for a maximum of 2 primary doses in children <1 year of age [248].

Development of such multicomponent vaccines also requires more thoughts about the clinical development pathway considering current regulatory guidelines [180]. Despite some difficulties in the selection of an optimal combination of a *Shigella* vaccine, this work represents the first evidence of the possibility to combine *Shigella* with *Salmonella* bivalent glycoconjugates and presents main criteria that could drive the development of multi-component vaccines, highlighting their benefits to address huge medical needs with strong impact on global health.

5. Development of novel analytical methods for identification and quantification of each single polysaccharide antigen in *Shigella* and *Salmonella* OAg-based multivalent formulations

5.1. INTRODUCTION

Polysaccharide-based vaccines are characterized by many critical quality attributes (CQAs) that need to be evaluated during the manufacturing process, in order to ensure and confirm vaccine's identity, content, potency, stability, purity and sterility. In particular, the quantification of PS, as active ingredient, is crucial for vaccine release, to monitor stability, to ensure appropriate immune response and to serve as a measure of the vaccine's potency. Consequently, it is important to identify robust and precise analytical methods, whether physicochemical or biological, to accurately quantify the saccharide content [249]. In the case of multivalent vaccines, finding a single procedure that is suitable for the specific measurement of all the combined components is particularly challenging.

Many methods can be used for the determination of PS content [249]. HPAEC-PAD is a reliable technique for the quantification of the monosaccharides constituting the polysaccharide. This method is characterized by very high levels of precision, reproducibility, and specificity for saccharide quantification; moreover, it does not involve carbohydrate derivatization for sensitive detection [250, 251]. Polysaccharide antigens need to be analyzed after cleavage of their glycosidic bonds, to release the monosaccharide units. The hydrolysis step is typically specific to each polysaccharide, as it depends on the repeating unit structure, properties, and glycosidic linkage. Notably, when aiming to quantify each individual component in multivalent formulations, it is not possible to identify a single monosaccharide conserved across different polysaccharide antigens [252].

In this study, a novel analytical method based on HPAEC-PAD was developed, enabling the individual identification and quantification of each PS antigen in *Salmonella* OAg-based multivalent formulations.

Multivalent OAg-based vaccines containing the main disease-causing serovars of *Salmonella* enterica are under development [75]. For the non-*Salmonella* Typhi serotypes and *S.* Paratyphi A, OAg is the key target of protective immunity [164-166]. The *Salmonella* OAg share a common backbone constituted of repeating units of mannose, rhamnose, and galactose (glucose can be branched to galactose) and have a different 3,6-dideoxy monosaccharide linked to the backbone [167, 168] (**Figure 5.1**). Dideoxyhexoses such as paratose (Par), abequose (Abe), or tyvelose (Tyv) confer

Salmonella the serogroup specificity (SPa, STm, and SEn OAg, respectively) (**Figure 5.1**) [169-171]. Moreover, *Salmonella* OAg could show high levels of heterogeneity in terms of chain length and variation in O-acetylation and glucosylation of the repeating units [167, 168, 172-175].

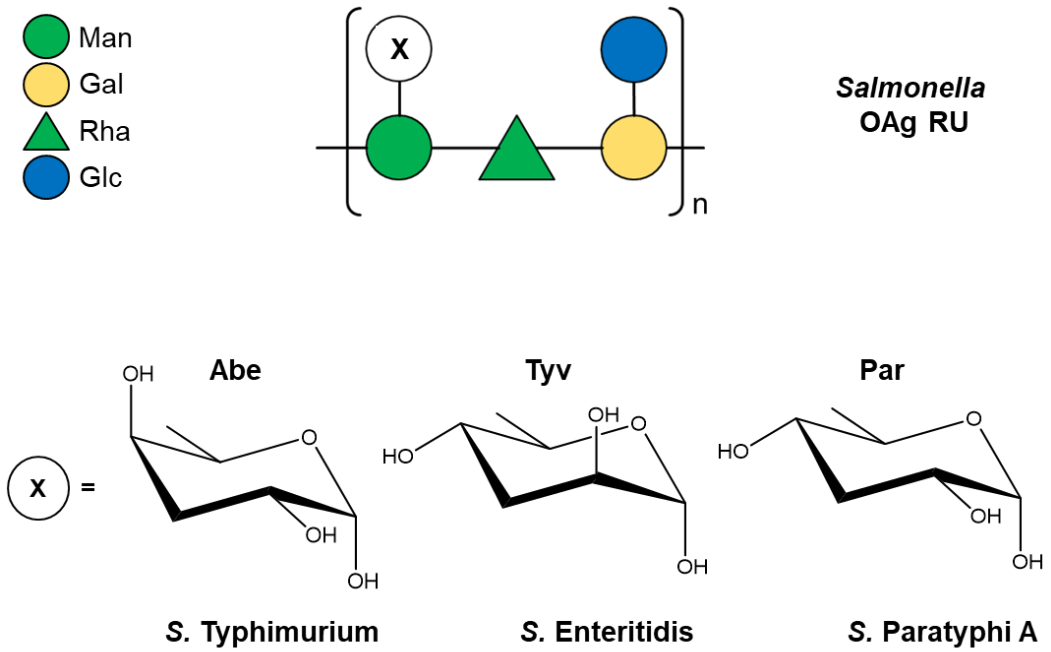

Figure 5.1. OAg repeating unit structures of *S.* Typhimurium, *S.* Enteritidis and *S.* Paratyphi A: common backbone constituted by mannose, rhamnose, and galactose, with a terminal glucose and a different terminal 3,6-dideoxyhexose such as paratose, abequose, or tyvelose conferring serogroup specificity (abequose for *S.* Typhimurium, tyvelose for *S.* Enteritidis and paratose for *S.* Paratyphi A).

In the past, as commercial standards for Abe and Par are not available, and the three dideoxyhexoses are unstable under the hydrolysis condition used for the quantification of the other monomers by HPAEC-PAD, the presence and amount of these sugars have been determined by ^{1}H-NMR [215] or, alternatively, by immunoassays such as competitive Enzyme-linked immunosorbent assay (cELISA) or Formulated Alhydrogel competitive ELISA (FacE) [253-255].

In my PhD project, a novel HPAEC-PAD analysis was developed for the precise and specific detection of the dideoxy monomers allowing identification and, consequentially, quantification of STm, SEn and SPa OAg, also in multivalent formulations.

Just like *Salmonella* serovars, *Shigella* is also associated with AMR, included in the list of pathogens prioritized by the WHO for vaccine development [15]. Different vaccine candidates are under development [73, 139], many of which based on the OAg [197-199], recognized as key target for

protective immunity [145, 200]. The most advanced *Shigella* vaccines share a 4-valent composition consisting of *Shigella flexneri* 2a, 3a, and either 6 or 1b, along with *Shigella sonnei* [148, 149].

While *S. sonnei* has a unique OAg structure **(1)** [216], all *S. flexneri* serotypes, except *S. flexneri* 6 [256], share a common OAg tetra-saccharide backbone **(2)** (corresponding to serotype Y) decorated with glucosylation and O-acetylation in different positions conferring serotype specificity [141, 142].

(→4)-α-L-Alt*p*NAcA-(1→3)-β-Fuc*p*NAc4N-(1→). **(1)**

(→2)-α-L-Rha*p*III-(1→2)-α-L-Rha*p*II-(1→3)-α-L-Rha*p*I-(1→3)-β-D-Glc*p*NAc-(1→). **(2)**

Although HPAEC-PAD methods have already been developed for the specific quantification of the *S. sonnei* and *S. flexneri* 6 OAg [256], the *S. flexneri* 1b, 2a, and 3a OAg, which have the same sugar composition as mentioned, cannot be distinguished using this technique, but can be quantified only as total OAg. Alternatively, immunoassays can be employed [253, 255].

In my project, a novel analytical method based on liquid chromatography (LC) coupled to mass spectrometry (MS) was put in place to quantify the *S. flexneri* 1b, 2a and 3a OAg in multivalent formulations. The OAg were permethylated, following the protocol for linkage analysis the monosaccharides were released by acid hydrolysis and their reducing end were derivatized with 1-phenyl-3-methyl-5-pyrazolone (PMP), to be able to identify specific target monomers differentiated for their linkage in the sugar chain [257, 258].

These novel methods will facilitate the characterization of multivalent *Salmonella* and *Shigella* OAg-based vaccines.

5.2. MATERIALS AND METHODS

5.2.1. HPAEC-PAD method development for *Salmonella* OAg

Materials

Purified STm, SEn and SPa OAg were obtained from GVGH [215, 217].

The OAg-CRM_{197} glycoconjugates were produced by random activation of the OAg chains with $NaIO_4$ and reductive amination with CRM_{197}, as reported for STm in [220]. Briefly, each OAg at 10 mg/mL in AcONa 100 mM pH 5 was stirred for 2 h in the dark with 3.75 mM $NaIO_4$. The mixtures were then quenched 15 minutes with 7.5 mM Na_2SO_3, desalted against water using PD-10 Desalting Columns (Cytiva Life Sciences, Marlborough, MA, USA; formerly GE Healthcare Life Sciences) and lyophilized. The oxidized OAg were then added to CRM_{197} in NaH_2PO_4 100 mM pH 7.2 to a final concentration of 10 mg/mL of oxidized OAg and 5 mg/mL of CRM_{197}. $NaBH_3CN$ was added immediately after at the final concentration of 5 mg/mL, and the reaction mixtures were stirred overnight at 37 °C. Finally, $NaBH_4$ ($NaBH_4$:OAg w/w ratio of 1 to 1) was added to quench residual unreacted aldehydic groups of oxidized OAg. The conjugates were purified by hydrophobic interaction chromatography (HIC), on a Phenyl HP column (Cytiva Life Sciences), loading 500 µg of protein for mL of resin in 20 mM NaH_2PO_4 3 M NaCl pH 7.2. The purified conjugate was eluted against 20 mM NaH_2PO_4 pH 7.2 and the collected fractions were exhanged against PBS by Amicon Ultra (Merck, Darmstadt, Germany) 30 kDa cut-off.

Glucose, Galactose, Mannose, Fucose, Rhamnose, N-acetylglucosamine, Glucosamine, trifluoroacetic acid, $NaIO_4$, Na_2SO_3, $NaBH_3CN$, NaH_2PO_4, NaH_2PO_4, NaCl were purchased from Sigma-Aldrich (Burlington, MA, USA). Tyvelose was purchased from Toronto Research Chemicals (Toronto, ON, Canada). Sodium Hydroxyde 50% was purchased from JT Baker (Radnor, PA, USA).

Optimized hydrolysis conditions

Using an Xstream Electronic Pipettor (Eppendorf, Hamburg, Germany), 30 µL of TFA 4 M were added to 450 µL of a solution containing sample/standard in a 2 mL screw cap vial; the lid was then closed and the content mixed by vortexing. The hydrolysis vials containing samples/standards were placed in a SBH130D/3 Stuart Thermoblock equipped with three preheated SHT1 12 33 Stuart aluminum blocks, at 75 °C for 1.5 hour. The temperature was monitored with a glass thermometer inserted in the aluminum block.

After hydrolysis, the vials were removed from the block heater and cooled to room temperature. The content of the vials was then evaporated to dryness through centrifugal evaporator.

After drying, the content of each vial was redissolved in 450 µL of water and accurately mixed by vortexing. The content of each vial was transferred into a AcroPrep Advance 96 Filter Plate 0.2 µm (Pall, Port Washington, NY, USA), placed over a 96 conical BTM plate (Thermo, Waltham, MA, USA) and centrifuged (Allegra X-15 with SX4750 swinging-bucket rotor and 393070 microplate carrier; Beckmann-Coulter, Brea, CA, USA) at 524 rcf for 2 min to collect filtered samples.

The plate containing filtered sample/standard solutions was covered with the Pre-Slit well Cap for 96 well PP Plate (Thermo, Waltham, MA, USA) and put in the HPAEC-PAD autosampler compartment.

Optimized chromatographic conditions

The chromatographic runs were performed on ICS-6000, ICS-5000 or ICS-3000 equipped with Chromeleon 7.2 (Thermo, Waltham, MA, USA) using the pulsed amperometric mode with gold working electrode and Ag/AgCl reference electrode applying standard quad carbohydrate waveform.

The separation was performed on a Thermo CarboPac MA1 4 × 250 analytical column with Thermo CarboPac MA1 4 × 50 guard column. The column and detector compartments were held at 25 °C, and the sample compartment was held at 10 °C.

Chromatographic condition were the following ones: 10 µL injection volume (partial loop mode), flow rate 0.4 mL/min, total run time 85 minutes.

Eluent program: (I) monosaccharides elution: 45 min, NaOH 60 mM, Sodium acetate 70 mM; (II) washing step: 15 min, NaOH 500 mM; (III) column conditioning: 15 min, NaOH 60 mM, Sodium acetate 70 mM.

For quantification, two calibration curves were run, one at the beginning and one at the end of the sample list. A solution containing standardized STm, SEn and SPa purified OAg was used to build the calibration curves. Each sample was analyzed in triplicate, and the results were averaged.

Characterization of the method

Standard linearity

To assess the linearity of the method, three different replicates of the calibration curve were tested at concentrations of 1.5, 4, 7, 11 and 15 µg/mL per each OAg. The preparation order of the standards and their chromatographic run order were randomized.

A linear regression analysis on the data generated was performed.

Accuracy (spike recovery)

The spike recovery was evaluated on a solution containing a mixture of STm, SEn and SPa OAg-CRM_{197} glycoconjugates. In four different analysis sessions the sample was analyzed diluted to 2 µg/mL, without spiking as a reference and respectively spiked with at 2, 5 and 8 µg/mL of the standard curve. Both sample preparation order and chromatographic run order were randomized. Confidence interval of the spike recovery values was calculated among the different analysis sessions.

Statistical Analysis

Statistical analyses were performed using Minitab 18.1.0 (Minitab Inc., State College, PA, USA).

5.2.2. LC-MS method development for *Shigella flexneri* OAg

Materials

Purified OAg from *S. flexneri* 1b (strain *S. flexneri* 1b Stansfield ΔtolR::frt ΔmsbB1a::frt ΔmsbB1b::frt), 2a (strain *S. flexneri* 2a 2457T ΔtolR::kan, ΔmsbB::cat), 3a (strain *S. flexneri* 3a 6885 ΔtolR::kan) GMMA, were obtained from GVGH [217].

Shigella flexneri 1b, 2a and 3a GMMA were obtained from GVGH [78].

Glucose, *N,N′,N″*-triacetylchitotriose, sucrose, iodomethane (MeI), PMP, acetonitrile (ACN), dichloromethane (DCM), dimethylsulfoxide (DMSO), trifluoroacetic acid (TFA), ammonia solution 28.0% in water, methanol, NH_4Ac were purchased from Sigma-Aldrich (Burlington, MA, USA). Sodium Hydroxyde 50% was purchased from JT Baker (Radnor, PA, USA).

Permethylation Reaction

Shigella flexneri 1b, 2a and 3a purified OAg (separately or in combination) and corresponding GMMA (in combination) were permethylated using iodomethane in a solution of DMSO and concentrated NaOH.

The NaOH-DMSO base was freshly prepared before each permethylation reaction [259]. First, 100 µL of a 50% w/w aqueous NaOH solution was mixed vigorously with 200 µL of methanol. Next, approximately 4 mL of DMSO was added to the mixture and shaken vigorously, causing the bicarbonates present in the NaOH solution to precipitate as a white, fluffy solid. The tube was then centrifuged at 3000 × g for 5 minutes, and the precipitated white solid at the top—along with the

excess DMSO—was carefully removed, ensuring that the bluish sol at the bottom was retained. This process was repeated four additional times until no further white solid precipitation was observed. Finally, the resulting NaOH-DMSO sol at the bottom was mixed with 1 mL of DMSO and used directly for the permethylation reaction.

The protocol reported in [259] was followed with slight modifications. Following lyophilization, the samples (10 or 100 µg of each purified OAg or GMMA) were resuspended in 50 µL of DMSO. Then, 75 µL of the NaOH base in DMSO were added, followed by 25 µL of MeI. The reaction mixtures were gently mixed for 30 minutes at RT. At the end, 100 µL of ice-cold water, which prevents temperature increases and degradation from the "peeling" reaction, was added.

To remove the excess of the reagents, a classic liquid-liquid extraction was performed with 1 mL DCM, followed by four washes with ice-cold water. The upper aqueous layers were discarded, and the remaining organic layer containing permethylated OAg was collected and dried.

To increase the throughput of the procedure, in alternative to the liquid-liquid extraction, the quenched mixtures were loaded onto C18 tips (Thermo Scientific, Waltham, MA, USA), preconditioned with ACN and preequilibrated with water. These tips retained the permethylated samples, while the solvents were expelled and discarded. Subsequently, the tips were washed five times with 100 µL of water, and the permethylated samples were eluted using 5 x 100 µL of ACN and then dried.

Acid Hydrolysis Conditions

Using screw cap vials, the dried permethylated samples were resuspended in a solution of 1:1 water to TFA 8 M v/v, resulting in a final concentration of TFA 4 M. The vials were placed in oven, at 100 °C for 4 hours. After hydrolysis, the content of the vials was evaporated to dryness through centrifugal evaporator.

Derivatization with PMP

The released permethylated monosaccharide residues were derivatized with PMP, following the procedure published in [260]. Briefly, the samples were added of 100 µL of water and mixed with 400 µL ammonia solution 28.0% in water and 400 µL 0.2 M PMP solution in methanol. The mixtures were placed in a Thermoblock at 70 °C for 30 minutes and then dried by vacuum centrifugation. Subsequently, the samples were resuspended in 500 µL of water.

Ultra Performance Liquid Chromatography coupled with Mass Spectrometry in Parallel Reaction Monitoring mode (UPLC-PRM MS analysis)

Separation and analysis of the permethylated PMP-labeled monosaccharides were carried out on a mass spectrometer Q-Exactive Plus (ThermoFisher) coupled to a liquid chromatographer Ultimate 3000 (ThermoFisher). For analysis, 2-20 µL of sample were injected on a ACQUITY UPLC BEH C18 Column (130Å, 1.7 µm, 2.1 mm X 50 mm) and separated using the following gradient with a constant flow rate of 0.2 mL/min. Mobile phase A was 25 mM NH_4Ac in 5% ACN/water (v/v), at pH 8.2; mobile phase B was 95% ACN/water (v/v). The following gradient conditions were used: 0.00−26.00 min, 17.00% B; 26.00−26.01 min, 17.00−99.00% B; 26.01−28.00 min, 99.00% B; 28.00−28.01 min, 99.00−17.00% B; 28.01−30.00 min, 17.00% B.

The mass spectrometer was equipped with an electrospray ionization (ESI) source operating in positive ion mode. Nitrogen drying and sheath gas were set at 20 and 5 a.u., while the capillary temperature was set at 290°C. The analysis was performed in Parallel Reaction Monitoring (PRM), setting in the inclusion list the parent mass of the derivatized monosaccharides of interest. Higher-energy collisional dissociation (HCD) was set at 25 or 30 a.u.

The raw data were then analyzed comparing the retention time and the fragmentation mass spectra of the derivatized samples.

Alternative methods to LC-MS

Permethylated PMP-labeled monosaccharides were analyzed via Reversed Phase-UPLC (UPLC-RP) using a Waters Acquity UPLC H-Class PLUS Bio System. Samples were injected (1 µL) on a ACQUITY UPLC BEH C18 Column (130Å, 1.7 µm, 2.1 mm X 50 mm) using the same mobile phases used for UPLC-PRM MS. The following gradient was used: 0.00−10.00 min, 17.00% B; 10.00−20.00 min, 17.00−90.00% B; 20.00−22.00 min, 90.00−17.00% B; 22.00−25.00 min, 17.00% B; with a constant flow rate of 0.7 mL/min. The column compartment was held at 50 °C, and the sample compartment was held at 20 °C. The samples were detected at 245 nm UV ABS.

Permethylated monosaccharides were analyzed via HPAEC-PAD. The chromatographic runs were performed on ICS-6000, ICS-5000 or ICS-3000 equipped with Chromeleon 7.2 (Thermo, Waltham, MA, USA) using the pulsed amperometric mode with gold working electrode and Ag/AgCl reference electrode applying standard quad carbohydrate waveform. The separation was performed on a Thermo CarboPac MA1 4 × 250 analytical column with Thermo CarboPac MA1 4 × 50 guard column. The column and detector compartments were held at 25 °C, and the sample compartment was held at

10 °C. Chromatographic conditions were: 10 µL injection volume (partial loop mode), flow rate 0.4 mL/min, total run time 85 minutes. Eluent program: (I) monosaccharides elution: 45 min, NaOH 60 mM, Sodium acetate 70 mM; (II) washing step: 15 min, NaOH 500 mM; (III) column conditioning: 15 min, NaOH 60 mM, Sodium acetate 70 mM.

5.3. RESULTS

5.3.1. *Salmonella* OAg HPAEC-PAD method development

Identification of optimal OAg hydrolysis conditions

For HPAEC-PAD identification and quantification of STm, SEn and SPa OAg targeting the dideoxy monomers, less stable with respect to the other backbone saccharides to hydrolysis with 2 M TFA, milder hydrolysis conditions allowing maximum release of the monosaccharides while avoiding their degradation needed to be identified.

Starting from acid hydrolysis conditions used for the backbone monosaccharides (2 M TFA, 100°C, 4 hours), each single purified OAg and the commercial Tyv, used as a reference, were tested in a hydrolysis kinetic experiment (from 1 to 5 hours). The results of this analysis showed a similar trend for both Tyv standard and the three OAg, with peak areas decreasing overtime (**Figure 5.2(A)**).

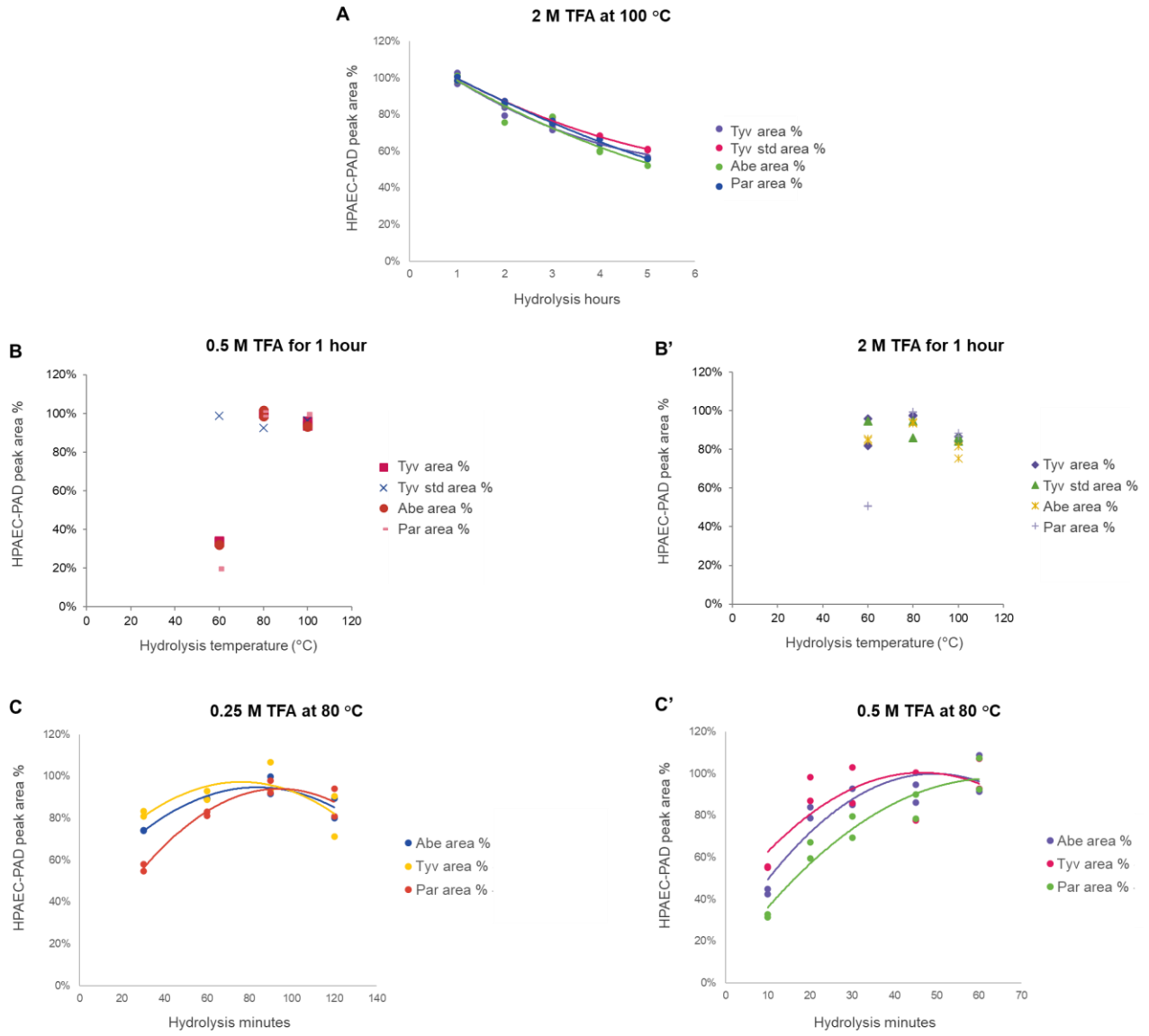

Figure 5.2. Identification of optimal *Salmonella* OAg hydrolysis conditions: (A) kinetic of hydrolysis with 2 M TFA at 100 °C, HPAEC-PAD peak area % normalized on peak area at 1 hour *vs* hydrolysis time is reported; (B, B') hydrolysis at the temperatures of 60°C, 80°C and 100°C with 2 M and 0.5 M TFA for 1 hour, HPAEC-PAD peak area % normalized on peak area at the conditions 0.5 M TFA, 80°C, 1 hour *vs* temperature is reported; (C, C') kinetic of hydrolysis with TFA 0.25 and 0.5 M at 80 °C, HPAEC-PAD peak area % normalized on peak area at the conditions 0.5 M TFA, 80°C, 1 hour *vs* hydrolysis time is reported.

The hydrolysis was repeated in milder conditions, keeping constant the time at 1 hour and changing the temperature (60°C, 80°C and 100°C) and the TFA concentration (2 M and 0.5 M). The most promising hydrolysis conditions were 0.5 M TFA at 80°C (**Figure 5.2(B, B')**). Moreover, with these conditions only 6% of Tyv standard was destroyed. Considering the similarities among the structures

of the *Salmonella* 3,6-dideoxyhexoses, a similar behavior for Abe and Par with respect to Tyv was hypothesized.

A further kinetic of hydrolysis experiment was then conducted in order to maximize the recovery of Abe, Tyv and Par and, at the same time, avoid the release of other monosaccharides coming from the hydrolysis of the OAg repeating unit and the core. The OAg were hydrolyzed at 80°C, with 0.5 M TFA (from 10 to 60 minutes) and 0.25 M TFA (from 30 minutes to 2 hours). The highest peaks were obtained with 0.25 M TFA at 80°C for 90 minutes (**Figure 5.2(C, C')**). The Rha peak originating from the OAg repeating unit was observed with a very low area when using 0.5 M TFA at 45 and 60 minutes, and with 0.25 M TFA at 90 and 120 minutes. Finally, the temperature was slightly decreased to 75°C, without affecting the area intensity of Abe, Tyv and Par with respect to 80°C, but avoiding complete release of the backbone monosaccharides.

Identification of optimal chromatographic conditions

HPAEC-PAD allows sensitive direct detection of carbohydrates with high-resolution separation. Two of the main factors affecting good separation are column and mobile phase composition. These two variables were screened during optimization of the chromatographic conditions.

Different columns were tested: CarboPac PA1, PA10 and MA1. CarboPac PA1 and PA10 columns have high selectivity for mono- and disaccharide, instead CarboPac MA1 is usually used for reduced mono- and disaccharide alditol analyses [261]. Since the CarboPac MA1 afforded greater retention of the 3,6-dideoxyhexoses, it was chosen for theseparation tests.

Several chromatographic conditions were tested (**Figure 5.3**), systematically changing concentrations of sodium hydroxide and/or sodium acetate. The trials were conducted in order not only to separate Abe, Tyv and Par, but also from other monosaccharides coming from the hydrolysis of the OAg repeating unit or the core. In particular, attention was focused on 3,6-dideoxyhexoses separation from fucose, which can be present as impurity [262], and rhamnose, one of the backbone monomers. Indeed, these sugars are the only ones appearing in the same retention time window of Abe, Tyv and Par, while glucose, galactose and mannose elute later (**Figure 5.4**).

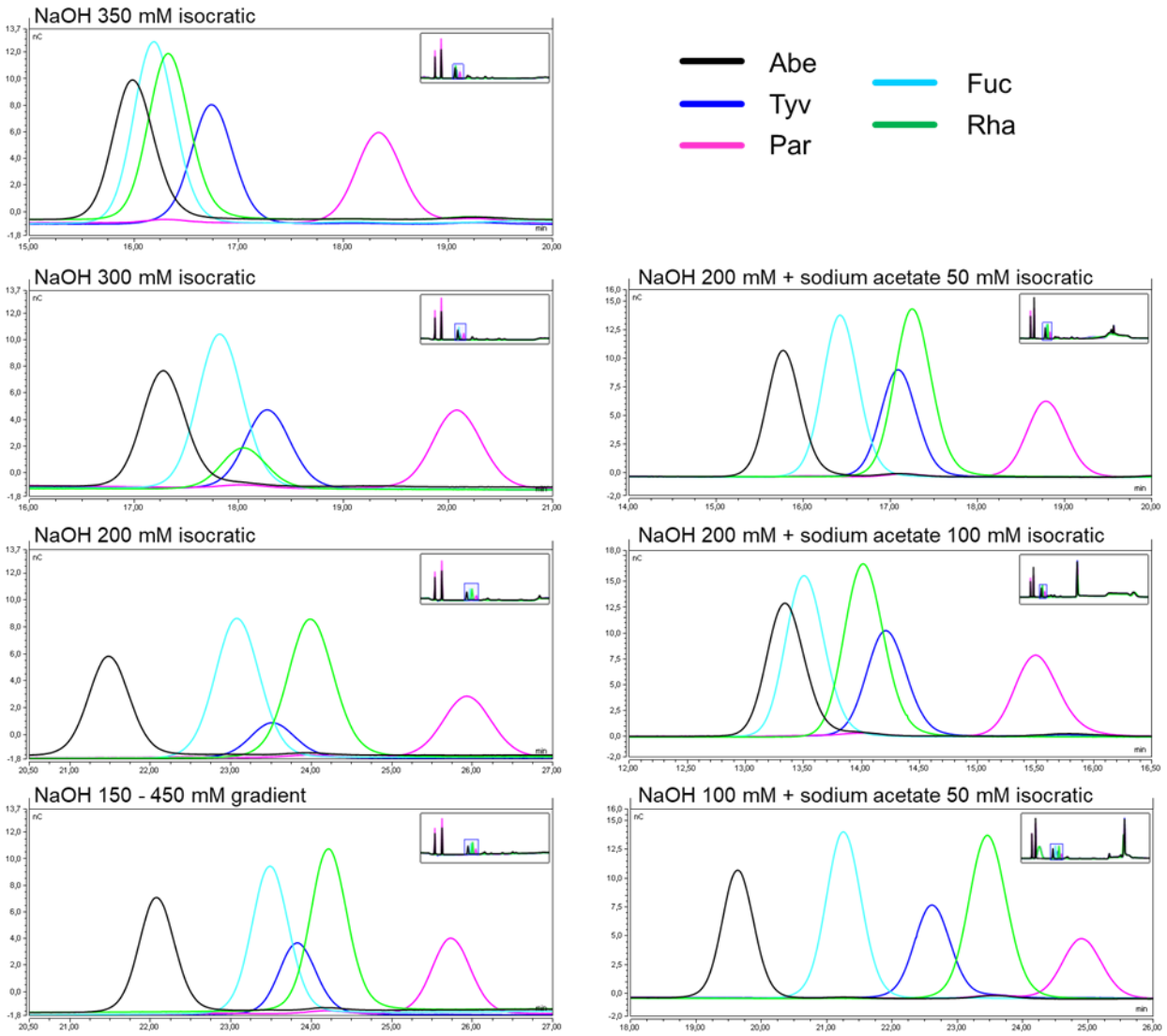

Figure 5.3. Preliminary chromatographic conditions tested by playing with concentrations of sodium hydroxide and/or sodium acetate in order to separate Abe (black), Tyv (blue) and Par (pink) among them and from Fuc (light blue) and Rha (green), using CarboPac MA1 column.

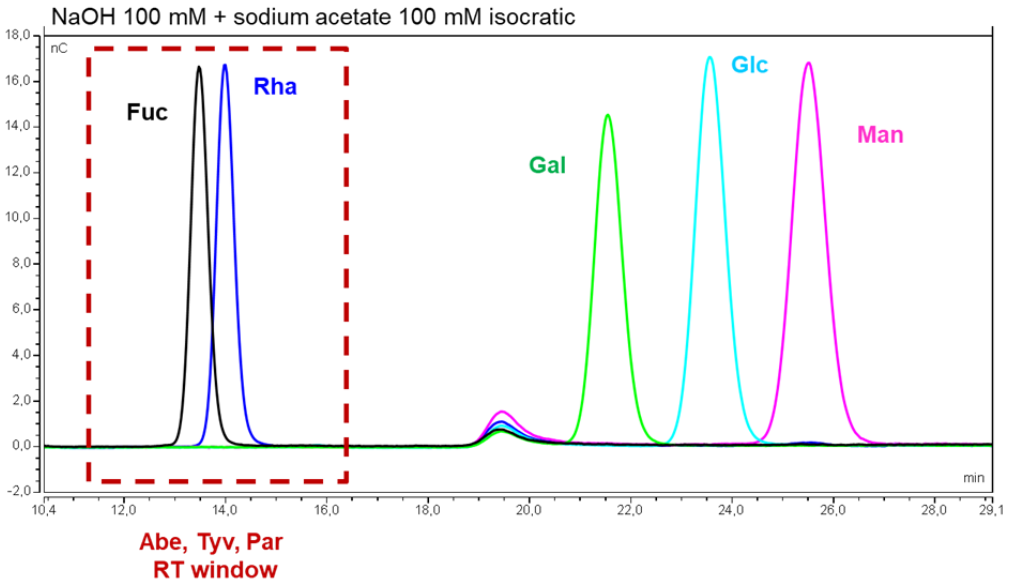

Figure 5.4. HPAEC-PAD chromatograms of Fuc (black), Rha (blue), Gal (green), Glc (light blue) and Man (pink) in CarboPac MA1 column, showing only Fuc and Rha eluting in the same retention time (RT) window of Abe, Tyv and Par.

The final selected conditions, NaOH 60 mM plus sodium acetate 70 mM, enabled complete separation of all sugar peaks (**Figure 5.5**). However, the Rha peak still partially overlapped with those of Tyv and Par. Nonetheless, the hydrolysis conditions were optimized to minimize the release of backbone monosaccharides.

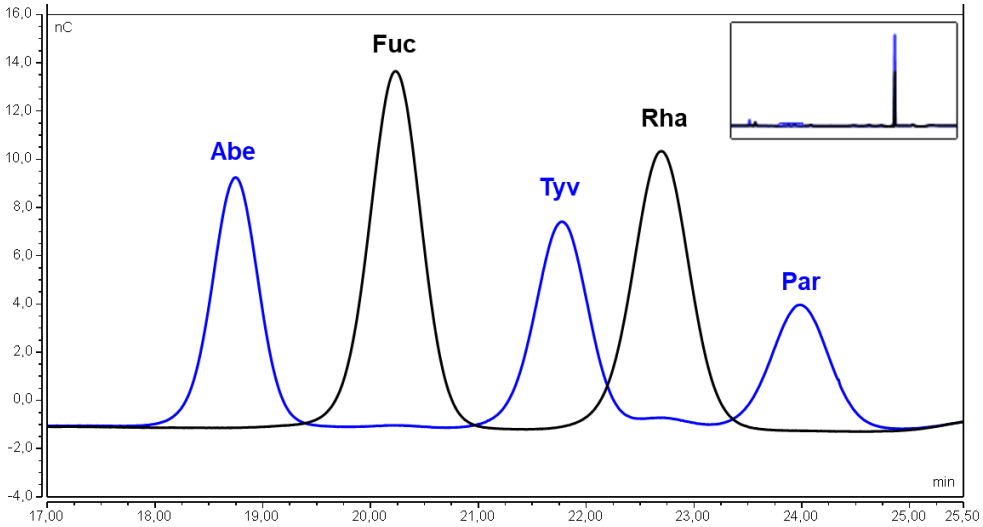

Figure 5.5. HPAEC-PAD chromatograms of (blue) Abe, Tyv and Par obtained after hydrolysis of STm, SEn and SPa OAg respectively, and (black) Fuc and Rha. Chromatographic run in CarboPac MA1 column with NaOH 60 mM + sodium acetate 70 mM as eluent.

5.3.2. *Salmonella* OAg HPAEC-PAD method characterization

Standard linearity determination

To assess the linearity of the novel method, after a first screening in the range 1 - 60 μg/mL, three different replicates of the calibration curve made with STm, SEn and SPa OAg mixed together were run at the concentrations of 1.5, 4, 7, 11 and 15 μg/mL (each OAg).

A regression analysis on the data generated showed significant linear models for each OAg and not significant lack of fit with the residuals normally distributed (**Table 5.1** and **Figure 5.6**).

Table 5.1. Standard linearity determination for quantification of STm, SEn and SPa OAg by acid hydrolysis followed by HPAEC-PAD: ANOVA on 3 replicates for the OAg calibration curve.

	STm	**SEn**	**SPa**
Lack of fit (p)	0.849	0.571	0.856
Residual normality (p, AD)	0.080	0.544	0.258
Linear coefficient (p)	<0.001	<0.001	<0.001
R^2	99.73%	99.59%	99.49%

A

Regression Analysis: STm versus ug/mL

Method

Rows unused 1

Analysis of Variance

Source	DF	Seq SS	Contribution	Adj SS	Adj MS	F-Value	P-Value
Regression	1	16.9660	99.73%	16.9660	16.9660	4483.36	0.000
ug/mL	1	16.9660	99.73%	16.9660	16.9660	4483.36	0.000
Error	12	0.0454	0.27%	0.0454	0.0038		
Lack-of-Fit	3	0.0037	0.02%	0.0037	0.0012	0.27	0.849
Pure Error	9	0.0417	0.25%	0.0417	0.0046		
Total	13	17.0114	100.00%				

Model Summary

S	R-sq	R-sq(adj)	PRESS	R-sq(pred)
0.0615160	99.73%	99.71%	0.0749561	99.56%

Coefficients

Term	Coef	SE Coef	95% CI	T-Value	P-Value	VIF
Constant	0.0009	0.0299	(-0.0642; 0.0660)	0.03	0.977	
ug/mL	0.22380	0.00334	(0.21652; 0.23108)	66.96	0.000	1.00

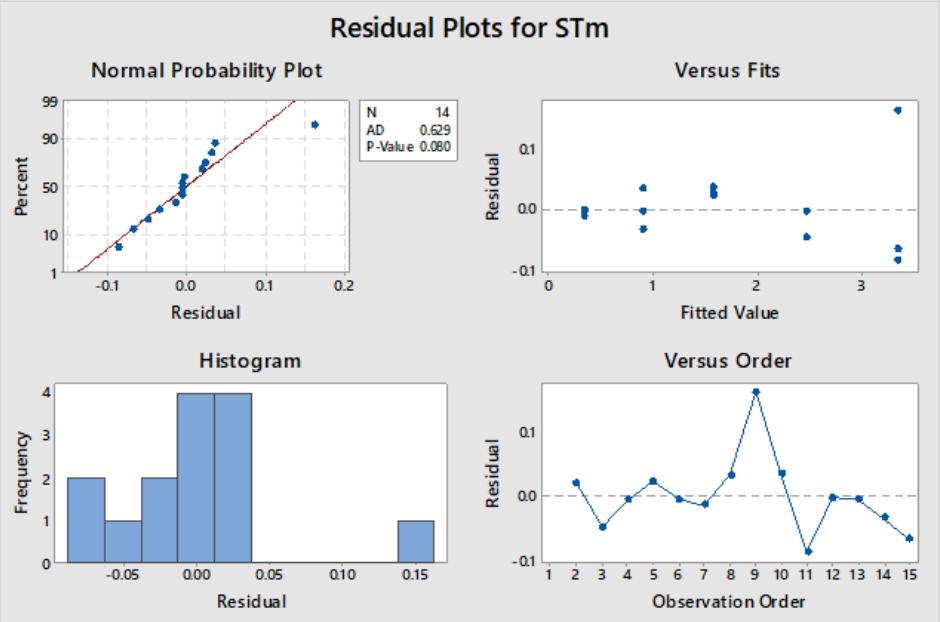

B

Regression Analysis: SEn versus ug/mL

Method

Rows unused 1

Analysis of Variance

Source	DF	Seq SS	Contribution	Adj SS	Adj MS	F-Value	P-Value
Regression	1	7.45591	99.62%	7.45591	7.45591	3144.84	0.000
ug/mL	1	7.45591	99.62%	7.45591	7.45591	3144.84	0.000
Error	12	0.02845	0.38%	0.02845	0.00237		
Lack-of-Fit	3	0.00544	0.07%	0.00544	0.00181	0.71	0.571
Pure Error	9	0.02301	0.31%	0.02301	0.00256		
Total	13	7.48436	100.00%				

Model Summary

S	R-sq	R-sq(adj)	PRESS	R-sq(pred)
0.0486912	99.62%	99.59%	0.0437492	99.42%

Coefficients

Term	Coef	SE Coef	95% CI	T-Value	P-Value	VIF
Constant	0.0100	0.0236	(-0.0415; 0.0615)	0.42	0.680	
ug/mL	0.14836	0.00265	(0.14260; 0.15413)	56.08	0.000	1.00

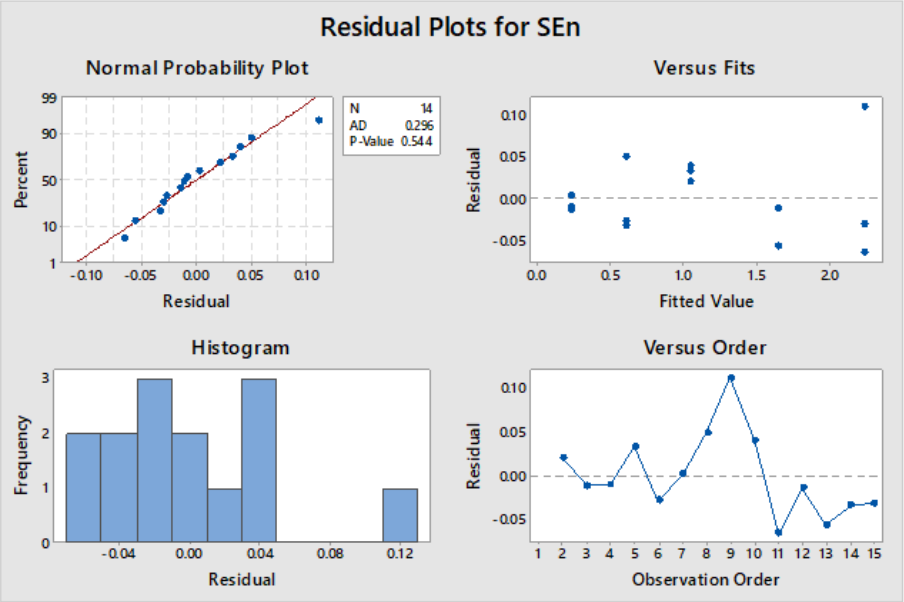

C

Regression Analysis: SPa versus ug/mL

Method

Rows unused 1

Analysis of Variance

Source	DF	Seq SS	Contribution	Adj SS	Adj MS	F-Value	P-Value
Regression	1	2.93997	99.49%	2.93997	2.93997	2358.12	0.000
ug/mL	1	2.93997	99.49%	2.93997	2.93997	2358.12	0.000
Error	12	0.01496	0.51%	0.01496	0.00125		
Lack-of-Fit	3	0.00117	0.04%	0.00117	0.00039	0.25	0.856
Pure Error	9	0.01379	0.47%	0.01379	0.00153		
Total	13	2.95493	100.00%				

Model Summary

S	R-sq	R-sq(adj)	PRESS	R-sq(pred)
0.0353092	99.49%	99.45%	0.0238243	99.19%

Coefficients

Term	Coef	SE Coef	95% CI	T-Value	P-Value	VIF
Constant	-0.0136	0.0171	(-0.0510; 0.0237)	-0.80	0.442	
ug/mL	0.09316	0.00192	(0.08898; 0.09734)	48.56	0.000	1.00

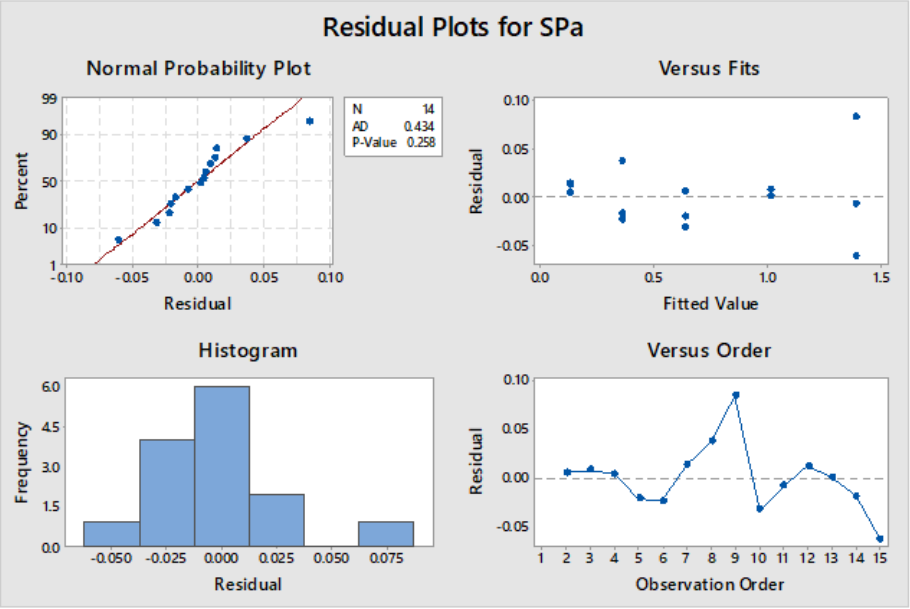

Figure 5.6. Standard linearity determination for quantification of STm (A), SEn (B) and SPa (C) OAg by acid hydrolysis followed by HPAEC-PAD: ANOVA on 3 replicates for the OAg calibration curve.

Accuracy determination

The accuracy of the method was estimated through the spike recovery technique. The sample was a solution containing a mixture of STm, SEn and SPa OAg-CRM_{197} glycoconjugates.

Two µg/mL of OAg conjugates were spiked with three different concentration levels of the purified OAg used for building the calibration curve (at 2, 5 and 8 µg/mL) to assess the accuracy at three different levels of the calibration curve.

To assess spike recovery, a total of four analysis sessions were performed on four different days. For each analysis session, the amount of polysaccharide recovered was calculated relative to the theoretical spike. Recoveries were in the range of 95-102% (**Table 5.2,** statistical analysis reported in **Figure 5.7**).

Table 5.2. Determination of accuracy for the HPAEC-PAD method: spike recovery values at different spike concentrations.

Sample	**STm**			**SEn**			**SPa**		
	N	**Mean**	**(90% CI)**	**Mean**	**(90% CI)**		**Mean**	**(90% CI)**	
Spike level 1 (+ 2 µg/mL)	4	97%	(92% 101%)	97%	(89%	105%)	102%	(99%	106%)
Spike level 2 (+ 5 µg/mL)	4	100%	(96% 105%)	102%	(96%	108%)	102%	(99%	106%)
Spike level 3 (+ 8 µg/mL)	4	95%	(91% 100%)	95%	(91%	100%)	100%	(96%	103%)

A

One-Sample T: STm CS1_1; STm CS2_1; STm CS3_1

Descriptive Statistics

Sample	N	Mean	StDev	SE Mean	90% CI for μ
STm CS1_1	4	0.9683	0.0381	0.0190	(0.9235; 1.0131)
STm CS2_1	4	1.0046	0.0369	0.0185	(0.9612; 1.0481)
STm CS3_1	4	0.9547	0.0384	0.0192	(0.9095; 0.9999)

μ: mean of STm CS1_1; STm CS2_1; STm CS3_1

B

One-Sample T: SEn CS1_1; SEn CS2_1; SEn CS3_1

Descriptive Statistics

Sample	N	Mean	StDev	SE Mean	90% CI for μ
SEn CS1_1	4	0.9705	0.0681	0.0340	(0.8904; 1.0505)
SEn CS2_1	4	1.0185	0.0486	0.0243	(0.9614; 1.0757)
SEn CS3_1	4	0.9507	0.0383	0.0192	(0.9056; 0.9958)

μ: mean of SEn CS1_1; SEn CS2_1; SEn CS3_1

C

One-Sample T: SPa CS1_1; SPa CS2_1; SPa CS3_1

Descriptive Statistics

Sample	N	Mean	StDev	SE Mean	90% CI for μ
SPa CS1_1	4	1.0242	0.0274	0.0137	(0.9919; 1.0564)
SPa CS2_1	4	1.0231	0.0294	0.0147	(0.9885; 1.0578)
SPa CS3_1	4	0.9976	0.0277	0.0139	(0.9649; 1.0302)

μ: mean of SPa CS1_1; SPa CS2_1; SPa CS3_1

Figure 5.7. Spike recoveries and confidence intervals for HPAEC-PAD quantification of the mixture of STm (A), SEn (B) and SPa (C) OAg-CRM_{197} glycoconjugates (data from four analysis sessions).

5.3.3. *Shigella flexneri* OAg LC-MS method development

Identification of target monosaccharides for quantification of *S. flexneri* 1b, 2a and 3a OAg via LC-MS

The method was based on a LC-MS platform to analyze glycosidic linkages in oligosaccharides and polysaccharides, combining permethylation with PMP derivatization [257]. First, free hydroxyl groups on the OAg were permethylated. Subsequently, acid hydrolysis at high temperatures broke the glycosidic bonds, releasing partially methylated monosaccharides. The hydrolysis process preserves the locations of these bonds as free hydroxyl groups. Lastly, the released monosaccharides were derivatized at the reducing end with PMP. This addition increased hydrophobicity and, thus, chromatographic separation via LC and facilitated the mass spectroscopy detection by enhancing the ionization efficiency in ESI-MS. Finally, the samples were analyzed via UPLC-PRM MS (**Figure 5.8(A)**).

To apply this method for independently quantifying the *S. flexneri* 1b, 2a, and 3a OAg, it was necessary to identify at least one monosaccharide unique to each OAg, distinguished by its linkage in the sugar chain. The monosaccharides selected as target for each OAg were: (3,4)-β-D-Glc*p*NAc in *S. flexneri* 1b OAg; (3,4)-α-L-Rha*p*I in *S. flexneri* 2a OAg; (2,3)-α-L-Rha*p*III in *S. flexneri* 3a OAg (**Table 5.3** and **Figure 5.8(B)**).

Table 5.3. *S. flexneri* 1b, 2a and 3a OAg structures [141, 142], highlighting the monosaccharides selected as target for method development.

OAg	Structure
S. flexneri 1b OAg	α-D-Glc*p* 1 ↓ **4** [→2)-α-L-Rha*p*III-(1→2)-α-L-Rha*p*II-(1→3)-α-L-Rha*p*I-(1→**3)-β-D-Glc*p*NAc-(1**→]$_n$
S. flexneri 2a OAg	α-D-Glc*p* 1 ↓ **4** [→2)-α-L-Rha*p*III-(1→2)-α-L-Rha*p*II-(1→**3)-α-L-Rha*p*I-(1**→3)-β-D-Glc*p*NAc-(1→]$_n$
S. flexneri 3a OAg	α-D-Glc*p* 1 ↓ **3** [→**2)-α-L-Rha*p*III-(1**→2)-α-L-Rha*p*II-(1→3)-α-L-Rha*p*I-(1→3)-β-D-Glc*p*NAc-(1→]$_n$

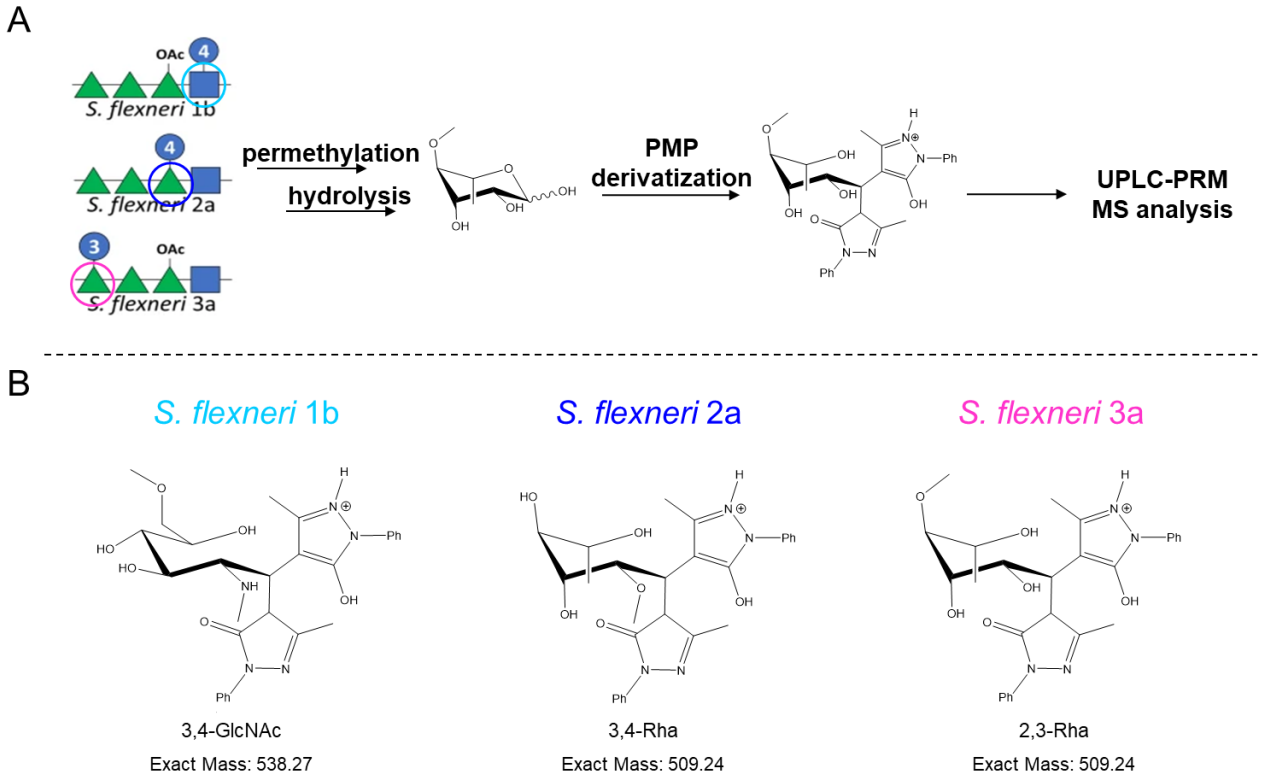

Figure 5.8. (A) Workflow of the LC-MS analysis for identification of the *S. flexneri* 1b, 2a and 3a OAg (in figure is reported *S. flexneri* 3a analyte as structure example); (B) monosaccharides unique to each OAg (as analytes)—(3,4)-β-D-Glc*p*NAc in *S. flexneri* 1b OAg; (3,4)-α-L-Rha*p*I in *S. flexneri* 2a OAg; (2,3)-α-L-Rha*p*III in *S. flexneri* 3a OAg—after OAg methylation, hydrolysis and derivatization with PMP.

Initially, the purified *S. flexneri* OAg were subjected to the derivatization workflow separately. It was verified that the derivatized target monomers can be identified based on chromatographic separation and their specific fragmentations (**Table 5.4** and **Figure 5.9**). The product ion masses obtained from the target residues of *S. flexneri* 2a and *S. flexneri* 3a OAg, following methylation, hydrolysis and PMP-labelling, matched the expected values according to the library published by [258]. Since the mass spectra for *S. flexneri* 1b 3,4-*N*-acetylglucosamine residue were not reported in literature, the spectral data obtained were confirmed by investigating the fragmentation profile of the commercial *N,N′,N″*-triacetylchitotriose (a trimer of the *N*-acetylglucosamine), after application of the same derivatization protocol. Using the permethylation conditions reported, the *N*-acetylglucosamine residues were also methylated at the amide. Then, after hydrolysis, as expected, the acetyl group was lost, thus releasing a secondary amine, as shown in **Figure 5.8(B)**.

For all monosaccharides analyzed, the most abundant fragment ion observed had an *m/z* of 175.09. This ion results from the cleavage between the PMP moiety and the C1 carbon of the derivatized

sugar. Additional product ions, listed in Table 5.4 and used for quantification, originate from fragmentation between the C2 and C3 carbons of the monosaccharide, along with the retention of one C1–PMP bond[257].

Table 5.4. Fragmentation profiles of *S. flexneri* OAg target monomers, following permethylation and PMP-labeling.

OAg	target residue	precursor ion (*m/z*)	product ions (*m/z*)
S. flexneri 1b OAg	3,4-*N*-acetylglucosamine	538.27	175.09, 230.13
S. flexneri 2a OAg	3,4-rhamnose	509.24	175.09, 231.11 [258]
S. flexneri 3a OAg	2,3-rhamnose	509.24	175.09, 217.10 [258]

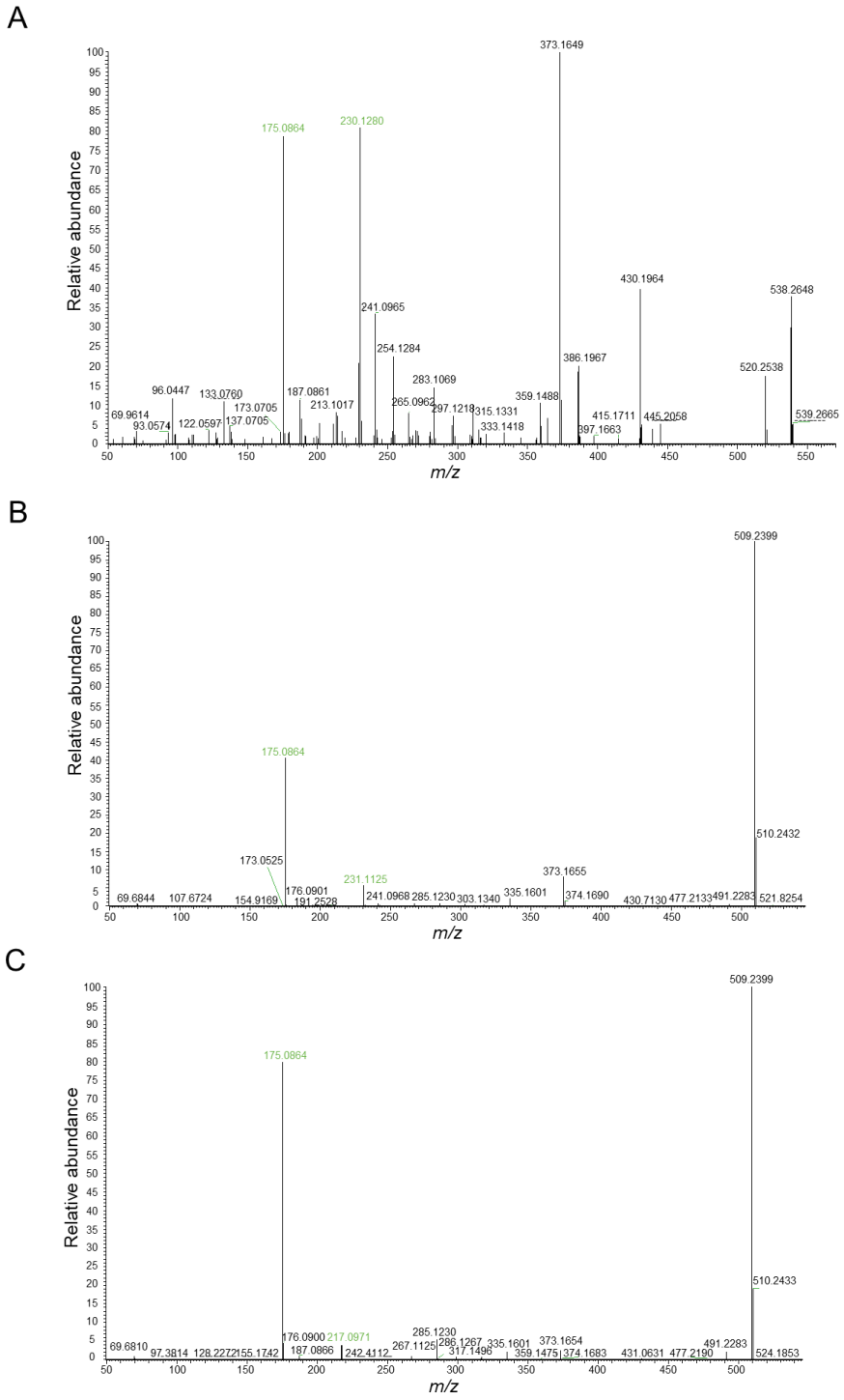

Figure 5.9. MS/MS spectra of the methylated PMP-labeled protonated precursor ion *m/z* 538.27 for identification of *S. flexneri* 1b OAg, releasing *m/z* 175.09 and *m/z* 230.13 specific fragment ions (A); MS/MS spectra of methylated PMP-labeled protonated precursor ions *m/z* 509.24 for identification of *S. flexneri* 2a releasing *m/z* 175.09 and *m/z* 231.11 specific fragment ions (B); MS/MS spectra of methylated PMP-labeled protonated precursor ions *m/z* 509.24 for identification of *S. flexneri* 3a OAg, releasing *m/z* 175.09 and *m/z* 217.10 specific fragment ions (C).

Each of the target monosaccharides also eluted at different retention time (rt). Importantly, the potential specificity of the analysis was verified, with < 4% impurity (calculated as the peak area in unrelated OAg MS chromatogram divided by the peak area in the corresponding OAg one).

Following initial trials with separate OAg, the three OAg were then combined in a mixture and derivatized in the same way. The ability to identify all the three *S. flexneri* target monosaccharides in a combined solution, using both purified OAg (**Figure 5.10(A)**) and GMMA (**Figure 5.10(B)**), was confirmed.

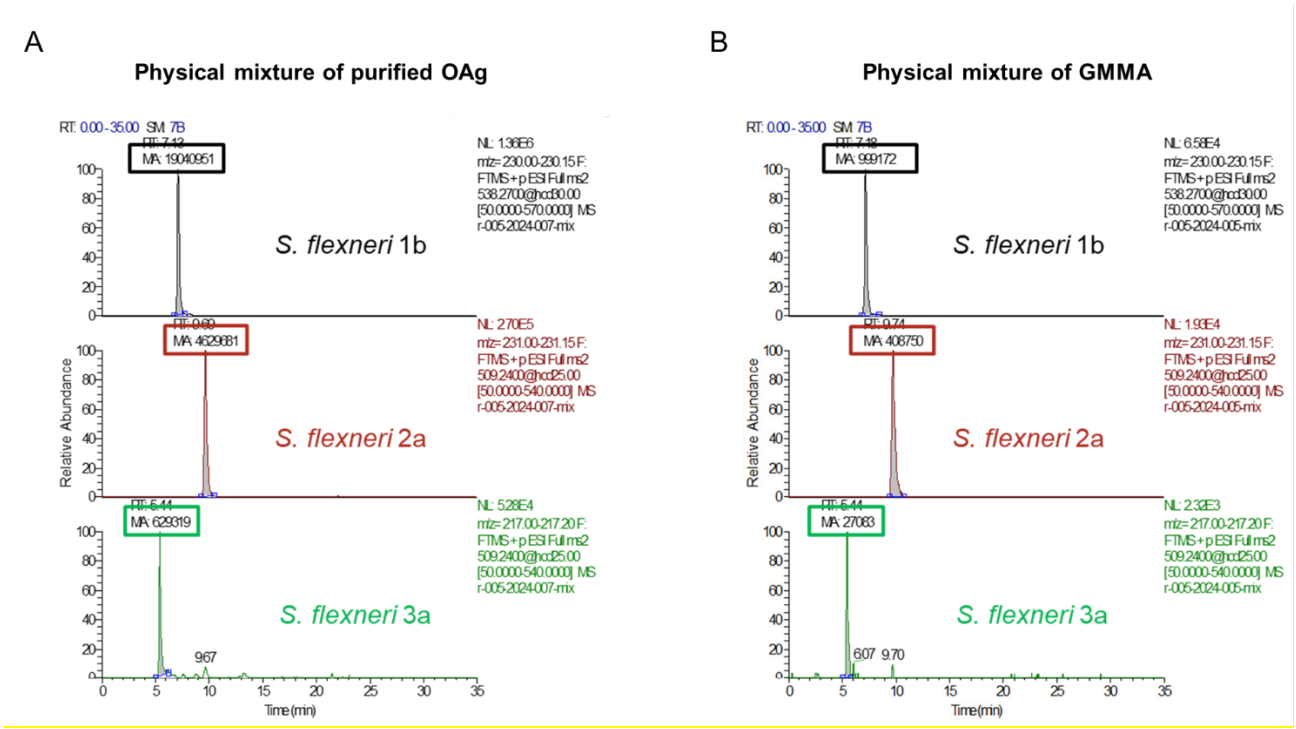

Figure 5.10. PRM chromatograms of the methylated PMP-labeled target monosaccharides obtained from the analysis of a physical mixture of purified *S. flexneri* 1b, 2a and 3a OAg (A) or GMMA (B). Peak area represents quantifying transitions.

Alternatives methods to LC-MS

Alternative methods to LC-MS were considered. In particular, since good chromatographic separation of the three methylated PMP-labeled target monosaccharides was achieved in LC-MS, UPLC-RP with UV detection was evaluated. The purified *S. flexneri* OAg were subjected, separately, to the same derivatization workflow used for the LC-MS method. Preliminary analyses were conducted and the chromatograms obtained were compared among them and with those of the commercial glucose and sucrose, both processed through the same derivatization protocol. Through these comparisons and considering each OAg RU structure, the peaks corresponding to the target monosaccharides were identified, along with other peaks from the other monomer residues belonging

to all the three OAg or to two out of the three (**Figure 5.11(A)**). However, when analyzing the OAg combination, the chromatograms resulted to be excessively crowded, making peak identification challenging. Moreover, since the final samples to be analyzed would be GMMA, the presence of additional potential chromophores derived from the hydrolysis of proteins in GMMA samples would make this approach even more complicated. Thus, it was not applied further.

Another alternative method tested was based on a different technique: HPAEC-PAD. The OAg were prepared using the same derivatization workflow but without PMP-labelling. After hydrolysis, the permethylated OAg were separately analysed using the same column and chromatographic conditions established for the *Salmonella* OAg in the beginning of this chapter. Peaks corresponding to the target monosaccharides were identified, but their intensities were very low, especially those of the *S. flexneri* 2a and 3a rhamnoses (**Figure 5.11(B)**). After different failing attempts trying to enhance the detection of such monomers, including using a platinum working electrode instead of gold one or applying different waveforms, this approach was not considered further.

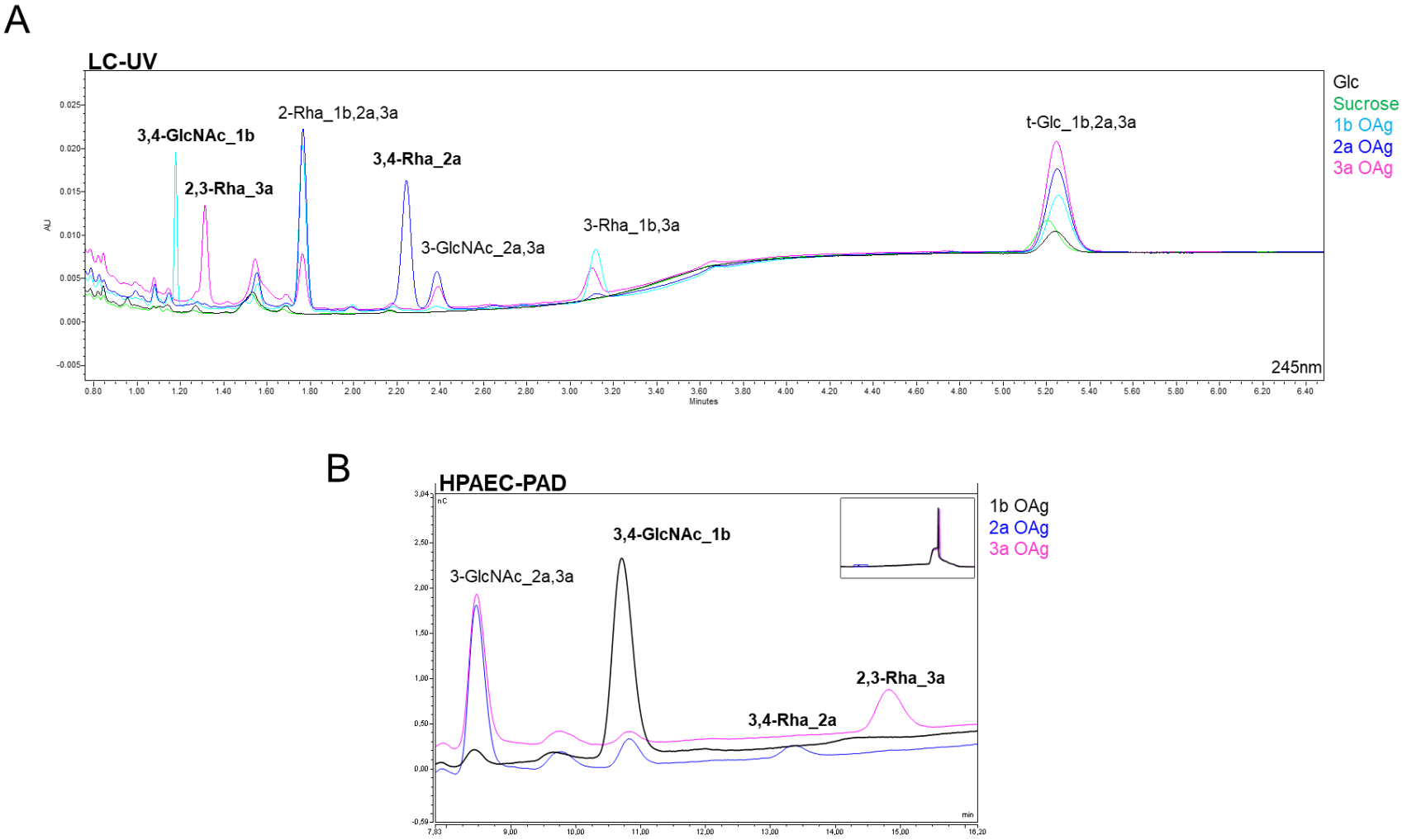

Figure 5.11. Alternative methods to LC-MS. (A) UPLC-RP chromatograms of the methylated PMP-labeled monosaccharides from the analysis of purified *S. flexneri* 1b, 2a and 3a OAg, glucose and sucrose. (B) HPAEC-PAD chromatograms of the methylated monosaccharides from the analysis of purified *S. flexneri* 1b, 2a and 3a OAg.

5.4. DISCUSSION

Multivalent vaccine formulations are complex, and there is the need to develop and validate appropriate assays to accurately characterize each component [180]. PS content is one of the critical quality attributes of a PS-based vaccine, and the availability of analytical methods to independently quantify each single PS antigen is fundamental for vaccine release, as well as to monitor its stability and ensure appropriate immune responses. However, finding a unique procedure that is suitable for the specific measurement of all the combined serotypes in a multivalent PS-based vaccine could be difficult.

Typically, the techniques most commonly used are the colorimetric and HPAEC-PAD methods. The ability of HPAEC-PAD to accurately distinguish between stereoisomeric sugars has enhanced its application in multivalent vaccines, addressing a key limitation of colorimetric tests. As a result, over time, this method has been instrumental in the development of various vaccines [249]. However, when it comes to multivalent vaccines, the use of HPAEC-PAD can be challenging, particularly when dealing with combinations of saccharide antigens that share repeating units made of same monomers. Currently, immunoassay methods based on Enzyme-Linked Immunosorbent Assay (ELISA) have emerged as valuable alternatives to HPAEC-PAD. In multiplex modality, ELISA is especially advantageous, as it can analyze multiple antigens simultaneously [253, 255, 263-265]. However, since these are immunological methods, the precision, accuracy, and reproducibility are lower than those of analytical methods such as HPAEC-PAD. Even more complicated is the quantification of each active ingredient in the presence of an adjuvant (e.g. Alhydrogel).

Multivalent OAg-based vaccines are currently in development against the principal serovars of *Salmonella enterica* [75] and *Shigella* serotypes [139]. For *Shigella*, particularly, among different serotypes, *S. flexneri* 1b, 2a and 3a, along with *S. flexneri* 6 and *S. sonnei*, have been proposed as components to reach broad coverage [148, 149]. Given the structural similarities among the OAg of *Salmonella* Typhimurium, Enteritidis, and Paratyphi A, which only differ in the 3,6-dideoxy monosaccharide linked to the backbone [167, 168], and among the OAg of *Shigella flexneri* 1b, 2a, and 3a, which share the same backbone with glucose positioned differently [141, 142], presently, the only available methods to directly and specifically quantify the OAg content of these *Salmonella* serovars and *Shigella flexneri* serotypes in multivalent formulations are the cELISA and FacE immunoassays [253-255].

In my thesis, two novel analytical methods were developed to identify and/or quantify these OAg.

Specifically, by targeting the dideoxy monomers, an HPAEC-PAD analysis was established that enabled the identification and subsequent quantification STm, SEn and SPa OAg, even in multivalent formulations. Mild hydrolysis conditions were identified to release the dideoxy monosaccharides, which are less stable than the other backbone saccharides, thus preventing their degradation. Additionally, chromatographic conditions were optimized for the detection of the resulting species. The range of linearity was determined, and the method proved to be accurate. However, for a more comprehensive characterization of the method, sample linearity and reproducibility will need to be assessed.

The *Shigella flexneri* 1b, 2a and 3a OAg share the same sugar composition and cannot be distinguished using HPAEC-PAD when in multivalent formulations. To address this limitation, a novel method was developed using a different technique, the LC-MS [257, 258]. This method identifies OAg through chromatographic separation of target monosaccharides alongside their specific fragmentations. The coupling of LC with MS enhances the ability to identify and characterize each OAg component in a complex mixture, due to the high resolution from chromatographic separation complemented by precise mass analysis. This method allowed the identification of individual *S. flexneri* OAg in mixture, using either purified OAg or GMMA, as they represent the final antigens to be analyzed in multivalent formulations. This method has potential for not only identifying but also quantifying each OAg. Improvement in the sample preparation workflow is necessary to increase throughput, and calibration curve linearity and internal standard for a precise quantification need to be evaluated.

These novel methods will facilitate the characterization of multivalent vaccines containing *Salmonella* and *Shigella* OAg as active ingredients. Although the HPAEC-PAD method for *Salmonella* is more specific, the LC-MS technique is potentially applicable to any polysaccharide structure and could be considered for other complex multivalent PS-based vaccines. Indeed, the method only requires one monosaccharide for each PS chain differently linked in the sugar chain. By specifically adjusting the sample preparation workflow, it may be possible to quantify a high number of PS in a single or few sessions.

6. Application of advanced kinetic modelling to tetravalent *Shigella* GMMA formulations to predict vaccine stability based on accelerated studies

6.1. INTRODUCTION

Assessing vaccine stability under specific storage and shipping conditions is crucial to maintain their safety and effectiveness. Vaccines are among the most cost-effective methods to combat infectious diseases, yet their stability often limits their access in developing regions with insufficient storage infrastructure [266]. Vaccine degradation can be influenced by many factors, with the World Health Organization (WHO) estimating cold chain breaks account for 50% of vaccine wastage [267], underscoring temperature's critical role in vaccine stability. Developing vaccines that maintain stability over extended periods could reduce financial burdens and enhance accessibility, particularly in remote areas, potentially preventing millions of deaths from vaccine-preventable diseases [266].

Extensive stability evaluations, including accelerated and stress condition studies, are essential to verify product stability and to thoroughly understand the product's properties and the impact of external stress factors on its quality [268]. According to regulatory guidelines from the International Conference on Harmonization (ICH) of Technical Requirements for Registration of Pharmaceuticals for Human Use—specifically chapters Q1 and Q5C—and additional WHO guidance for vaccines [269], the primary data to define vaccine shelf life must come from long-term, real-condition studies. These studies are required to support INDs/IMPDs or marketing applications. Initial licensing demands stability data from a minimum of three batches for at least six months when requesting expiry beyond six months, for up to twice the last stability timepoint and no more than one year [270].

Although ICH guidelines do not extensively address the use of data from stress or accelerated conditions, stability modelling—leveraging advanced statistical analyses—provides a valuable means to predict the degradation profile of vaccines. This approach aids not only in predicting shelf life but also in managing temperature excursions (cold chain breaks), assessing the impact of degradation on product quality, and facilitating post-approval changes or comparability studies following manufacturing modifications [270]. As per ICH guidelines, also predictions are valid for up to twice the last stability timepoint analysed for a maximum of one-year extension.

In this project, the stability modelling approach was applied to tetravalent *Shigella* vaccine altSonflex1-2-3, with Alum-formulated GMMA as alternative delivery system for *Shigella* OAg [78, 202, 230].

The altSonflex1-2-3 vaccine is in its final development stages. A large panel of analytical methods has been established to allow characterization of GMMA and Alum-formulated GMMA [78, 214, 253, 254], ensuring consistency of manufacture and to monitor stability over time. These analyses have confirmed the ability to detect changes in critical quality attributes (CQAs) affecting vaccine immunogenicity [253].

In this study, altSonflex1-2-3 stability data under accelerated conditions (2–8 °C, 25 °C and 40 °C for up to 6 months) were collected. Predictive models were established using the advanced kinetic modelling based on the truncated Šesták–Berggren equation [270], to anticipate vaccine behavior during storage. Multiple software tools were employed, obtaining similar models. Furthermore, stability data collected in real time (2–8 °C up to 36 months) were compared with predictions, to validate the kinetic models obtained.

Beyond altSonflex1-2-3, this approach was extended to tetravalent *Shigella* GMMA formulated without Alum, providing valuable insights into vaccine stability and identifying the impact of aging on specific quality attributes (QAs) in the absence of Alum. Recent studies indicate that Alum is unnecessary for enhancing GMMA magnitude, quality, or functionality of the antibody response induced [194, 213]. Also, *Shigella* GMMA formulated without Alum demonstrated good tolerance in rabbits [213] and assessments using a human monocyte activation test (MAT) revealed that GMMA, regardless of Alum presence, induced similar levels of IL-6 release [213, 246].

Advanced kinetic modelling can be a valuable tool to predict the stability of complex tetravalent *Shigella* GMMA formulations and can be applied to other multivalent OAg-based vaccines.

6.2. MATERIAL AND METHODS

Shigella GMMA production

Shigella GMMA were obtained from GVGH [78].

Shigella GMMA formulation with and without Alum

Formulation with Alum (4 GMMA + Alum) was prepared by adsorbing *S. sonnei* and *S. flexneri* 1b, 2a and 3a GMMA in NaCl 154 mM, NaH_2PO_4 10 mM pH 6.5 on 0.7 mg/mL (Al^{3+}) Alum at the final concentration of 120 µg/mL total OAg (30 µg/mL each OAg).

Formulation without Alum (4 GMMA) was prepared by diluting *S. sonnei* and *S. flexneri* 1b, 2a and 3a GMMA in NaCl 154 mM, NaH_2PO_4 10 mM pH 6.5 at the final concentration of 120 µg/mL total OAg (30 µg/mL each OAg).

Accelerated stability studies

GMMA formulations, both with and without Alum, were stored in 8 mL Wheaton glass screw cap tubes filled with 8 mL of the formulations. They were kept at temperatures of 2–8°C and subjected to heating at 25 and 40°C for 6 months. Timepoint samples were collected at day 0 (a common starting point for all temperatures), and subsequently at 2 weeks, and 1, 1.5, 2, 2.5, and 6 months (**Figure 6.1**). Each timepoint was characterized as described below.

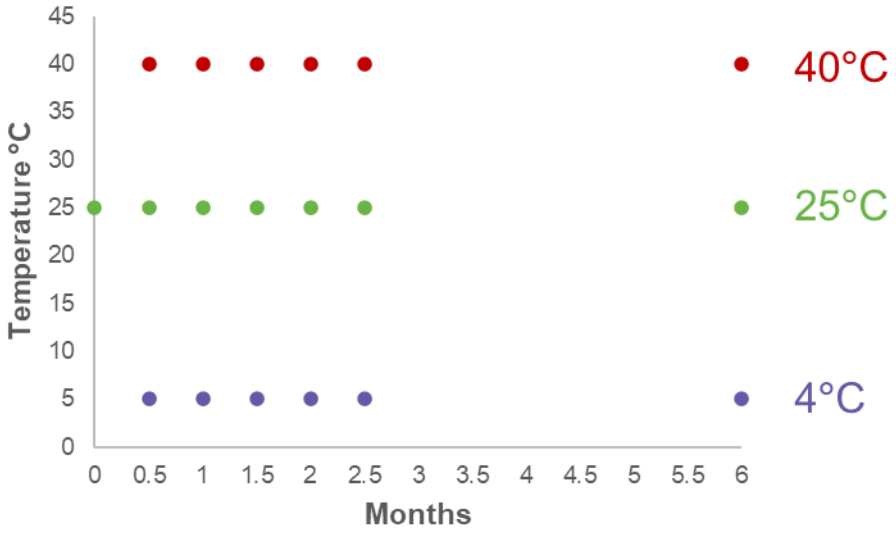

Figure 6.1. Schematic representation detailing the temperatures and timepoints at which samples were collected during accelerated stability studies of 4 GMMA, both with and without Alum.

Formulations characterization

Samples collected at different timepoints during the accelerated stability studies of GMMA formulations, both with and without Alum, were characterized using the analytical methods reported in **Table 6.1**.

Table 6.1. Selected QAs and corresponding analytical methods used to characterize tetravalent *Shigella* GMMA formulations, both with and without Alum, at various timepoints during accelerated stability studies.

Formulation	Quality attributes	Analytical methods
4 GMMA + Alum	Size	laser diffraction, D[4,3] and D(90)
	pH	pH meter
	Quantification of lipid A in supernatant	HPLC-MS after 0.2 μm filtration
	Quantification of free OAg in supernatant	HPAEC-PAD after 0.2 μm filtration
	Quantification of free proteins in supernatant	μBCA after 0.2 μm filtration
4 GMMA	Size/aggregation	DLS, Z-av
	pH	pH meter
	Integrity	HPLC-SEC, GMMA(t)/GMMA (t_0) % peak area
	Quantification of free OAg in supernatant	HPAEC-PAD after ultracentrifugation

Characterization of GMMA formulation with Alum

The tetravalent *Shigella* GMMA formulated with Alum was characterized at each timepoint for pH and particle size. The pH was measured using the Seven Excellence pH meter equipped with an Inlab micro-electrode (Mettler Toledo), with temperature corrections made following calibration with standard buffers at pH 4.01, 7.00 and 10.00 (Mettler Toledo, Columbus, OH, USA). Particle size was assessed using the Mastersizer 3000 (Malvern, UK) equipped with a Hidro SV small volume dispersion unit, using D(90) and D[4,3] as indicators for particle size distribution—respectively representing the diameter below which 90% of particles fall and the volume-weighted mean diameter.

The settings applied included: stirrer speed at 1000 rpm, non-spherical particle type mode, refractive index of 1.53, absorption index of 0.01, density of 1, dispersant refractive index of 1.33, a measurement duration of 30 seconds, six measurement replicates, measurement obscuration between 1-20%, and data processed using a general-purpose algorithm [254].

At each timepoint, supernatants from the Alum-formulated GMMA were collected using centrifugal filtration devices (Nanosep MF Centrifugal Devices with Bio-Inert Membrane 0.2 μm, PALL code ODM02C34). Initially, 500 μL of the Alum-formulated GMMA were loaded into the device and centrifuged for 20 minutes at 300 rcf using a fixed-angle rotor to prime the filter; the filtrate from this step was discarded. Subsequently, additional Alum-formulated GMMA were loaded and centrifuged under the same conditions [253]. The filtrates collected from these steps were then frozen until the completion of the accelerated stability studies.

These supernatants were then analyzed in randomized order for: free protein content assessed by micro BCA using bovine serum albumin (BSA) as a reference according to the manufacturer's instructions (Thermo Scientific, Waltham, MA, USA); free *S. sonnei* OAg and total *S. flexneri* OAg sugar content measured by High Performance Anion Exchange Chromatography with Pulsed Amperometric Detection (HPAEC-PAD) [167, 216] and free lipid A determined by High Performance Liquid Chromatography coupled to Mass Spectrometry (HPLC-MS) [214]. The HPAEC-PAD and HPLC-MS methods are described in Chapters 3 and 4, respectively.

Characterization of GMMA formulation without Alum

The tetravalent *Shigella* GMMA formulated without Alum was characterized at each timepoint for pH, as reported above, and for particle size through Dynamic Light Scattering (DLS) as described in Chapter 3 [214].

At each timepoint, part of the formulation was directly frozen, and the rest was ultracentrifuged using a Thermo Scientific (Waltham, MA, USA) Sorvall MX 150+ Micro-Ultracentrifuge (4°C, 30 min, 110,000 rpm, with a Thermo Scientific fixed-angle rotor K factor 15) to collect supernatants. Both formulation aliquots and supernatants were frozen until the completion of the accelerated stability studies. Then, the formulation aliquots were analyzed, in randomized order, for GMMA integrity by Size Exclusion High Performance Liquid Chromatography (HPLC-SEC) [214]. A Waters Acquity UPLC H-Class PLUS Bio System was utilized with the following settings: the column compartment was maintained at 30 °C, the autosampler compartment at 4 °C, and the fluorimeter detector was set with an excitation wavelength of 280 nm and an emission wavelength of 336 nm. An 80 μL sample was injected onto a Tosoh (King of Prussia, PA, USA) TSK gel 6000 PW column (30 cm × 7.5 mm)

connected in series with a Tosoh TSK gel 4000 PW column (30 cm × 7.5 mm) and a Tosoh TSK gel PWH guard column (7.5 cm × 7.5 mm). The analytes were eluted with PBS at a flow rate of 0.5 mL/min over a 70-minute run. Finally, the supernatants in randomized order were characterized by HPAEC-PAD for the evaluation of released *S. sonnei* OAg and total *S. flexneri* OAg, as described in Chapter 3 [167, 216].

Advanced kinetic modelling

Kinetic modelling was performed using Thermokinetics 5.4 (AKTS) by setting a one-step model with the truncated Šesták–Berggren equation, without accounting for any autocatalytic behavior. In addition, zero-order, first-order, and *n*-order integrated kinetic equations (equations (1), (2), and (3), respectively) were tested for non-linear fitting of the data at multiple temperatures using Minitab 22 (Minitab LLC, State College, PA, USA) and JMP 17 (SAS Institute Inc., Cary, NC, USA). AKTS was not used for all the models, while Minitab and JMP were utilized for all of them.

$$\boldsymbol{Ci + time\ Sign\ Exp\left(LnA - \frac{Exp\ (LnEa)}{((temperature\ °C + 273.15)\ 8.314463)}\right)} \quad (1)$$

$$\boldsymbol{Cf + (Ci - Cf)\ Exp\left(-time\ Exp\left(LnA - \frac{Exp\ (LnEa)}{((temperature\ °C + 273.15)\ 8.314463)}\right)\right)} \quad (2)$$

$$\boldsymbol{Cf + (Ci - Cf)\left(1 - (1 - N)\ time\ Exp\left(LnA - \frac{Exp\ (LnEa)}{((temperature\ °C + 273.15)\ 8.314463)}\right)\right)^{\left(\frac{1}{(1-N)}\right)}} \quad (3)$$

The models were chosen based on the goodness of fit by checking the sum of squares error (SSE) and the root mean square error (RMSE), and were optimized for the following parameters (equations are also reported in **Tables 6.2 and 6.3**): values of starting (t_0) and final (t_∞, referring to the maximum or minimum value that can potentially be reached as an asymptote) QA, the pre-exponential factor (A), the activation energy (E_a), and the order of reaction (*n*). Prediction intervals (PI) of 95% were calculated using all three software packages, Minitab and JMP estimate the PI starting from the covariance matrix of the parameter estimates, while AKTS employs a bootstrap method (n = 1000) with resampling residuals. With Minitab, evaluations of residuals normality (through Anderson-Darling test) and of residuals versus fitted values, time and temperature were performed.

The QAs were not subjected to modelling if no trend in changes over time was observed.

To compare the prediction models with real time data, for free protein and free lipid A %, the trends identified using confidence intervals were compared to the stability data of Good Manufacturing Practice (GMP) batches.

6.3. RESULTS

6.3.1. Modelling the stability of tetravalent *Shigella* GMMA formulation with Alum, and comparison with available long-term real time data

Shigella GMMA formulated with Alum were subjected to accelerated stability studies at the three temperatures of 2–8 °C, 25 °C and 40 °C. Sample timepoints were collected up to 6 months (**Figure 6.1**). Higher temperatures were used to accelerate degradation processes, considering that potential changes in certain QAs might be slow and difficult to track within a short timeframe at 2–8 °C. This approach allowed to identify kinetic models that best describe the changes in various QAs as a function of time and temperature.

At the end of the stability period, stressed formulations were characterized using a comprehensive panel of analytical methods (**Table 6.1**), to detect eventual physico-chemical changes. The quality attributes investigated—pH, particle size and free lipid A, OAg, proteins in the supernatant—were selected based on previous stability studies with similar formulations, in which major changes after thermal stress were observed particularly in terms of increase of *S. sonnei* OAg not adsorbed to Alhydrogel, free lipid A and protein in the supernatant, together with an increased particle size expressed as D[4,3] [253]. The pH was monitored as any change in this feature can adversely affect the overall stability and structural integrity of GMMA, as well as the immunogenicity of its components [102, 254].

After incubation at the three different temperatures, no significant changes in pH were observed. In terms of formulation size, D[4,3] and D(90) remained constant. Furthermore, no changes were observed in the total *S. flexneri* OAg in the drug product supernatant (**Figure 6.2**).

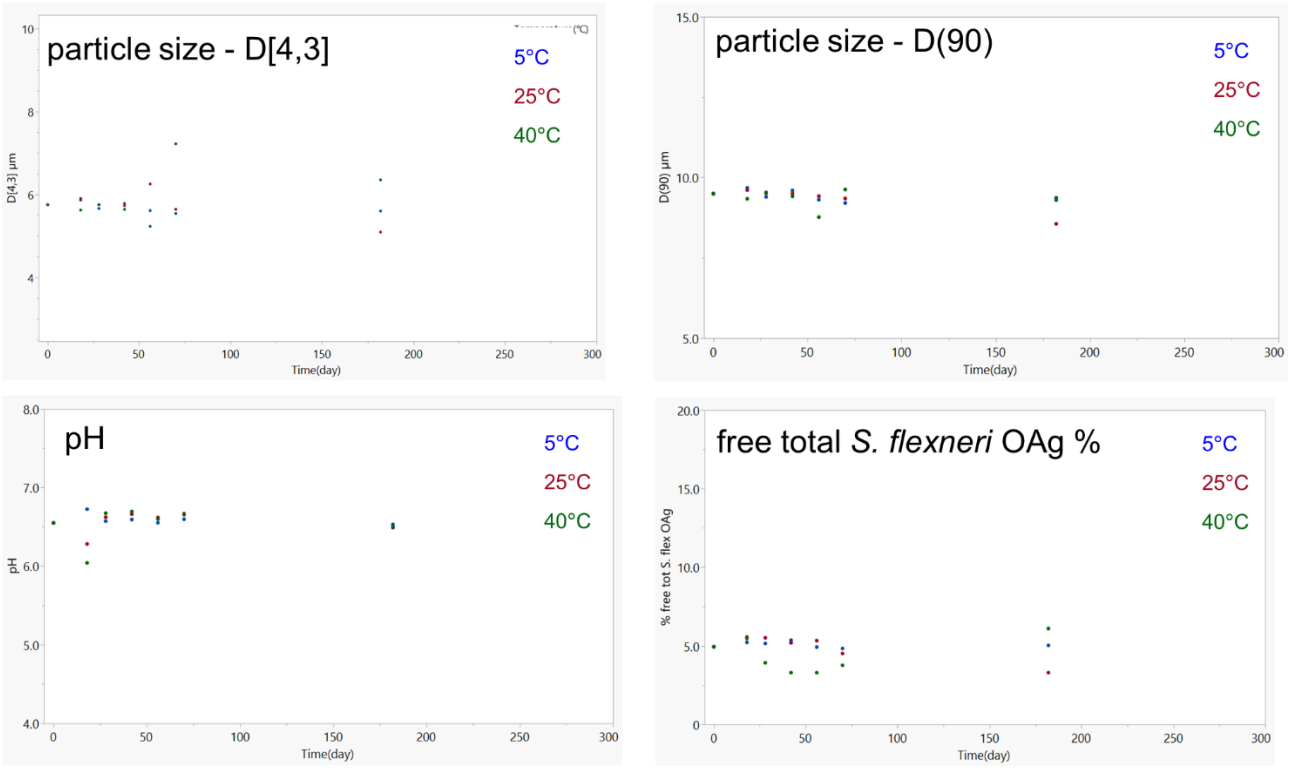

Figure 6.2. Accelerated stability studies of 4 GMMA + Alum at different temperatures, showing no changes over time in particle size (both D[4,3] and D(90)), pH and free total *S. flexneri* OAg in the supernatant.

A significant increase was instead observed for free lipid A, *S. sonnei* OAg and proteins in the supernatants. The stability profiles were evaluated using the integrated kinetic equation (**Table 6.2**) to perform a statistical analysis of stability data at the different incubation temperatures. First-order kinetic models were identified as the best models to predict such changes over time at each temperature (**Figure 6.3(A-C)**). Modelling was performed with different software, and the resulting models and prediction intervals were consistent (**Figure 6.3(A-C)** and **Table 6.2**). Moreover, the residuals were normally distributed, and no trends were observed in the residuals versus fitted values, time and temperature (**Figure 6.4(A-C)**).

Table 6.2. Optimized parameters of the kinetic equation found for the stability modelling of QAs of GMMA formulated with Alum.

$\frac{d[Y]}{dt} = A\ e^{-\frac{E_a}{RT}}\ [Y]^n$	Software	Final Y (t_∞)	Initial Y (t_0)	*n*	A (1/s)	E_a (KJ/mol)	Model SSE	Model RMSE
Free lipid A % in supernatant	JMP	24.0	3.8	1	11345146.7	82.0	8.5	0.75
	Minitab	24.0	3.8	1	11345787.0	82.0	8.5	0.75
Free *S. sonnei* OAg % in supernatant	JMP	63.4	0.2	1	210956.2	71.3	253.6	4.1
	Minitab	63.4	0.2	1	210946.0	71.3	253.6	4.1
	AKTS	63.1	0.3	1	241590.6	71.6	249.1	4.1
Free proteins % in supernatant	JMP	114.6	5.3	1	0.25	42.6	83.9	2.4
	Minitab	114.6	5.3	1	0.25	42.6	83.9	2.4

A: pre-exponential factor; E_a: activation energy; *n*: reaction order; Initial Y: CQA value at starting time; Final Y: CQA value at asymptote of the curve; SSE: model sum of squares error; and RMSE: model root mean square error.

A

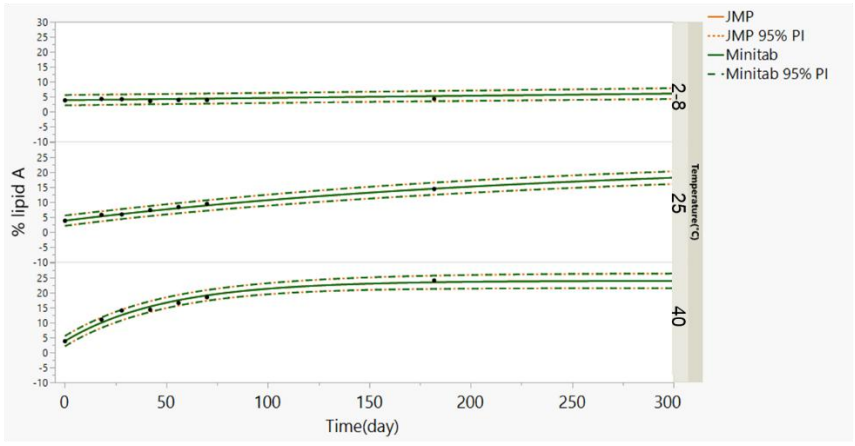

B

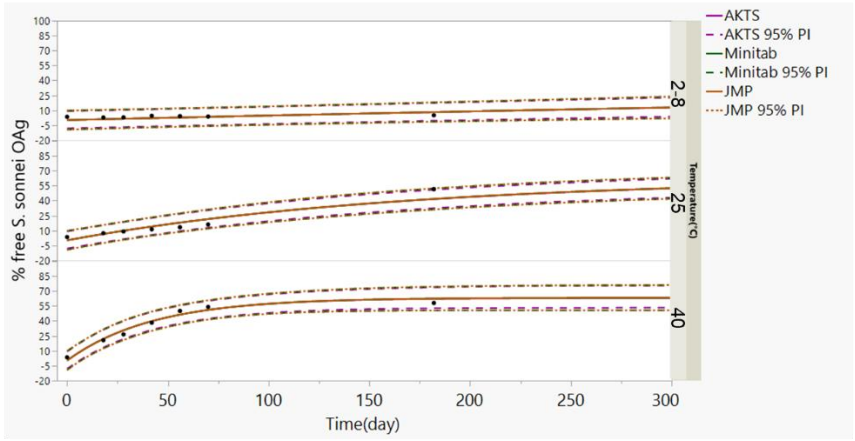

C

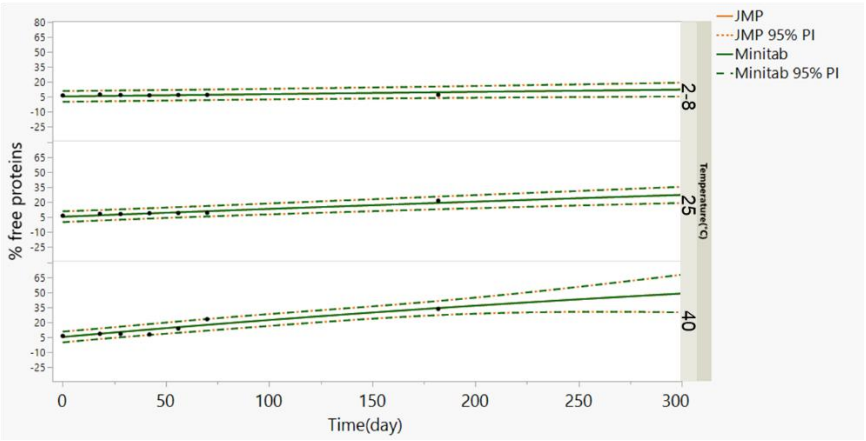

Figure 6.3. Models for free lipid A (A), *S. sonnei* OAg (B) and proteins (C) found in 4 GMMA+Alum supernatant, obtained from the integrated kinetic equation at different temperatures. Predictions (solid lines) obtained using AKTS (purple), JMP (orange) and/or Minitab (green) software with 95% prediction intervals (dashed and dotted lines). The experimental data are reported as black dots.

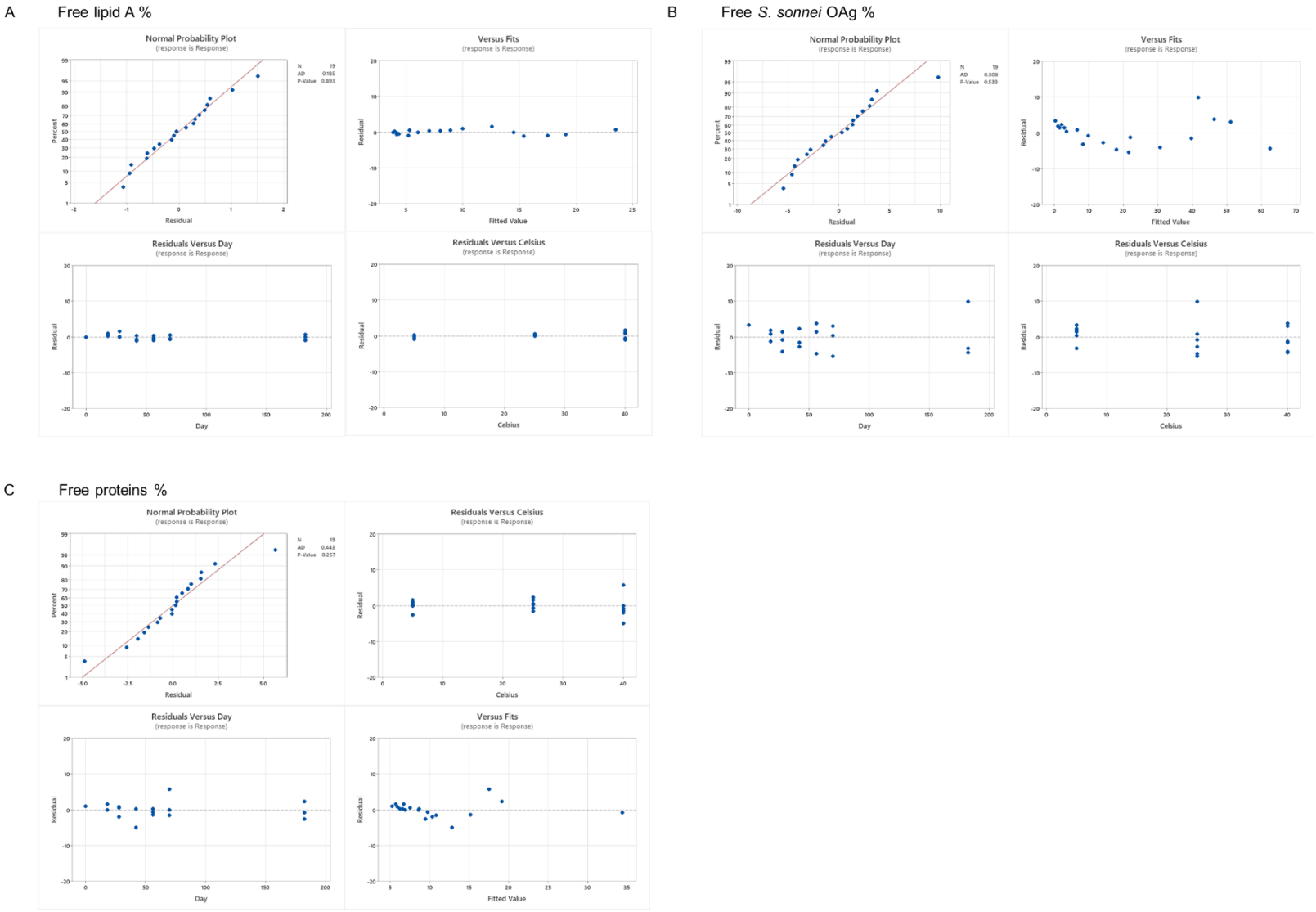

Figure 6.4. Analysis of the residuals for the models obtained for free lipid A (A), *S. sonnei* OAg (B) and proteins (C) in the supernatant of 4 GMMA+Alum.

After determination of the best kinetic models, the JMP software was used to simulate the reaction progress during arbitrarily chosen aging time and under any temperature profiles within the range tested [271]. **Figure 6.5** shows an example of a 3D surface plot of one of the models, specifically the free lipid A percentage one, along with its prediction interval.

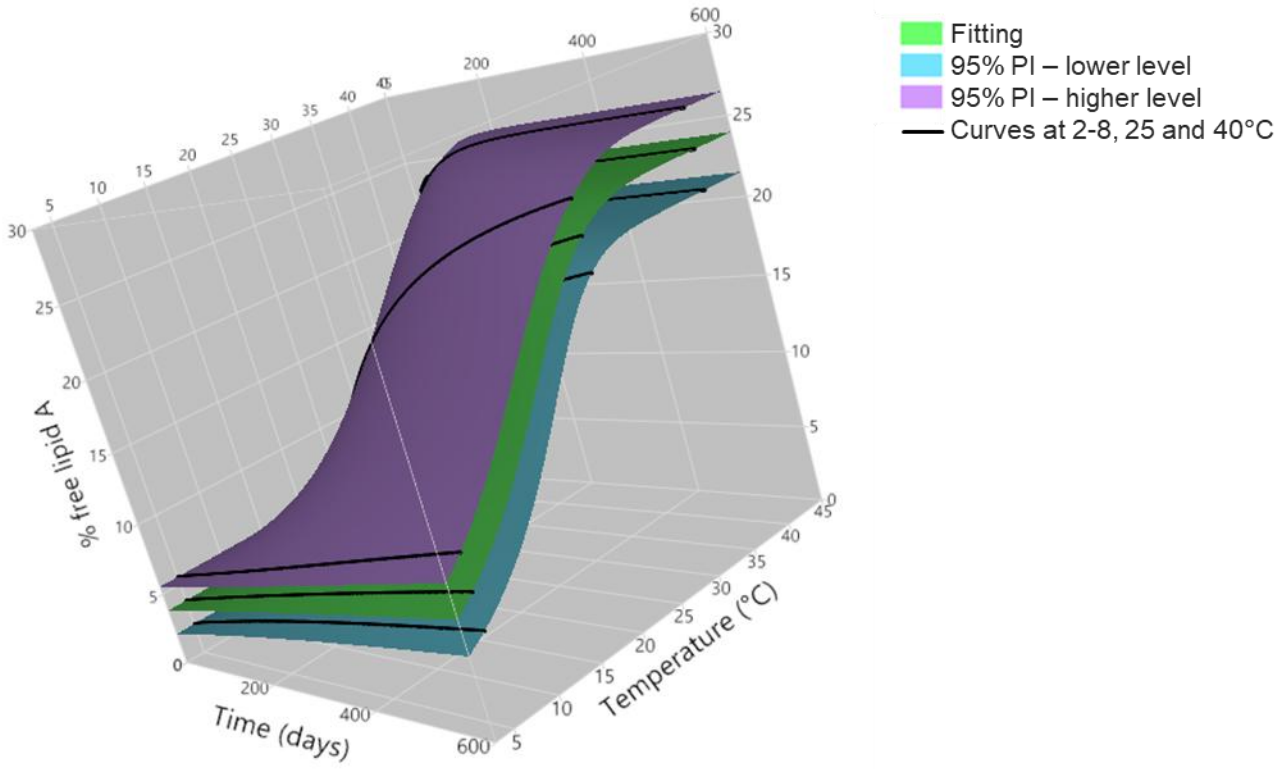

Figure 6.5. 3D surface plot of the free lipid A model obtained for 4 GMMA+Alum, showing the QA percentage over time, 0 to 600 days, and temperature ranging from 2–8°C to 40°C (green surface). Additionally, 3D surfaces representing the 95% prediction intervals are displayed (blue and violet surfaces), and the actual curves obtained at 2–8°C, 25°C, and 40°C are depicted as black lines.

The models developed for free lipid A and free protein in the supernatant of the 4 GMMA + Alum formulation at 2–8 °C were compared with long-term experimental data from real time stability assessments of three altSonflex1-2-3 GMP lots (**Figure 6.6(A-F)**). The real time values seem to be aligned with the model prediction intervals for the initial timepoints, roughly up to one year, but subsequently they fall below the lower prediction levels. Thus, the models represent a "least favorable scenario", indicating that the product is more stable than predicted. This divergence may be due to the models' use of data from higher temperatures, potentially influenced by other degradation phenomena that occur at elevated temperatures but are absent at 2–8 °C, hence not appearing in real time data.

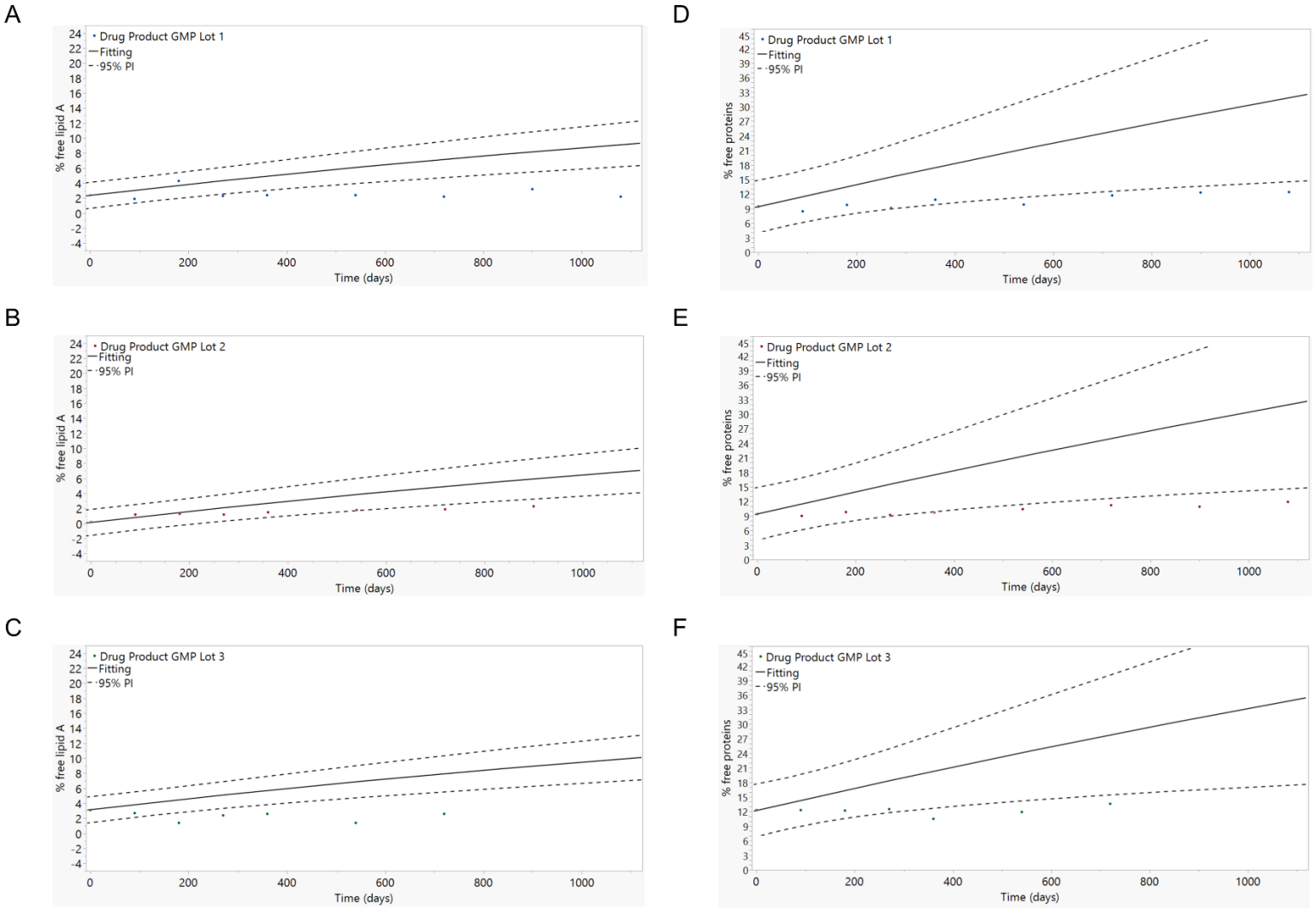

Figure 6.6. Comparison at 2–8°C of the models for free lipid A (A-C) and proteins (D-F), found for 4 GMMA+Alum in the supernatant,with available long-term data coming from the real time stability of three drug product GMP lots, represented as dots in blue, red and green respectively. The predictions are in black, reported as solid lines with 95% prediction intervals reported as dashed lines.

6.3.2. Modelling the stability of tetravalent *Shigella* GMMA formulation without Alum

The tetravalent *Shigella* GMMA formulation without Alum was placed under accelerated stability testing at the same temperatures of Alum-formulated GMMA, and timepoints were collected up to 6 months (**Figure 6.1**). This was done to acquire valuable insights into the stability profile of this formulation, an alternative to the tetravalent *Shigella* GMMA vaccine typically adsorbed on Alum. At the end of the stability studies, the QAs examined—which are the one impacting more on GMMA immunogenicity—included pH, GMMA size and integrity, and the percentage of free OAg in the supernatant post-ultracentrifugation (**Table 6.1**).

As for GMMA with Alum, post-incubation at different temperatures, pH levels remained stable, and no changes were observed in the total *S. flexneri* OAg in the supernatant following ultracentrifugation (**Figure 6.7**).

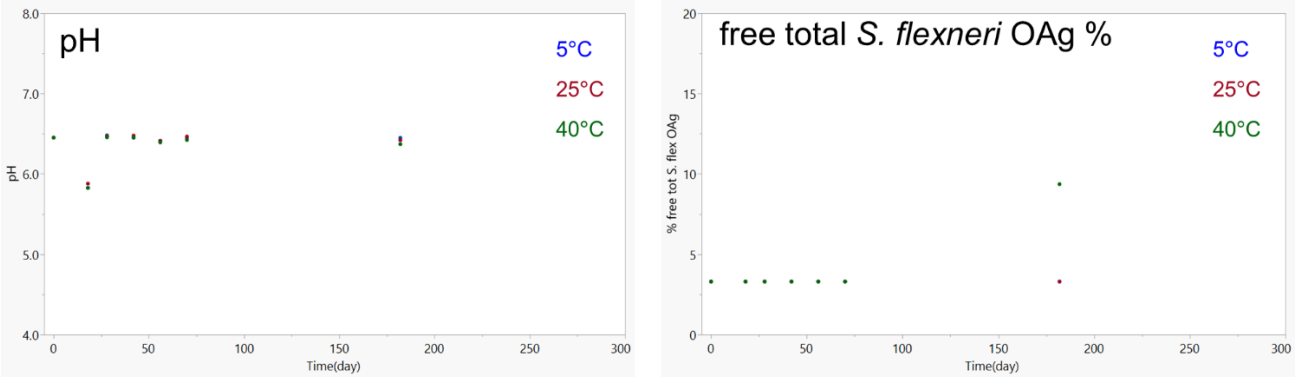

Figure 6.7. Accelerated stability studies of 4 GMMA without Alum at different temperatures, showing no changes over time in pH and free total *S. flexneri* OAg in the supernatant after ultracentrifugation. Outlayers due to analytical variability.

Changes were instead observed in terms of GMMA size and integrity, assessed by DLS and HPLC-SEC respectively, and free *S. sonnei* OAg in the supernatant. These stability profiles were evaluated using the advanced kinetic modelling approach (**Table 6.3**).

Table 6.3. Optimized parameters of the kinetic equation found for the stability modelling of QAs of GMMA formulated without Alum.

$\frac{d[Y]}{dt} = A\ e^{-\frac{E_a}{RT}}\ [Y]^n$	Software	Final Y (t_∞)	Initial Y (t_0)	*n*	A (1/s)	E_a (KJ/mol)	Model SSE	Model RMSE
GMMA size Z-average	JMP	108	122	2.4	3.60E+11	103	7.4	0.73
	Minitab	108	122	2.4	3.30E+11	103	7.4	0.7
	AKTS	108	122	2.4	3.60E+11	104	7.4	0.7
Integrity GMMA (t)/GMMA (t_0) % peak area	JMP	-0.4	94.9	1	2.5E+16	142.6	145.3	3.1
	Minitab	0	94.9	1	2.5E+16	142.6	145.3	3.1
	AKTS	0.4	94.9	1	2.6E+16	142.7	145.3	3.1
Free *S. sonnei* OAg % in supernatant	JMP	40.8	2.4	1	11106.3	64.4	180	3.5
	Minitab	40.8	2.4	1	11098.4	64.4	180	3.5

A: pre-exponential factor; E_a: activation energy; *n*: reaction order; Initial Y: CQA value at starting time; Final Y: CQA value at asymptote of the curve; SSE: model sum of squares error; and RMSE: model root mean square error

In particular, a 2.4th-order model was determined to be the most suitable option for predicting the reduction in GMMA size across different temperatures and over time (**Figure 6.8(A)**). In contrast, a first-order kinetic model was constructed to describe the decline in GMMA integrity (**Figure 6.8(B)**). For free *S. sonnei* OAg increase, a first-order model was selected to predict this change (**Figure 6.8(C)**). Similar to the formulation with Alum, modelling for this formulation was performed using various software, and the resulting models and prediction intervals displayed consistency (**Figure 6.8(A-C)** and **Table 6.3**). Residuals for the integrity of GMMA followed a normal distribution, whereas the p-values from the Anderson-Darling test were significant for GMMA size and free *S. sonnei* OAg levels. No observable trends were detected against fitted values, time or temperature (**Figure 6.9(A-C)**).

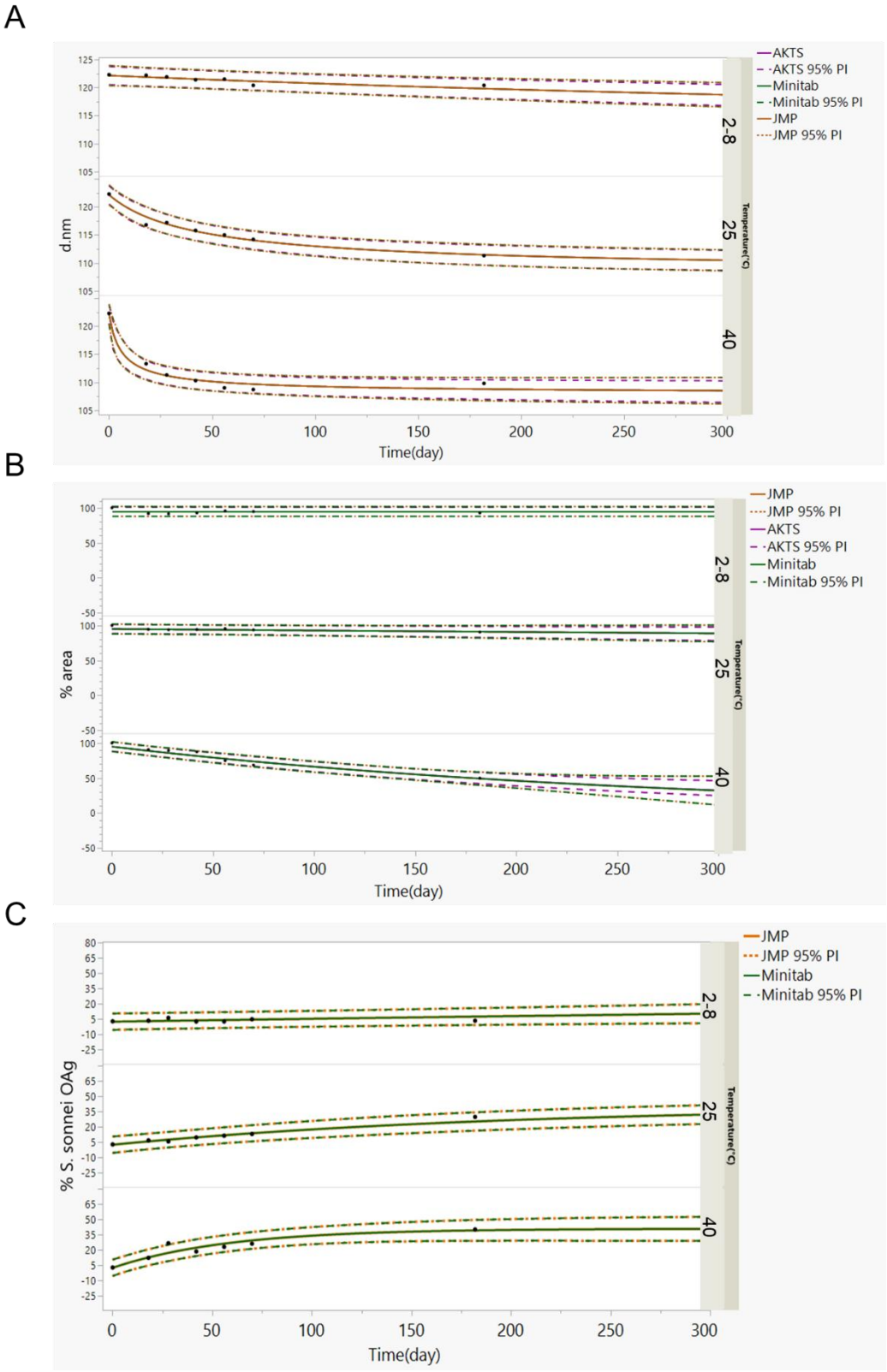

Figure 6.8. Models for GMMA size (A), GMMA integrity (B) and free *S. sonnei* OAg in the supernatant (C) in 4 GMMA without Alum, obtained from the Šesták–Berggren truncated equation at different temperatures. Predictions (solid lines) obtained using AKTS (purple), JMP (orange) and/or Minitab (green) software with 95% prediction intervals (dashed and dotted lines). The experimental data are reported as black dots.

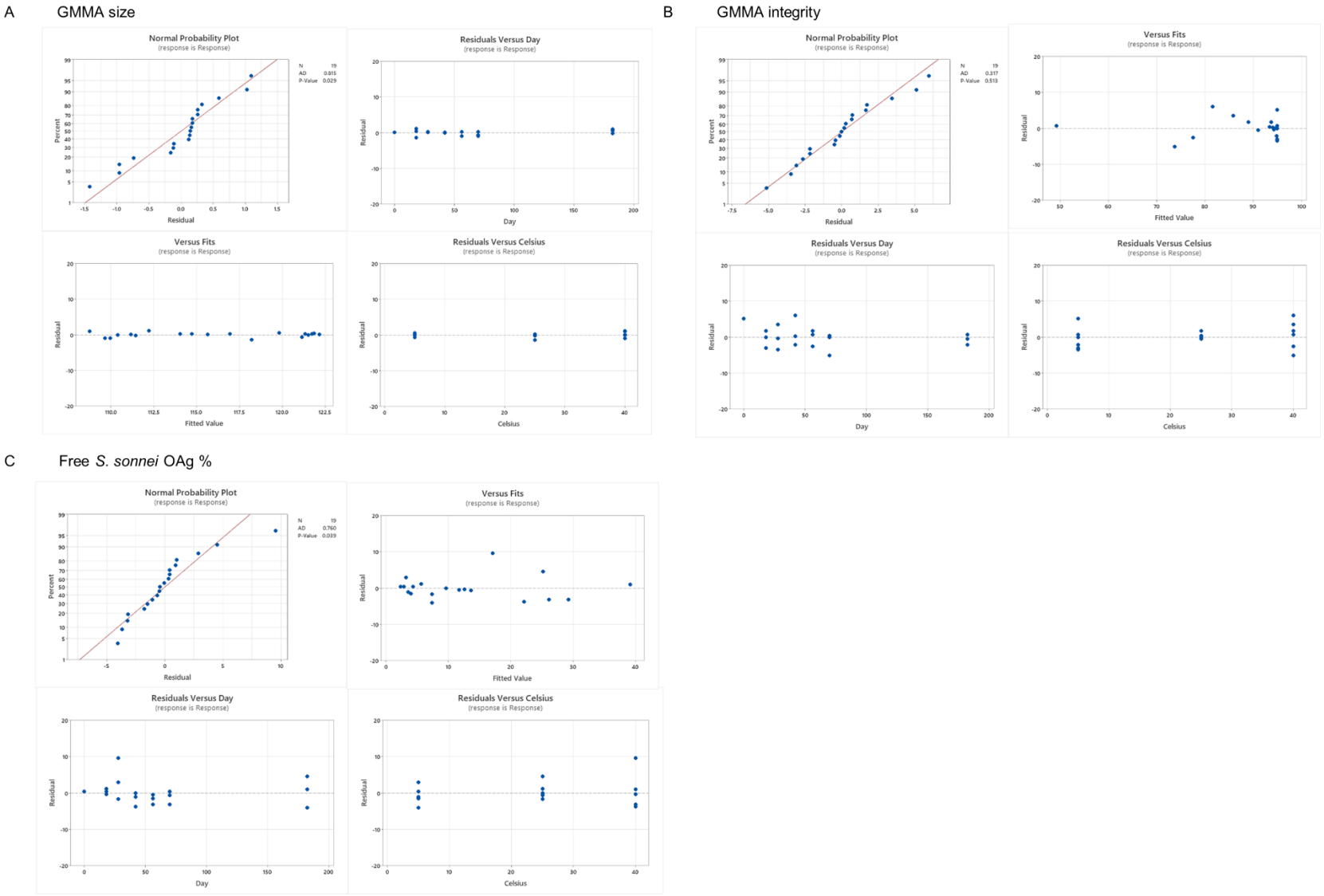

Figure 6.9. Analysis of the residuals for the models obtained for GMMA size (A), GMMA integrity (B) and free *S. sonnei* OAg in the supernatant (C) in 4 GMMA without Alum.

6.4. DISCUSSION

GMMA have been proposed for developing a tetravalent vaccine against *Shigella*, known as altSonflex1-2-3, aiming to provide broad protection against the most prevalent *Shigella* serotypes, which primarily affect infants in LMICs [78, 202]. GMMA are known for their ease of manufacturing and have potential for low-cost production [99]. They represent a promising platform for developing multivalent vaccines. However, the complex composition of GMMA makes characterization challenging, particularly in multivalent vaccines. A wide array of analytical methods has been implemented to ensure comprehensive characterization of GMMA [214, 254], ensuring manufacturing consistency and assessing stability over time. These analytics are able to detect changes that could affect vaccine immunogenicity [253].

When stability evaluations rely solely on real time data, they may hinder rapid vaccine development. Therefore, accelerated stability studies and predictive modelling are essential tools for predicting stability within a shorter timeframe. Predictive stability modelling has successfully predicted degradation profiles across various vaccine platforms, including inactivated virus, protein-based vaccines, glycoconjugates, emulsion-based adjuvants, and mRNA vaccines [178, 268, 270-275].

In this study, this approach was applied to tetravalent *Shigella* GMMA formulations, both with and without Alum. Accelerated stability assessments were performed at 2–8 °C, 25 °C and 40 °C, with data collected up to six months. Stability models were constructed using advanced kinetic modelling [270] with different software, comparing predictions with available long-term real time data.

The GMMA + Alum (altSonflex1-2-3) was selected due to its late-stage development status and the abundance of real time stability data. This approach was extended to tetravalent *Shigella* GMMA formulated without Alum, providing valuable insights into vaccine stability and identifying the impact of aging on specific QAs, even in the absence of Alum. Recent studies indicate that Alum is not essential for improving GMMA antibody response magnitude, quality or functionality [194, 213]. Additionally, *Shigella* GMMA formulated without Alum exhibited good tolerance in rabbits [213], and human monocyte activation tests (MAT) indicated that, regardless of Alum inclusion, GMMA induced comparable levels of IL-6 release [213, 246]. Therefore, the advanced kinetic modelling approach become crucial for obtaining new insights on this formulation and useful to support eventual testing of GMMA without Alum in humans.

For GMMA formulated with Alum, stress tests at different temperatures revealed notable changes, such as increased free proteins and lipid A percentage in the supernatant, consistent with previous studies [253]. Additionally, there was an increase in *S. sonnei* OAg not adsorbed to Alum, whereas

the percentage of free *S. flexneri* OAg did not increase. The increase for the *S. sonnei* OAg component likely results from the capsular polysaccharide of the *S. sonnei* GMMA, which shares the same structure as OAg repeats but is longer and lacks the core-lipid A anchored to the membrane [224]. Importantly, the pH was not affected during stability testing. Since pH is a critical parameter for the physico-chemical stability of GMMA and can influence immunogenicity [102, 254], its monitoring was essential. Furthermore, in contrast to previous findings, particle size remained constant across different temperatures [253].

Models developed for free lipid A and protein in the supernatant of 4 GMMA + Alum formulation at 2–8 °C were compared with long-term experimental data from real time stability studies of three altSonflex1-2-3 GMP lots. The trend found for real time data seems to agree with the model prediction bands for initial timepoints, generally up to one year, then, later, fell below lower prediction levels. Thus, the models demonstrate a "worst-case scenario", indicating greater product stability than predicted up to one year. Indeed, as per ICH guidelines, predictions are valid for up to twice the last stability timepoint analysed for a maximum of one-year extension. The discrepancy between real time results and kinetic modelling might arise from the models incorporating data obtained at higher temperatures, where additional degradation phenomena occur that are not present in the 2–8 °C conditions observed in real time data. Accurately selecting temperatures for accelerated stability studies is therefore crucial.

Without Alum, tetravalent *Shigella* GMMA were found to be stable in terms of pH. This was different from what reported in reference [253], in which a pH decrease was observed testing the monovalent stressed *Shigella* GMMA. This may be due to different buffers, saline versus formulation buffer used here. Significant changes were observed, with particle size decreasing (as determined via DLS), likely due to loss of long capsular polysaccharide chains from *S. sonnei* GMMA [224]. Indeed, an increase in *S. sonnei* OAg not adsorbed to Alum was noted. The percentage of free *S. flexneri* OAg remained instead constant, as in Alum-formulated vaccine. Moreover, a decrease in the intensity of fluorescence emission profiles by HPLC-SEC was observed, indicating a reduction in GMMA integrity. The results obtained are summarized in **Table 6.4**.

Table 6.4. Impact of accelerated stability testing at different temperatures on the stability profiles of quality attributes investigated for GMMA with and without Alum.

Quality attribute	4 GMMA + Alum	4 GMMA
pH	No change	No change
Size	No change (both D[4,3] and D(90))	Reduction
free lipid A in supernatant	Increase	—
free OAg in supernatant	No change in total *S. flexneri* OAg, increase in *S. sonnei* OAg	No change in total *S. flexneri* OAg, increase in *S. sonnei* OAg
free proteins in supernatant	Increase	—
Integrity	—	Reduction

It would be important to verify whether observed physico-chemical changes in the formulation without Alum could impact GMMA immunogenicity. A potency method would be key for monitoring potential loss in vaccine efficacy. An *in vitro* relative potency (IVRP) assay developed for tetravalent GMMA *Shigella* with Alum could also be applicable without it. The IVRP is based on recognizing OAg by monoclonal antibodies selected to target key epitopes of different OAg active ingredients, replacing animal use [253].

In general, advanced kinetic modelling can be useful to: (1) provide essential data on vaccine stability, including during cold chain disruptions, crucial for LMICs; (2) assist in selecting optimal vaccine candidates and formulations early in the development process, reducing the risk of failure; (3) identify how aging affects critical quality attributes. Beyond establishing shelf life, kinetic models are valuable during development for understanding the specific degradation patterns characteristic of a given product, allowing for more comprehensive characterization. Moreover, these degradation patterns can assist in selecting the optimal storage conditions of a vaccine early in the development stages (e.g., buffer, pH, excipients).

The proposed work can be extended to other multivalent vaccines with OAg as a key active ingredient. In general, this type of modelling can be applied to vaccines produced using the same technology or targeting the same pathogen; however, its applicability and reliability depend on several factors, including product and platform knowledge, the development stage, and the

availability of appropriate analytical methods for product characterization. Moreover, the selection of the right temperature ranges for accelerated stability studies is fundamental.

Applying this approach to other OAg-based GMMA vaccines would be valuable to determine whether comparable models can be obtained. If similar models emerge, they may reflect intrinsic properties of the GMMA platform rather than pathogen-specific characteristics. This could enable the consolidation of such models across GMMA-based vaccines, thereby facilitating their use for new targets.

7. CONCLUSIONS

In recent years, the growing threat posed by antibiotic-resistant bacteria has increasingly underscored the critical role that vaccines can play in reducing the global burden of infectious diseases [21]. In particular, multivalent polysaccharide-based vaccines have emerged as promising candidates to address the AMR challenge by providing broad protection against diverse serotypes.

My PhD work has aimed to advance the development of such vaccines, targeting pathogens that significantly impact LMICs. By addressing critical technological and analytical challenges, the research has not only demonstrated technical feasibility but has also provided important insights into the immunological and manufacturing aspects essential to combating AMR.

My project focused on two key bacterial pathogens implicated in AMR: *Shigella* and *Salmonella*. *Shigella* remains the leading bacterial cause of diarrheal disease, particularly in regions where access to clean water and adequate healthcare is limited [121]. Similarly, *Salmonella* serovars, including Typhi and Paratyphi A, contribute significantly to morbidity and mortality in resource-constrained settings [276].

Two advanced vaccine technologies were explored: GMMA and glycoconjugation. GMMA, which are outer membrane vesicles derived from genetically modified Gram-negative bacteria, offer several advantages. They display a cocktail of antigens in the natural membrane context and carry immunostimulatory molecules such as lipopolysaccharides and lipoproteins. These features promote a robust immune response, and GMMA can be produced via a simple, detergent-free manufacturing process that is both cost-effective and scalable. The ability to introduce additional mutations to modulate lipid A content further reduces the endotoxicity of the GMMA, thereby enhancing their safety profile [81].

Alternatively, glycoconjugate vaccines, which involve the covalent linkage of a polysaccharide antigen to a carrier protein, remain a well-established strategy. This approach enhances the immunogenicity of polysaccharide antigens, which are naturally T-cell independent, leading to improved memory responses, class switching, and increased antibody production in infants [59].

In this work these two approaches were compared for an OAg-based vaccine against *Shigella*. The OAg, a key component of the lipopolysaccharide on the bacterial surface, is essential for directing protective immunity against *Shigella* infections [145, 200]. GMMA and glycoconjugates targeting *S. sonnei* and *S. flexneri* strains 1b, 2a, and 3a were formulated into tetravalent vaccines, with and without the adjuvant Alhydrogel, and in murine and rabbit models. In mice, GMMA elicited

significantly stronger bactericidal titers against all the tested *Shigella* strains compared to glycoconjugate formulations. In rabbits, a similar trend was observed for *S. sonnei*, while responses to *S. flexneri* serotypes were comparable between the two platforms. Moreover, GMMA did not require Alhydrogel to achieve robust immunogenicity, which points to an intrinsic advantage in formulation simplicity. This part of my PhD thesis has been already published [194].

Building on these promising results, the *Shigella* GMMA tetravalent formulation was expanded to a hexavalent formulation by addition of the glycoconjugate antigens against *Salmonella* Typhi and Paratyphi A. This combination approach not only addresses two significant pathogens simultaneously but also meets an important need by broadening the protective spectrum of the vaccine. As these two pathogens coexist in many geographical areas, combining them into a single infant vaccine could substantially contribute to reducing enteric disease burden, AMR, increase commercial attractiveness through reduced cost of goods, and improve acceptance among end users and health-care providers, ultimately leading to higher and more equitable vaccination coverage. Importantly, the technical feasibility of combining these six antigens was rigorously demonstrated, with data showing that each component maintained its ability to elicit a robust humoral immune response in different animal models, indicating no adverse immunological interference among the antigens.

Another major focus of my PhD project was the development of novel analytical methods to ensure the quality of complex vaccine formulations—a key aspect of both regulatory approval and long-term vaccine efficacy. Polysaccharide content is one of the critical quality attributes (CQA) for PS-based vaccines; thus, accurate and precise methods for antigen quantification are essential [249]. One particularly challenging aspect was the quantification of *S. flexneri* 1b, 2a and 3a OAg, which share identical sugar compositions. To address this, a LC-MS method was developed. This method differentiates monomers based on their unique linkage patterns in the OAg chain after derivatization, enabling the identification of individual *S. flexneri* OAg components in multivalent combinations of either GMMA or purified OAg samples.. This method has potential for not only identifying but also quantifying such OAg. Improvement in the sample preparation workflow is necessary to increase throughput, while the calibration curve linearity and quantification by means of an internal standard need to be evaluated.

For the *Salmonella* antigens, a distinct analytical strategy was necessary. The development of a HPAEC-PAD method allowed the selective quantification of OAg from *Salmonella* Typhimurium, Enteritidis, and Paratyphi A. These serovars contain a common polysaccharide backbone but differ by a specific di-deoxy monosaccharide linked to the RU structure [167, 168]. By optimizing mild hydrolysis conditions to release these less stable sugars without degrading the rest of the OAg, and

optimizing chromatographic conditions, it was possible to separate and accurately quantify these sugars even within complex mixtures.

The analytical progress not only enhances quality control during vaccine production but also contributes to a better understanding of product stability—a crucial aspect for vaccine safety and efficacy [266]. Another significant achievement of this project was the application of advanced kinetic modelling, based on accelerated stability studies applied to tetravalent *Shigella* GMMA formulations, both with and without Alhydrogel. By collecting data at multiple temperatures and generating predictive models, this approach allowed estimation of quality attributes values over time with known uncertainty. This is the first application of such predictive models to multivalent formulations, enabling early detection of stability issues and accelerating product development.

Overall, the results of this work represent a significant advance in the development of multivalent, saccharide-based vaccines, further confirming that multivalent vaccine strategies can deliver broad-spectrum protection, translating into a meaningful impact on public health. While this work focuses on human pathogens, the underlying principle of using vaccines to reduce infection and antibiotic use has broader relevance. Similar strategies could, in theory, also be applied to animal health to curb AMR at its source, reinforcing the One Health perspective and highlighting the global importance of vaccine innovation.

LIST OF PUBLICATIONS

- Di Benedetto R[#], Mancini F[#], Caradonna V, Aruta MG, Giannelli C, Rossi O, Micoli F. Comparison of *Shigella* GMMA and glycoconjugate four-component formulations in animals. Front Mol Biosci. 2023 Nov 16;10:1284515. doi: 10.3389/fmolb.2023.1284515. PMID: 38046812; PMCID: PMC10690372. #contributed equally

- Nappini R, Alfini R, Durante S, Salvini L, Raso MM, Palmieri E, Di Benedetto R, Carducci M, Rossi O, Cescutti P, Micoli F, Giannelli C. Modeling 1-Cyano-4-Dimethylaminopyridine Tetrafluoroborate (CDAP) Chemistry to Design Glycoconjugate Vaccines with Desired Structural and Immunological Characteristics. Vaccines (Basel). 2024 Jun 24;12(7):707. doi: 10.3390/vaccines12070707. PMID: 39066345; PMCID: PMC11281720.

- Boero E[#], Di Benedetto R[#], Vezzani G, Alfini R, Ceyssens PJ, Tansarli GS, Fang FC, Fontana C, Rossi A, Carrara S, Mancini F, Iturriza M, Sala C, Giannelli C, Rossi O, Micoli F. Antibodies elicited by altSonflex1-2-3 GMMA vaccine are bactericidal against a panel of drug-resistant *Shigella* clinical isolates. Front Immunol. 2025 Sep 4;16:1652460. doi: 10.3389/fimmu.2025.1652460. PMID: 40977721; PMCID: PMC12443847. #contributed equally

In preparation:

- Evaluation of multivalent combinations against *Shigella* and *Salmonella* infections

- Application of advanced kinetic modelling to tetravalent *Shigella* GMMA formulations to predict vaccine stability based on accelerated studies

- Review on OAg-based vaccines

TRANSPARENCY, 3R AND ETHICAL STATEMENTS

Transparency statement

This work was undertaken at the request of and sponsored by GlaxoSmithKline Biologicals SA. Roberta Di Benedetto is an employee of the GSK group of companies and participates in a PhD program at GSK. GSK Vaccines Institute for Global Health Srl is an affiliate of GlaxoSmithKline Biologicals SA.

3Rs and ethical statement

GSK is committed to the replacement, reduction and refinement of animal studies (3Rs). Non-animal models and alternative technologies are part of our strategy and employed where possible. When animals are required, application of robust study design principles and peer review minimizes animal use, reduces harm and improves benefit in studies..All animal studies were ethically reviewed and carried out in accordance with European Directive 2010/63/EU, national legislation D.Lgs. 26/2014 and the GSK Policy on Care, Welfare and Treatment of Animals.

REFERENCES

1. Hutchings, M.I., A.W. Truman, and B. Wilkinson, *Editorial overview: Antimicrobials: Tackling AMR in the 21st century.* Curr Opin Microbiol, 2019. **51**: p. iii-v.
2. Jansen, K.U. and A.S. Anderson, *The role of vaccines in fighting antimicrobial resistance (AMR).* Hum Vaccin Immunother, 2018. **14**(9): p. 2142-2149.
3. O'Neill, J., *Tackling drug-resistant infections globally: final report and recommendations.* Tackling drug-resistant infections globally: final report and recommendations, 2016: p. 84 pp.
4. Resistance, R.o.A., et al., *Antimicrobial Resistance: Tackling a Crisis for the Health and Wealth of Nations : December 2014*. 2014: Review on Antimicrobial Resistance.
5. Hay, S.I., et al., *Measuring and mapping the global burden of antimicrobial resistance.* BMC Med, 2018. **16**(1): p. 78.
6. Resistance, I.C.G.o.A., *No time to wait: securing the future from drug-resistant infections.* Report to the Secretary General of the United Nations, 2019.
7. Gautam, A., *Antimicrobial Resistance: The Next Probable Pandemic.* JNMA J Nepal Med Assoc, 2022. **60**(246): p. 225-228.
8. Sulis, G., S. Sayood, and S. Gandra, *Antimicrobial resistance in low-and middle-income countries: current status and future directions.* Expert review of anti-infective therapy, 2022. **20**(2): p. 147-160.
9. Murray, C.J., et al., *Global burden of bacterial antimicrobial resistance in 2019: a systematic analysis.* The lancet, 2022. **399**(10325): p. 629-655.
10. Miller, W.R. and C.A. Arias, *ESKAPE pathogens: antimicrobial resistance, epidemiology, clinical impact and therapeutics.* Nat Rev Microbiol, 2024. **22**(10): p. 598-616.
11. Naghavi, M., et al., *Global burden of bacterial antimicrobial resistance 1990–2021: a systematic analysis with forecasts to 2050.* The Lancet, 2024. **404**(10459): p. 1199-1226.
12. Organization, W.H., *Global action plan on antimicrobial resistance. Geneva, Switzerland; 2015*. 2019.
13. Organization, W.H., *Global Antimicrobial Resistance Surveillance System (GLASS): molecular methods for antimicrobial resistance (AMR) diagnostics to enhance the Global antimicrobial Resistance Surveillance System*, in *Global Antimicrobial Resistance Surveillance System (GLASS): Molecular Methods for Antimicrobial Resistance (AMR) Diagnostics to Enhance the Global Antimicrobial Resistance Surveillance System*. 2019.
14. Tacconelli, E., et al., *Discovery, research, and development of new antibiotics: the WHO priority list of antibiotic-resistant bacteria and tuberculosis.* The Lancet infectious diseases, 2018. **18**(3): p. 318-327.
15. Organization, W.H., *WHO bacterial priority pathogens list, 2024: bacterial pathogens of public health importance, to guide research, development, and strategies to prevent and control antimicrobial resistance*. 2024: World Health Organization.

16. Organization, W.H., *New Multi-Partner Trust Fund launched to combat antimicrobial resistance globally*. 2019.

17. Kapoor, G., S. Saigal, and A. Elongavan, *Action and resistance mechanisms of antibiotics: A guide for clinicians.* J Anaesthesiol Clin Pharmacol, 2017. **33**(3): p. 300-305.

18. Mladenovic-Antic, S., et al., *Correlation between antimicrobial consumption and antimicrobial resistance of Pseudomonas aeruginosa in a hospital setting: a 10-year study.* J Clin Pharm Ther, 2016. **41**(5): p. 532-7.

19. Klein, E.Y., et al., *Global increase and geographic convergence in antibiotic consumption between 2000 and 2015.* Proc Natl Acad Sci U S A, 2018. **115**(15): p. E3463-e3470.

20. Saikia, S. and P. Chetia, *Antibiotics: From Mechanism of Action to Resistance and Beyond.* Indian J Microbiol, 2024. **64**(3): p. 821-845.

21. Micoli, F., et al., *The role of vaccines in combatting antimicrobial resistance.* Nat Rev Microbiol, 2021. **19**(5): p. 287-302.

22. Blair, J.M., et al., *Molecular mechanisms of antibiotic resistance.* Nat Rev Microbiol, 2015. **13**(1): p. 42-51.

23. Brüssow, H., *The antibiotic resistance crisis and the development of new antibiotics.* Microb Biotechnol, 2024. **17**(7): p. e14510.

24. Aslam, B., et al., *Antibiotic resistance: a rundown of a global crisis.* Infect Drug Resist, 2018. **11**: p. 1645-1658.

25. Baker, S.J., et al., *Technologies to address antimicrobial resistance.* Proc Natl Acad Sci U S A, 2018. **115**(51): p. 12887-12895.

26. La Guidara, C., et al., *Vaccines and monoclonal antibodies as alternative strategies to antibiotics to fight antimicrobial resistance.* International journal of molecular sciences, 2024. **25**(10): p. 5487.

27. Lipsitch, M. and G.R. Siber, *How Can Vaccines Contribute to Solving the Antimicrobial Resistance Problem?* mBio, 2016. **7**(3).

28. Bloom, D.E., et al., *Antimicrobial resistance and the role of vaccines.* Proc Natl Acad Sci U S A, 2018. **115**(51): p. 12868-12871.

29. Rappuoli, R., A. Santoni, and A. Mantovani, *Vaccines: An achievement of civilization, a human right, our health insurance for the future.* J Exp Med, 2019. **216**(1): p. 7-9.

30. Atkins, K.E., et al., *Use of mathematical modelling to assess the impact of vaccines on antibiotic resistance.* Lancet Infect Dis, 2018. **18**(6): p. e204-e213.

31. Mishra, R.P., et al., *Vaccines and antibiotic resistance.* Curr Opin Microbiol, 2012. **15**(5): p. 596-602.

32. Klugman, K.P. and S. Black, *Impact of existing vaccines in reducing antibiotic resistance: primary and secondary effects.* Proceedings of the National Academy of Sciences, 2018. **115**(51): p. 12896-12901.

33. Troisi, M., et al., *Vaccines as remedy for antimicrobial resistance and emerging infections.* Curr Opin Immunol, 2020. **65**: p. 102-106.

34. Rappuoli, R., D.E. Bloom, and S. Black, *Deploy vaccines to fight superbugs.* Nature, 2017. **552**(7684): p. 165-167.

35. Tagliabue, A. and R. Rappuoli, *Changing Priorities in Vaccinology: Antibiotic Resistance Moving to the Top.* Front Immunol, 2018. **9**: p. 1068.

36. Kennedy, D.A. and A.F. Read, *Why does drug resistance readily evolve but vaccine resistance does not?* Proc Biol Sci, 2017. **284**(1851).

37. Bagnoli, F. and D.J. Payne, *Reaction: Alternative Modalities to Address Antibiotic-Resistant Pathogens.* Chem, 2017. **3**(3): p. 369-372.

38. Kennedy, D.A. and A.F. Read, *Why the evolution of vaccine resistance is less of a concern than the evolution of drug resistance.* Proc Natl Acad Sci U S A, 2018. **115**(51): p. 12878-12886.

39. Organization, W.H., *Leveraging vaccines to reduce antibiotic use and prevent antimicrobial resistance.* WHO: Geneva, Switzerland, 2021: p. 1-40.

40. Tekle, Y.I., et al., *Controlling antimicrobial resistance through targeted, vaccine-induced replacement of strains.* PLoS One, 2012. **7**(12): p. e50688.

41. Mba, I.E., et al., *Vaccine development for bacterial pathogens: Advances, challenges and prospects.* Tropical Medicine & International Health, 2023. **28**(4): p. 275-299.

42. Delany, I., R. Rappuoli, and E. De Gregorio, *Vaccines for the 21st century.* EMBO Mol Med, 2014. **6**(6): p. 708-20.

43. Pollard, A.J. and E.M. Bijker, *A guide to vaccinology: from basic principles to new developments.* Nat Rev Immunol, 2021. **21**(2): p. 83-100.

44. Laidlaw, B.J., J.E. Craft, and S.M. Kaech, *The multifaceted role of CD4(+) T cells in CD8(+) T cell memory.* Nat Rev Immunol, 2016. **16**(2): p. 102-11.

45. Xie, Q., J. Ding, and Y. Chen, *Role of CD8(+) T lymphocyte cells: Interplay with stromal cells in tumor microenvironment.* Acta Pharm Sin B, 2021. **11**(6): p. 1365-1378.

46. Wieczorek, M., et al., *Major Histocompatibility Complex (MHC) Class I and MHC Class II Proteins: Conformational Plasticity in Antigen Presentation.* Front Immunol, 2017. **8**: p. 292.

47. Micoli, F., P. Costantino, and R. Adamo, *Potential targets for next generation antimicrobial glycoconjugate vaccines.* FEMS Microbiol Rev, 2018. **42**(3): p. 388-423.

48. Stefanetti, G., et al., *Immunobiology of Carbohydrates: Implications for Novel Vaccine and Adjuvant Design Against Infectious Diseases.* Front Cell Infect Microbiol, 2021. **11**: p. 808005.

49. Taylor, C.M. and I.S. Roberts, *Capsular Polysaccharides and.* Concepts in bacterial virulence, 2004. **12**: p. 55-66.

50. Luong, P. and D.H. Dube, *Dismantling the bacterial glycocalyx: Chemical tools to probe, perturb, and image bacterial glycans.* Bioorg Med Chem, 2021. **42**: p. 116268.

51. Jones, C., *Vaccines based on the cell surface carbohydrates of pathogenic bacteria.* An Acad Bras Cienc, 2005. **77**(2): p. 293-324.

52. Costantino, P., R. Rappuoli, and F. Berti, *The design of semi-synthetic and synthetic glycoconjugate vaccines.* Expert Opin Drug Discov, 2011. **6**(10): p. 1045-66.

53. Mac, L.C. and R.G. Hodges, *Prevention of pneumococcal pneumonia by immunization with specific capsular polysaccharides.* J Exp Med, 1945. **82**: p. 445-65.

54. Gold, R. and M.S. Artenstein, *Meningococcal infections. 2. Field trial of group C meningococcal polysaccharide vaccine in 1969-70.* Bull World Health Organ, 1971. **45**(3): p. 279-82.

55. Artenstein, M.S., et al., *Prevention of meningococcal disease by group C polysaccharide vaccine.* N Engl J Med, 1970. **282**(8): p. 417-20.

56. Jha, V. and E.N. Janoff, *Complementary Role of CD4+ T Cells in Response to Pneumococcal Polysaccharide Vaccines in Humans.* Vaccines (Basel), 2019. **7**(1).

57. Peltola, H., et al., *Clinical efficacy of meningococcus group A capsular polysaccharide vaccine in children three months to five years of age.* N Engl J Med, 1977. **297**(13): p. 686-91.

58. Peltola, H.K., H.; Sivonen A, *Haemophilus influenzae Type b capsular polysaccharide vaccine in children: A double-blind field study of 100,000 vaccinees 3 months to 5 years of age in Finland.* Pediatrics, 1977. **60**: p. 727-32.

59. Rappuoli, R., *Glycoconjugate vaccines: Principles and mechanisms.* Sci Transl Med, 2018. **10**(456).

60. Berti, F. and F. Micoli, *Improving efficacy of glycoconjugate vaccines: from chemical conjugates to next generation constructs.* Curr Opin Immunol, 2020. **65**: p. 42-49.

61. Klugman, K.P., *Herd protection induced by pneumococcal conjugate vaccine.* Lancet Glob Health, 2014. **2**(7): p. e365-6.

62. Gilsdorf, J.R., *Hib Vaccines: Their Impact on Haemophilus influenzae Type b Disease.* J Infect Dis, 2021. **224**(12 Suppl 2): p. S321-s330.

63. Ramsay, M.E., et al., *Herd immunity from meningococcal serogroup C conjugate vaccination in England: database analysis.* Bmj, 2003. **326**(7385): p. 365-6.

64. FiercePharma. *On a vaccine roll, Pfizer scores FDA nod for Prevnar 13 follow-up ahead of rival Merck*. 2021 Accessed: 28/09/2025]; Available from: https://www.fiercepharma.com/pharma/a-vaccine-roll-pfizer-gains-fda-nod-for-its-20-valent-pneumococcal-follow-to-prevnar-13.

65. Guttormsen, H.K., et al., *Cognate stimulatory B-cell-T-cell interactions are critical for T-cell help recruited by glycoconjugate vaccines.* Infect Immun, 1999. **67**(12): p. 6375-84.

66. Borriello, F., et al., *B7-1 and B7-2 have overlapping, critical roles in immunoglobulin class switching and germinal center formation.* Immunity, 1997. **6**(3): p. 303-13.

67. Tangye, S.G. and D.M. Tarlinton, *Memory B cells: effectors of long-lived immune responses.* Eur J Immunol, 2009. **39**(8): p. 2065-75.

68. Pichichero, M.E., *Booster vaccinations: can immunologic memory outpace disease pathogenesis?* Pediatrics, 2009. **124**(6): p. 1633-41.

69. Insel, R.A. and P.W. Anderson, *Oligosaccharide-protein conjugate vaccines induce and prime for oligoclonal IgG antibody responses to the Haemophilus influenzae b capsular polysaccharide in human infants.* J Exp Med, 1986. **163**(2): p. 262-9.

70. Guirola, M., et al., *Immunologic memory response induced by a meningococcal serogroup C conjugate vaccine using the P64k recombinant protein as carrier.* FEMS Immunol Med Microbiol, 2006. **46**(2): p. 169-79.

71. Goldblatt, D., A.R. Vaz, and E. Miller, *Antibody avidity as a surrogate marker of successful priming by Haemophilus influenzae type b conjugate vaccines following infant immunization.* J Infect Dis, 1998. **177**(4): p. 1112-5.

72. Sayeed, M.A., et al., *A Cholera Conjugate Vaccine Containing O-specific Polysaccharide (OSP) of V. cholerae O1 Inaba and Recombinant Fragment of Tetanus Toxin Heavy Chain (OSP:rTTHc) Induces Serum, Memory and Lamina Proprial Responses against OSP and Is Protective in Mice.* PLoS Negl Trop Dis, 2015. **9**(7): p. e0003881.

73. Mani, S., T. Wierzba, and R.I. Walker, *Status of vaccine research and development for Shigella.* Vaccine, 2016. **34**(26): p. 2887-2894.

74. Huttner, A., et al., *Safety, immunogenicity, and preliminary clinical efficacy of a vaccine against extraintestinal pathogenic Escherichia coli in women with a history of recurrent urinary tract infection: a randomised, single-blind, placebo-controlled phase 1b trial.* Lancet Infect Dis, 2017. **17**(5): p. 528-537.

75. MacLennan, C.A., et al., *Salmonella Combination Vaccines: Moving Beyond Typhoid.* Open Forum Infectious Diseases, 2023. **10**(Supplement_1): p. S58-S66.

76. Obaro, S.K., *The new pneumococcal vaccine.* Clin Microbiol Infect, 2002. **8**(10): p. 623-33.

77. Riddle, M.S., et al., *Challenges and opportunities in developing a Shigella-containing combination vaccine for children in low- and middle-income countries: Report of an expert convening.* Vaccine, 2023. **41**(16): p. 2634-2644.

78. Rossi, O., et al., *A next-generation GMMA-based vaccine candidate to fight shigellosis.* NPJ vaccines, 2023.

79. Micoli, F., R. Adamo, and P. Costantino, *Protein Carriers for Glycoconjugate Vaccines: History, Selection Criteria, Characterization and New Trends.* Molecules, 2018. **23**(6).

80. Dagan, R., J. Poolman, and C.A. Siegrist, *Glycoconjugate vaccines and immune interference: A review.* Vaccine, 2010. **28**(34): p. 5513-23.

81. Piccioli, D., E. Bartolini, and F. Micoli, *GMMA as a 'plug and play' technology to tackle infectious disease to improve global health: context and perspectives for the future.* Expert Rev Vaccines, 2022. **21**(2): p. 163-172.

82. van der Pol, L., M. Stork, and P. van der Ley, *Outer membrane vesicles as platform vaccine technology.* Biotechnol J, 2015. **10**(11): p. 1689-706.

83. Jan, A.T., *Outer Membrane Vesicles (OMVs) of Gram-negative Bacteria: A Perspective Update.* Front Microbiol, 2017. **8**: p. 1053.

84. Gnopo, Y.M.D., et al., *Designer outer membrane vesicles as immunomodulatory systems - Reprogramming bacteria for vaccine delivery.* Adv Drug Deliv Rev, 2017. **114**: p. 132-142.

85. Li, M., et al., *Bacterial outer membrane vesicles as a platform for biomedical applications: An update.* J Control Release, 2020. **323**: p. 253-268.

86. Micoli, F. and C.A. MacLennan, *Outer membrane vesicle vaccines.* Seminars in Immunology, 2020. **50**: p. 101433.

87. Akira, S., S. Uematsu, and O. Takeuchi, *Pathogen recognition and innate immunity.* Cell, 2006. **124**(4): p. 783-801.

88. Kawai, T. and S. Akira, *The role of pattern-recognition receptors in innate immunity: update on Toll-like receptors.* Nat Immunol, 2010. **11**(5): p. 373-84.

89. Iwasaki, A. and R. Medzhitov, *Regulation of adaptive immunity by the innate immune system.* Science, 2010. **327**(5963): p. 291-5.

90. Mancini, F., et al., *OMV Vaccines and the Role of TLR Agonists in Immune Response.* Int J Mol Sci, 2020. **21**(12).

91. Moyer, T.J., A.C. Zmolek, and D.J. Irvine, *Beyond antigens and adjuvants: formulating future vaccines.* J Clin Invest, 2016. **126**(3): p. 799-808.

92. Benne, N., et al., *Orchestrating immune responses: How size, shape and rigidity affect the immunogenicity of particulate vaccines.* J Control Release, 2016. **234**: p. 124-34.

93. Bachmann, M.F. and G.T. Jennings, *Vaccine delivery: a matter of size, geometry, kinetics and molecular patterns.* Nat Rev Immunol, 2010. **10**(11): p. 787-96.

94. Tan, K., et al., *Outer Membrane Vesicles: Current Status and Future Direction of These Novel Vaccine Adjuvants.* Front Microbiol, 2018. **9**: p. 783.

95. Rappuoli, R., et al., *Meningococcal B vaccine (4CMenB): the journey from research to real world experience.* Expert Review of Vaccines, 2018. **17**(12): p. 1111-1121.

96. Toneatto, D., et al., *Emerging experience with meningococcal serogroup B protein vaccines.* Expert Rev Vaccines, 2017. **16**(5): p. 433-451.

97. Holst, J., et al., *Properties and clinical performance of vaccines containing outer membrane vesicles from Neisseria meningitidis.* Vaccine, 2009. **27 Suppl 2**: p. B3-12.

98. Ferrari, G., et al., *Outer membrane vesicles from group B Neisseria meningitidis delta gna33 mutant: proteomic and immunological comparison with detergent-derived outer membrane vesicles.* Proteomics, 2006. **6**(6): p. 1856-66.

99. Kis, Z., et al., *Emerging Technologies for Low-Cost, Rapid Vaccine Manufacture.* Biotechnol J, 2019. **14**(1): p. e1800376.

100. Berlanda Scorza, F., et al., *High yield production process for Shigella outer membrane particles.* PLoS One, 2012. **7**(6): p. e35616.

101. Gerke, C., et al., *Production of a Shigella sonnei Vaccine Based on Generalized Modules for Membrane Antigens (GMMA), 1790GAHB.* PLoS One, 2015. **10**(8): p. e0134478.

102. Giannelli, C., et al., *Quality by Design Framework Applied to GMMA Purification.* Aaps j, 2024. **26**(2): p. 32.

103. Rossi, O., et al., *Toll-Like Receptor Activation by Generalized Modules for Membrane Antigens from Lipid A Mutants of Salmonella enterica Serovars Typhimurium and Enteritidis.* Clin Vaccine Immunol, 2016. **23**(4): p. 304-14.

104. Rossi, O., et al., *Modulation of endotoxicity of Shigella generalized modules for membrane antigens (GMMA) by genetic lipid A modifications: relative activation of TLR4 and TLR2 pathways in different mutants.* J Biol Chem, 2014. **289**(36): p. 24922-35.

105. Gupta, R.K., *Aluminum compounds as vaccine adjuvants.* Adv Drug Deliv Rev, 1998. **32**(3): p. 155-172.

106. HogenEsch, H., D.T. O'Hagan, and C.B. Fox, *Optimizing the utilization of aluminum adjuvants in vaccines: you might just get what you want.* NPJ Vaccines, 2018. **3**: p. 51.

107. Kool, M., K. Fierens, and B.N. Lambrecht, *Alum adjuvant: some of the tricks of the oldest adjuvant.* J Med Microbiol, 2012. **61**(Pt 7): p. 927-934.

108. Piccioli, D., et al., *Antigen presentation by Follicular Dendritic cells to cognate B cells is pivotal for Generalised Modules for Membrane Antigens (GMMA) immunogenicity.* Vaccine, 2022. **40**(44): p. 6305-6314.

109. Micoli, F., et al., *GMMA Is a Versatile Platform to Design Effective Multivalent Combination Vaccines.* Vaccines (Basel), 2020. **8**(3).

110. MacLennan, C.A. *Vaccines for low-income countries*. in *Seminars in immunology*. 2013. Elsevier.

111. Rappuoli, R., S. Black, and D.E. Bloom, *Vaccines and global health: In search of a sustainable model for vaccine development and delivery.* Science Translational Medicine, 2019. **11**(497): p. eaaw2888.

112. Micoli, F., et al., *Comparative immunogenicity and efficacy of equivalent outer membrane vesicle and glycoconjugate vaccines against nontyphoidal Salmonella.* Proc Natl Acad Sci U S A, 2018. **115**(41): p. 10428-10433.

113. Koeberling, O., et al., *A broadly-protective vaccine against meningococcal disease in sub-Saharan Africa based on generalized modules for membrane antigens (GMMA).* Vaccine, 2014. **32**(23): p. 2688-95.

114. Kapulu, M.C., et al., *Complement-mediated serum bactericidal activity of antibodies elicited by the Shigella sonnei GMMA vaccine in adults from a shigellosis-endemic country: Exploratory analysis of a Phase 2a randomized study.* Front Immunol, 2022. **13**: p. 971866.

115. Launay, O., et al., *Safety Profile and Immunologic Responses of a Novel Vaccine Against Shigella sonnei Administered Intramuscularly, Intradermally and Intranasally: Results From*

Two Parallel Randomized Phase 1 Clinical Studies in Healthy Adult Volunteers in Europe. EBioMedicine, 2017. **22**: p. 164-172.

116. Launay, O., et al., *Booster Vaccination With GVGH Shigella sonnei 1790GAHB GMMA Vaccine Compared to Single Vaccination in Unvaccinated Healthy European Adults: Results From a Phase 1 Clinical Trial.* Front Immunol, 2019. **10**: p. 335.

117. Micoli, F., et al., *Antibodies Elicited by the Shigella sonnei GMMA Vaccine in Adults Trigger Complement-Mediated Serum Bactericidal Activity: Results From a Phase 1 Dose Escalation Trial Followed by a Booster Extension.* Front Immunol, 2021. **12**: p. 671325.

118. Obiero, C.W., et al., *A Phase 2a Randomized Study to Evaluate the Safety and Immunogenicity of the 1790GAHB Generalized Modules for Membrane Antigen Vaccine against Shigella sonnei Administered Intramuscularly to Adults from a Shigellosis-Endemic Country.* Front Immunol, 2017. **8**: p. 1884.

119. Leroux-Roels, I., et al., *Safety and Immunogenicity of a 4-Component Generalized Modules for Membrane Antigens Shigella Vaccine in Healthy European Adults: Randomized, Phase 1/2 Study.* J Infect Dis, 2024. **230**(4): p. e971-e984.

120. Hanumunthadu, B., et al., *Safety and immunogenicity of the invasive non-typhoidal Salmonella (iNTS)-GMMA vaccine: a first-in-human, randomised, dose escalation trial.* EBioMedicine, 2025. **119**: p. 105903.

121. Khalil, I.A., et al., *Morbidity and mortality due to shigella and enterotoxigenic Escherichia coli diarrhoea: the Global Burden of Disease Study 1990-2016.* Lancet Infect Dis, 2018. **18**(11): p. 1229-1240.

122. Troeger, C., et al., *Estimates of global, regional, and national morbidity, mortality, and aetiologies of diarrhoeal diseases: a systematic analysis for the Global Burden of Disease Study 2015.* The Lancet infectious diseases, 2017. **17**(9): p. 909-948.

123. Nasrin, D., et al., *Pathogens Associated With Linear Growth Faltering in Children With Diarrhea and Impact of Antibiotic Treatment: The Global Enteric Multicenter Study.* J Infect Dis, 2021. **224**(12 Suppl 2): p. S848-s855.

124. Rogawski, E.T., et al., *Use of quantitative molecular diagnostic methods to investigate the effect of enteropathogen infections on linear growth in children in low-resource settings: longitudinal analysis of results from the MAL-ED cohort study.* Lancet Glob Health, 2018. **6**(12): p. e1319-e1328.

125. Taneja, N. and A. Mewara, *Shigellosis: Epidemiology in India.* Indian J Med Res, 2016. **143**(5): p. 565-76.

126. Qiu, S., et al., *Multidrug-resistant atypical variants of Shigella flexneri in China.* Emerg Infect Dis, 2013. **19**(7): p. 1147-50.

127. Chung The, H., et al., *South Asia as a Reservoir for the Global Spread of Ciprofloxacin-Resistant Shigella sonnei: A Cross-Sectional Study.* PLoS Med, 2016. **13**(8): p. e1002055.

128. Organization, W.H., *Bacterial vaccines in clinical and preclinical development 2021: an overview and analysis.* 2022.

129. Liu, B., et al., *Structure and genetics of Shigella O antigens.* FEMS Microbiol Rev, 2008. **32**(4): p. 627-53.

130. Kotloff, K.L., et al., *Shigellosis.* Lancet, 2018. **391**(10122): p. 801-812.

131. Qu, F., et al., *Genotypes and antimicrobial profiles of Shigella sonnei isolates from diarrheal patients circulating in Beijing between 2002 and 2007.* Diagn Microbiol Infect Dis, 2012. **74**(2): p. 166-70.

132. Kahsay, A.G. and S. Muthupandian, *A review on Sero diversity and antimicrobial resistance patterns of Shigella species in Africa, Asia and South America, 2001-2014.* BMC Res Notes, 2016. **9**(1): p. 422.

133. Puzari, M., M. Sharma, and P. Chetia, *Emergence of antibiotic resistant Shigella species: A matter of concern.* J Infect Public Health, 2018. **11**(4): p. 451-454.

134. Thompson, C.N., P.T. Duy, and S. Baker, *The Rising Dominance of Shigella sonnei: An Intercontinental Shift in the Etiology of Bacillary Dysentery.* PLoS Negl Trop Dis, 2015. **9**(6): p. e0003708.

135. Killackey, S.A., M.T. Sorbara, and S.E. Girardin, *Cellular Aspects of Shigella Pathogenesis: Focus on the Manipulation of Host Cell Processes.* Front Cell Infect Microbiol, 2016. **6**: p. 38.

136. Tribble, D.R., *Resistant pathogens as causes of traveller's diarrhea globally and impact(s) on treatment failure and recommendations.* J Travel Med, 2017. **24**(suppl_1): p. S6-s12.

137. Ouyang-Latimer, J., et al., *In vitro antimicrobial susceptibility of bacterial enteropathogens isolated from international travelers to Mexico, Guatemala, and India from 2006 to 2008.* Antimicrob Agents Chemother, 2011. **55**(2): p. 874-8.

138. Raso, M.M., et al., *Toward a Shigella Vaccine: Opportunities and Challenges to Fight an Antimicrobial-Resistant Pathogen.* Int J Mol Sci, 2023. **24**(5).

139. MacLennan, C.A., et al., *The Shigella Vaccines Pipeline.* Vaccines (Basel), 2022. **10**(9).

140. Kubler-Kielb, J., et al., *Immunochemical studies of Shigella flexneri 2a and 6, and Shigella dysenteriae type 1 O-specific polysaccharide-core fragments and their protein conjugates as vaccine candidates.* Carbohydr Res, 2010. **345**(11): p. 1600-8.

141. Perepelov, A.V., et al., *A similarity in the O-acetylation pattern of the O-antigens of Shigellaflexneri types 1a, 1b, and 2a.* Carbohydr Res, 2009. **344**(5): p. 687-92.

142. Perepelov, A.V., et al., *Shigella flexneri O-antigens revisited: final elucidation of the O-acetylation profiles and a survey of the O-antigen structure diversity.* FEMS Immunol Med Microbiol, 2012. **66**(2): p. 201-10.

143. Robbins, J.B., et al., *Synthesis, characterization, and immunogenicity in mice of Shigella sonnei O-specific oligosaccharide-core-protein conjugates.* Proc Natl Acad Sci U S A, 2009. **106**(19): p. 7974-8.

144. Cohen, D., et al., *Threshold protective levels of serum IgG to Shigella lipopolysaccharide: re-analysis of Shigella vaccine trials data.* Clin Microbiol Infect, 2023. **29**(3): p. 366-371.

145. Cohen, D., et al., *Serum IgG antibodies to Shigella lipopolysaccharide antigens - a correlate of protection against shigellosis.* Hum Vaccin Immunother, 2019. **15**(6): p. 1401-1408.

146. Conti, V., et al., *Putative correlates of protection against shigellosis assessing immunomarkers across responses to S. sonnei investigational vaccine.* NPJ Vaccines, 2024. **9**(1): p. 56.

147. Levine, M.M., et al., *Clinical trials of Shigella vaccines: two steps forward and one step back on a long, hard road.* Nat Rev Microbiol, 2007. **5**(7): p. 540-53.

148. Citiulo, F., et al., *Rationalizing the design of a broad coverage Shigella vaccine based on evaluation of immunological cross-reactivity among S. flexneri serotypes.* PLoS Negl Trop Dis, 2021. **15**(10): p. e0009826.

149. Livio, S., et al., *Shigella isolates from the global enteric multicenter study inform vaccine development.* Clin Infect Dis, 2014. **59**(7): p. 933-41.

150. Van De Verg, L.L., et al., *Cross-reactivity of Shigella flexneri serotype 2a O antigen antibodies following immunization or infection.* Vaccine, 1996. **14**(11): p. 1062-8.

151. Tennant, S.M., et al., *Nontyphoidal salmonella disease: Current status of vaccine research and development.* Vaccine, 2016. **34**(26): p. 2907-2910.

152. Sima, C.M., et al., *Emerging Strategies against Non-Typhoidal Salmonella: From Pathogenesis to Treatment.* Curr Issues Mol Biol, 2024. **46**(7): p. 7447-7472.

153. Marchello, C.S., M. Birkhold, and J.A. Crump, *Complications and mortality of non-typhoidal salmonella invasive disease: a global systematic review and meta-analysis.* Lancet Infect Dis, 2022. **22**(5): p. 692-705.

154. *Global burden of 369 diseases and injuries in 204 countries and territories, 1990-2019: a systematic analysis for the Global Burden of Disease Study 2019.* Lancet, 2020. **396**(10258): p. 1204-1222.

155. Kuehn, R., et al., *Enteric (typhoid and paratyphoid) fever.* Lancet, 2025. **406**(10509): p. 1283-1294.

156. Deen, J., et al., *Community-acquired bacterial bloodstream infections in developing countries in south and southeast Asia: a systematic review.* Lancet Infect Dis, 2012. **12**(6): p. 480-7.

157. Aslam, S., et al., *Clinical presentation and outcome of enteric fever in adult patients with cancer: a perspective from Pakistan.* Access Microbiology, 2024. **6**(5): p. 000719. v3.

158. Browne, A.J., et al., *Drug-resistant enteric fever worldwide, 1990 to 2018: a systematic review and meta-analysis.* BMC Med, 2020. **18**(1): p. 1.

159. Marchello, C.S., S.D. Carr, and J.A. Crump, *A Systematic Review on Antimicrobial Resistance among Salmonella Typhi Worldwide.* Am J Trop Med Hyg, 2020. **103**(6): p. 2518-2527.

160. Tack, B., et al., *Invasive non-typhoidal Salmonella infections in sub-Saharan Africa: a systematic review on antimicrobial resistance and treatment.* BMC Med, 2020. **18**(1): p. 212.

161. Szu, S.C., et al., *Relation between structure and immunologic properties of the Vi capsular polysaccharide.* Infect Immun, 1991. **59**(12): p. 4555-61.

162. Sahastrabuddhe, S. and T. Saluja, *Overview of the Typhoid Conjugate Vaccine Pipeline: Current Status and Future Plans.* Clin Infect Dis, 2019. **68**(Suppl 1): p. S22-s26.

163. Steele, A.D., et al., *Typhoid Conjugate Vaccines and Enteric Fever Control: Where to Next?* Clin Infect Dis, 2020. **71**(Suppl 2): p. S185-s190.

164. Goh, Y.S., et al., *Monoclonal Antibodies of a Diverse Isotype Induced by an O-Antigen Glycoconjugate Vaccine Mediate In Vitro and In Vivo Killing of African Invasive Nontyphoidal Salmonella.* Infect Immun, 2015. **83**(9): p. 3722-31.

165. Nyirenda, T.S., et al., *Sequential acquisition of T cells and antibodies to nontyphoidal Salmonella in Malawian children.* The Journal of infectious diseases, 2014. **210**(1): p. 56-64.

166. Rondini, S., et al., *Invasive African Salmonella Typhimurium induces bactericidal antibodies against O-antigens.* Microb Pathog, 2013. **63**: p. 19-23.

167. Micoli, F., et al., *Structural analysis of O-polysaccharide chains extracted from different Salmonella Typhimurium strains.* Carbohydr Res, 2014. **385**: p. 1-8.

168. Ravenscroft, N., et al., *Structural analysis of the O-acetylated O-polysaccharide isolated from Salmonella paratyphi A and used for vaccine preparation.* Carbohydr Res, 2015. **404**: p. 108-16.

169. Hellerqvist, C., et al., *Structural studies on the O-specific side-chains of the cell-wall lipopolysaccharide from Salmonella typhimurium LT2.* Carbohydrate research, 1969. **9**(2): p. 237-241.

170. Konadu, E., et al., *Synthesis, characterization, and immunological properties in mice of conjugates composed of detoxified lipopolysaccharide of Salmonella paratyphi A bound to tetanus toxoid with emphasis on the role of O acetyls.* Infection and immunity, 1996. **64**(7): p. 2709-2715.

171. Rahman, M.M., J. Guard-Petter, and R.W. Carlson, *A virulent isolate of Salmonella enteritidis produces a Salmonella typhi-like lipopolysaccharide.* Journal of bacteriology, 1997. **179**(7): p. 2126-2131.

172. Lanzilao, L., et al., *Strain Selection for Generation of O-Antigen-Based Glycoconjugate Vaccines against Invasive Nontyphoidal Salmonella Disease.* PLoS One, 2015. **10**(10): p. e0139847.

173. Onsare, R.S., et al., *Relationship between antibody susceptibility and lipopolysaccharide O-antigen characteristics of invasive and gastrointestinal nontyphoidal Salmonellae isolates from Kenya.* Plos neglected tropical diseases, 2015. **9**(3): p. e0003573.

174. Parker, C.T., et al., *Lipopolysaccharide O-chain microheterogeneity of Salmonella serotypes Enteritidis and Typhimurium.* Environmental Microbiology, 2001. **3**(5): p. 332-342.

175. Rondini, S., et al., *Design of glycoconjugate vaccines against invasive African Salmonella enterica serovar Typhimurium.* Infect Immun, 2015. **83**(3): p. 996-1007.

176. Hanumunthadu, B., et al., *Salmonella Vaccine Study in Oxford (SALVO) trial: protocol for an observer-participant blind randomised placebo-controlled trial of the iNTS-GMMA vaccine within a European cohort.* BMJ Open, 2023. **13**(11): p. e072938.

177. Skidmore, P.D., R. Canals, and M.N. Ramasamy, *The iNTS-GMMA vaccine: a promising step in non-typhoidal Salmonella vaccine development.* Expert Rev Vaccines, 2023. **22**(1): p. 918-920.

178. Alfini, R., et al., *Design of a Glycoconjugate Vaccine Against Salmonella Paratyphi A.* Vaccines (Basel), 2024. **12**(11).

179. Ibarz-Pavon, A.B., et al., *Consultation report - considerations for a regulatory pathway for bivalent Salmonella Typhi/Paratyphi A vaccines for use in endemic countries.* Vaccine, 2025. **56**: p. 127189.

180. Hausdorff, W.P., et al., *Facilitating the development of urgently required combination vaccines.* The Lancet Global Health, 2024. **12**(6): p. e1059-e1067.

181. Fatima, M. and K.-J. Hong, *Innovations, Challenges, and Future Prospects for Combination Vaccines Against Human Infections.* Vaccines, 2025. **13**(4): p. 335.

182. Liu, B., et al., *Immunogenicity and Safety of Childhood Combination Vaccines: A Systematic Review and Meta-Analysis.* Vaccines (Basel), 2022. **10**(3).

183. Berlanda Scorza, F., et al., *A strategic model for developing vaccines against neglected diseases: An example of industry collaboration for sustainable development.* Hum Vaccin Immunother, 2022. **18**(6): p. 2136451.

184. Maman, K., et al., *The value of childhood combination vaccines: From beliefs to evidence.* Hum Vaccin Immunother, 2015. **11**(9): p. 2132-41.

185. Esposito, S., et al., *Hexavalent vaccines for immunization in paediatric age.* Clin Microbiol Infect, 2014. **20 Suppl 5**: p. 76-85.

186. Vidor, E. and B. Soubeyrand, *Manufacturing DTaP-based combination vaccines: industrial challenges around essential public health tools.* Expert Rev Vaccines, 2016. **15**(12): p. 1575-1582.

187. Feemster, K., et al. *Immunogenicity of current and next-generation pneumococcal conjugate vaccines in children: current challenges and upcoming opportunities*. in *Open forum infectious diseases*. 2024. Oxford University Press US.

188. Dagan, R., et al., *Reduction of antibody response to an 11-valent pneumococcal vaccine coadministered with a vaccine containing acellular pertussis components.* Infection and immunity, 2004. **72**(9): p. 5383-5391.

189. *Penmenvy - a second pentavalent meningococcal vaccine.* Med Lett Drugs Ther, 2025. **67**(1726): p. 57-59.

190. *Penbraya: A pentavalent meningococcal vaccine.* Med Lett Drugs Ther, 2024. **66**(1698): p. 43-45.

191. Haidara, F.C., et al., *Meningococcal ACWYX conjugate vaccine in 2-to-29-year-olds in Mali and Gambia.* New England Journal of Medicine, 2023. **388**(21): p. 1942-1955.

192. Valmas, C., et al., *A policy review of the introduction of the MenACWY vaccine in toddlers across multiple countries.* Expert Review of Vaccines, 2022. **21**(11): p. 1637-1646.

193. Pizza, M., R. Bekkat-Berkani, and R. Rappuoli, *Vaccines against meningococcal diseases.* Microorganisms, 2020. **8**(10): p. 1521.

194. Di Benedetto, R., et al., *Comparison of Shigella GMMA and glycoconjugate four-component formulations in animals.* Front Mol Biosci, 2023. **10**: p. 1284515.

195. Kotloff, K.L., et al., *The incidence, aetiology, and adverse clinical consequences of less severe diarrhoeal episodes among infants and children residing in low-income and middle-income countries: a 12-month case-control study as a follow-on to the Global Enteric Multicenter Study (GEMS).* Lancet Glob Health, 2019. **7**(5): p. e568-e584.

196. Ranjbar, R. and A. Farahani, *Shigella: Antibiotic-Resistance Mechanisms And New Horizons For Treatment.* Infect Drug Resist, 2019. **12**: p. 3137-3167.

197. Cohen, D., et al., *Detoxified O-Specific Polysaccharide (O-SP)-Protein Conjugates: Emerging Approach in the Shigella Vaccine Development Scene.* Vaccines (Basel), 2022. **10**(5).

198. Martin, P. and C. Alaimo, *The Ongoing Journey of a Shigella Bioconjugate Vaccine.* Vaccines (Basel), 2022. **10**(2).

199. Phalipon, A. and L.A. Mulard, *Toward a Multivalent Synthetic Oligosaccharide-Based Conjugate Vaccine against Shigella: State-of-the-Art for a Monovalent Prototype and Challenges.* Vaccines (Basel), 2022. **10**(3).

200. Robbins, J.B., C. Chu, and R. Schneerson, *Hypothesis for vaccine development: protective immunity to enteric diseases caused by nontyphoidal salmonellae and shigellae may be conferred by serum IgG antibodies to the O-specific polysaccharide of their lipopolysaccharides.* Clin Infect Dis, 1992. **15**(2): p. 346-61.

201. Mancini, F., et al., *GMMA-Based Vaccines: The Known and The Unknown.* Front Immunol, 2021. **12**: p. 715393.

202. Micoli, F., U.N. Nakakana, and F. Berlanda Scorza, *Towards a Four-Component GMMA-Based Vaccine against Shigella.* Vaccines (Basel), 2022. **10**(2).

203. Frenck, R.W., Jr., et al., *Efficacy, safety, and immunogenicity of the Shigella sonnei 1790GAHB GMMA candidate vaccine: Results from a phase 2b randomized, placebo-controlled challenge study in adults.* EClinicalMedicine, 2021. **39**: p. 101076.

204. Schneerson, R., et al., *Preparation, characterization, and immunogenicity of Haemophilus influenzae type b polysaccharide-protein conjugates.* J Exp Med, 1980. **152**(2): p. 361-76.

205. Passwell, J.H., et al., *Age-related efficacy of Shigella O-specific polysaccharide conjugates in 1-4-year-old Israeli children.* Vaccine, 2010. **28**(10): p. 2231-2235.

206. Barel, L.A. and L.A. Mulard, *Classical and novel strategies to develop a Shigella glycoconjugate vaccine: from concept to efficacy in human.* Hum Vaccin Immunother, 2019. **15**(6): p. 1338-1356.

207. Robbins, J.B., R. Schneerson, and S.C. Szu, *Perspective: hypothesis: serum IgG antibody is sufficient to confer protection against infectious diseases by inactivating the inoculum.* J Infect Dis, 1995. **171**(6): p. 1387-98.

208. Cohen, D., et al., *Double-blind vaccine-controlled randomised efficacy trial of an investigational Shigella sonnei conjugate vaccine in young adults.* Lancet, 1997. **349**(9046): p. 155-9.

209. Cohen, D., et al., *Safety and immunogenicity of a synthetic carbohydrate conjugate vaccine against Shigella flexneri 2a in healthy adult volunteers: a phase 1, dose-escalating, single-blind, randomised, placebo-controlled study.* Lancet Infect Dis, 2021. **21**(4): p. 546-558.

210. Riddle, M.S., et al., *Safety and Immunogenicity of a Candidate Bioconjugate Vaccine against Shigella flexneri 2a Administered to Healthy Adults: a Single-Blind, Randomized Phase I Study.* Clin Vaccine Immunol, 2016. **23**(12): p. 908-917.

211. HogenEsch, H., *Mechanisms of stimulation of the immune response by aluminum adjuvants.* Vaccine, 2002. **20 Suppl 3**: p. S34-9.

212. Rosenqvist, E., et al., *Effect of aluminium hydroxide and meningococcal serogroup C capsular polysaccharide on the immunogenicity and reactogenicity of a group B Neisseria meningitidis outer membrane vesicle vaccine.* Developments in biological standardization, 1998. **92**: p. 323-333.

213. Mancini, F., et al., *Testing S. sonnei GMMA with and without Aluminium Salt-Based Adjuvants in Animal Models.* Pharmaceutics, 2024. **16**(4).

214. Micoli, F., R. Alfini, and C. Giannelli, *Methods for Assessment of OMV/GMMA Quality and Stability.* Methods Mol Biol, 2022. **2414**: p. 227-279.

215. Micoli, F., et al., *A scalable method for O-antigen purification applied to various Salmonella serovars.* Anal Biochem, 2013. **434**(1): p. 136-45.

216. Giannelli, C., et al., *Development of a Specific and Sensitive HPAEC-PAD Method for Quantification of Vi Polysaccharide Applicable to other Polysaccharides Containing Amino Uronic Acids.* Anal Chem, 2020. **92**(9): p. 6304-6311.

217. Micoli, F., C. Giannelli, and R. Di Benedetto, *O-Antigen Extraction, Purification, and Chemical Conjugation to a Carrier Protein.* Methods Mol Biol, 2021. **2183**: p. 267-304.

218. Shafer, D.E., et al., *Activation of soluble polysaccharides with 1-cyano-4-dimethylaminopyridinium tetrafluoroborate (CDAP) for use in protein-polysaccharide conjugate vaccines and immunological reagents. II. Selective crosslinking of proteins to CDAP-activated polysaccharides.* Vaccine, 2000. **18**(13): p. 1273-81.

219. Angela, B., R. Stefano, and P. Daniela, *SEPARATION OF UNCONJUGATED AND CONJUGATED SACCHARIDE BY SOLID PHASE EXTRACTION*. 2005, Chiron SRL.

220. Stefanetti, G., et al., *Impact of conjugation chemistry on the immunogenicity of S. Typhimurium conjugate vaccines.* Vaccine, 2014. **32**(46): p. 6122-9.

221. Caboni, M., et al., *An O antigen capsule modulates bacterial pathogenesis in Shigella sonnei.* PLoS Pathog, 2015. **11**(3): p. e1004749.

222. Aruta, M.G., et al., *Increasing the High Throughput of a Luminescence-Based Serum Bactericidal Assay (L-SBA).* BioTech (Basel), 2021. **10**(3).

223. Necchi, F., A. Saul, and S. Rondini, *Development of a high-throughput method to evaluate serum bactericidal activity using bacterial ATP measurement as survival readout.* PLoS One, 2017. **12**(2): p. e0172163.

224. Gasperini, G., et al., *Effect of O-Antigen Chain Length Regulation on the Immunogenicity of Shigella and Salmonella Generalized Modules for Membrane Antigens (GMMA).* Int J Mol Sci, 2021. **22**(3).

225. Micoli, F., G. Stefanetti, and C.A. MacLennan, *Exploring the variables influencing the immune response of traditional and innovative glycoconjugate vaccines.* Front Mol Biosci, 2023. **10**: p. 1201693.

226. Raso, M.M., et al., *GMMA and Glycoconjugate Approaches Compared in Mice for the Development of a Vaccine against Shigella flexneri Serotype 6.* Vaccines (Basel), 2020. **8**(2).

227. Mancini, F., et al., *Exploring the Role of GMMA Components in the Immunogenicity of a 4-Valent Vaccine against Shigella.* Int J Mol Sci, 2023. **24**(3).

228. Ndungo, E. and M.F. Pasetti, *Functional antibodies as immunological endpoints to evaluate protective immunity against Shigella.* Hum Vaccin Immunother, 2020. **16**(1): p. 197-205.

229. Piccioli, D., et al., *Enhanced Systemic Humoral Immune Response Induced in Mice by Generalized Modules for Membrane Antigens (GMMA) Is Associated with Affinity Maturation and Isotype Switching.* Vaccines (Basel), 2023. **11**(7).

230. Mancini, F., et al., *Dissecting the contribution of O-Antigen and proteins to the immunogenicity of Shigella sonnei generalized modules for membrane antigens (GMMA).* Sci Rep, 2021. **11**(1): p. 906.

231. Giersing, B.K., et al., *Clinical and regulatory development strategies for Shigella vaccines intended for children younger than 5 years in low-income and middle-income countries.* Lancet Glob Health, 2023. **11**(11): p. e1819-e1826.

232. Hausdorff, W.P., S. Scheele, and B.K. Giersing, *What Drives the Value of a Shigella Vaccine?* Vaccines (Basel), 2022. **10**(2).

233. *Vaccine Investment Strategy 2024. Appendix 1: Shigella Investment Case.* 2024.

234. WHO, *Bacterial Priority Pathogens List, 2024: bacterial pathogens of public health importance to guide research, development and strategies to prevent and control antimicrobial resistance. Geneva: World Health Organization; 2024.* 2024.

235. Micoli, F., et al., *Production of a conjugate vaccine for Salmonella enterica serovar Typhi from Citrobacter Vi.* Vaccine, 2012. **30**(5): p. 853-61.

236. Arcuri, M., et al., *The influence of conjugation variables on the design and immunogenicity of a glycoconjugate vaccine against Salmonella Typhi.* PLoS One, 2017. **12**(12): p. e0189100.

237. Nappini, R., et al., *Modeling 1-Cyano-4-Dimethylaminopyridine Tetrafluoroborate (CDAP) Chemistry to Design Glycoconjugate Vaccines with Desired Structural and Immunological Characteristics.* Vaccines, 2024. **12**(7): p. 707.

238. Lei, Q.P., et al., *Quantitation of low level unconjugated polysaccharide in tetanus toxoid-conjugate vaccine by HPAEC/PAD following rapid separation by deoxycholate/HCl.* J Pharm Biomed Anal, 2000. **21**(6): p. 1087-91.

239. Oldrini, D., et al., *Testing a Recombinant Form of Tetanus Toxoid as a Carrier Protein for Glycoconjugate Vaccines.* Vaccines (Basel), 2023. **11**(12).

240. Gasperini, G., et al., *O-Antigen decorations in Salmonella enterica play a key role in eliciting functional immune responses against heterologous serovars in animal models.* Front Cell Infect Microbiol, 2024. **14**: p. 1347813.

241. Mancini, F., F. Micoli, and O. Rossi, *Setup and Characterization of a High-Throughput Luminescence-Based Serum Bactericidal Assay (L-SBA) to Determine Functionality of Human Sera against Shigella flexneri.* BioTech (Basel), 2022. **11**(3).

242. Feng, J., et al., *A quadrivalent recombinant influenza Hemagglutinin vaccine induced strong protective immune responses in animal models.* Vaccine, 2024. **42**(22): p. 126008.

243. Zhang, Y., et al., *Safety and immunogenicity of a combined DTacP-sIPV-Hib vaccine in animal models.* Hum Vaccin Immunother, 2022. **18**(7): p. 2160158.

244. Anderson, J.D.t., et al., *Burden of enterotoxigenic Escherichia coli and shigella non-fatal diarrhoeal infections in 79 low-income and lower middle-income countries: a modelling analysis.* Lancet Glob Health, 2019. **7**(3): p. e321-e330.

245. Baker, S. and T.A. Scott, *Antimicrobial-resistant Shigella: where do we go next?* Nature Reviews Microbiology, 2023. **21**(7): p. 409-410.

246. Carson, D., et al., *Development of a Monocyte Activation Test as an Alternative to the Rabbit Pyrogen Test for Mono- and Multi-Component Shigella GMMA-Based Vaccines.* Microorganisms, 2021. **9**(7).

247. Vadrevu, K.M., et al., *Persisting antibody responses to Vi polysaccharide-tetanus toxoid conjugate (Typbar TCV®) vaccine up to 7 years following primary vaccination of children < 2 years of age with, or without, a booster vaccination.* Vaccine, 2021. **39**(45): p. 6682-6690.

248. Hausdorff, W.P., et al., *Vaccine value profile for Shigella.* Vaccine, 2023. **41 Suppl 2**: p. S76-s94.

249. Santostefano, G., et al., *Glycoconjugate Vaccine Quantification: An Overview on Present and Future Trends in Analytical Development.* Analytical Chemistry, 2025. **97**(18): p. 9541-9553.

250. Cataldi, T.R., C. Campa, and G.E. De Benedetto, *Carbohydrate analysis by high-performance anion-exchange chromatography with pulsed amperometric detection: the potential is still growing.* Fresenius J Anal Chem, 2000. **368**(8): p. 739-58.

251. Townsend, R.R. and M.R. Hardy, *Analysis of glycoprotein oligosaccharides using high-pH anion exchange chromatography.* Glycobiology, 1991. **1**(2): p. 139-47.

252. Corrado, A., et al., *A universal UHPLC-CAD platform for the quantification of polysaccharide antigens.* Sci Rep, 2023. **13**(1): p. 10646.

253. Necchi, F., et al., *From an in vivo to an in vitro relative potency (IVRP) assay to fully characterize a multicomponent O-antigen based vaccine against Shigella.* Carbohydr Polym, 2023. **314**: p. 120920.

254. Palmieri, E., et al., *Stability of Outer Membrane Vesicles-Based Vaccines, Identifying the Most Appropriate Methods to Detect Changes in Vaccine Potency.* Vaccines (Basel), 2021. **9**(3).

255. Rossi, O., et al., *Characterization of Competitive ELISA and Formulated Alhydrogel Competitive ELISA (FAcE) for Direct Quantification of Active Ingredients in GMMA-Based Vaccines.* Methods Protoc, 2020. **3**(3).

256. Raso, M.M., et al., *Comparison and Optimization of Quantification Methods for Shigella flexneri Serotype 6 O-antigen Containing Galacturonic Acid and Methyl-Pentose.* Int J Mol Sci, 2021. **22**(22).

257. Galermo, A.G., et al., *Liquid Chromatography-Tandem Mass Spectrometry Approach for Determining Glycosidic Linkages.* Anal Chem, 2018. **90**(21): p. 13073-13080.

258. Galermo, A.G., et al., *Development of an Extensive Linkage Library for Characterization of Carbohydrates.* Anal Chem, 2019. **91**(20): p. 13022-13031.

259. Shajahan, A., et al., *High-throughput automated micro-permethylation for glycan structure analysis.* Analytical chemistry, 2018. **91**(2): p. 1237-1240.

260. Xu, G., et al., *Revisiting monosaccharide analysis - quantitation of a comprehensive set of monosaccharides using dynamic multiple reaction monitoring.* Analyst, 2017. **143**(1): p. 200-207.

261. Corradini, C., A. Cavazza, and C. Bignardi, *High-performance anion-exchange chromatography coupled with pulsed electrochemical detection as a powerful tool to evaluate carbohydrates of food interest: principles and applications.* International Journal of Carbohydrate Chemistry, 2012. **2012**(1): p. 487564.

262. Palomares-Navarro, J.J., et al., *Antibiofilm action of plant terpenes in Salmonella strains: Potential inhibitors of the synthesis of extracellular polymeric substances.* Pathogens, 2022. **12**(1): p. 35.

263. Phugare, S., et al., *Quantitation of novel pentavalent meningococcal polysaccharide conjugate vaccine (Men A-TT, Men C-CRM, Men Y-CRM, Men W-CRM, Men X-TT) using sandwich ELISA.* Vaccine, 2020. **38**(49): p. 7815-7824.

264. Reyes, F., et al., *Development of four sandwich ELISAs for quantitation of capsular polysaccharides from Neisseria meningitidis serogroups A, C, W and Y in multivalent vaccines.* Journal of immunological methods, 2014. **407**: p. 58-62.

265. Saydam, M., P. Rigsby, and F. Mawas, *A novel Enzyme-Linked Immuno-Sorbent Assay (ELISA) for the quantification of total and free polysaccharide in Haemophilus influenzae b–Tetanus toxoid conjugate vaccines in monovalent and combined vaccine formulations.* Biologicals, 2014. **42**(1): p. 29-33.

266. Dumpa, N., et al., *Stability of vaccines.* Aaps Pharmscitech, 2019. **20**(2): p. 42.

267. Biologicals, I., *Monitoring vaccine wastage at country level: guidelines for programme managers.* Geneva, Switzerland: World Health Organization, 2005.

268. Schnetzinger, F., et al., *Stability Preparedness: The Not-So-Cold Case for Innovations in Vaccine Stability Modelling and Product Release.* Vaccines (Basel), 2024. **12**(9).

269. Organizaion, W.H., *Guidelines on stability evaluation of vaccines.* Biologicals, 2009. **37**(6): p. 424-434.

270. Campa, C., et al., *Use of Stability Modeling to Support Accelerated Vaccine Development and Supply.* Vaccines (Basel), 2021. **9**(10).

271. Clénet, D., *Accurate prediction of vaccine stability under real storage conditions and during temperature excursions.* Eur J Pharm Biopharm, 2018. **125**: p. 76-84.

272. Clénet, D., et al., *Advanced kinetic analysis as a tool for formulation development and prediction of vaccine stability.* J Pharm Sci, 2014. **103**(10): p. 3055-64.

273. Castellanos, M.M., et al., *CMC Strategies and Advanced Technologies for Vaccine Development to Boost Acceleration and Pandemic Preparedness.* Vaccines (Basel), 2023. **11**(7).

274. Fabre, A.-L., et al., *An efficient method for long-term room temperature storage of RNA.* European Journal of Human Genetics, 2014. **22**(3): p. 379-385.

275. Kis, Z., *Stability Modelling of mRNA Vaccine Quality Based on Temperature Monitoring throughout the Distribution Chain.* Pharmaceutics, 2022. **14**(2).

276. Lamichhane, B., et al., *Salmonellosis: An Overview of Epidemiology, Pathogenesis, and Innovative Approaches to Mitigate the Antimicrobial Resistant Infections.* Antibiotics (Basel), 2024. **13**(1).